UNIVERSITY OF OKLAHOMA

GRADUATE COLLEGE

THE SYNERGISTIC EFFECTS OF PREPREG HUMIDITY EXPOSURE, FABRICATION PRESSURE, AND HYDRAULIC FLUID ABSORPTION ON MICROSTRUCTURE AND MECHANICAL PROPERTIES OF HIGH-PERFORMANCE COMPOSITE LAMINATES

A DISSERTATION

SUBMITTED TO THE GRADUATE FACULTY

In partial fulfillment of the requirements for the

Degree of

DOCTOR OF PHILOSOPHY

By

KEITH R. HURDELBRINK II
Norman, Oklahoma
2017

THE SYNERGISTIC EFFECTS OF PREPREG HUMIDITY EXPOSURE, FABRICATION PRESSURE, AND HYDRAULIC FLUID ABSORPTION ON MICROSTRUCTURE AND MECHANICAL PROPERTIES OF HIGH-PERFORMANCE COMPOSITE LAMINATES

A DISSERTATION APPROVED FOR THE
SCHOOL OF AEROSPACE AND MECHANICAL ENGINEERING

BY

Dr. Zahed Siddique, Co-Chair

Dr. M. Cengiz Altan, Co-Chair

Dr. Shivakumar Raman

Dr. Mrinal C. Saha

Dr. David P. Miller

Dr. Landon R. Grace

DEDICATION PAGE

I would like to dedicate this work to my mother, whom I think of and miss everyday. I wish you could be here today to share in this accomplishment; however I am thankful for the nearly 30 years of your guidance in my life.

Additionally, I would like to dedicate this work to Anna. This achievement would not have been possible without your love and support, which has made the sacrifices and challenges easier to bear. I look forward to spending the rest of my life with you.

ACKNOWLEDGEMENTS

First, I would like to thank the members of my advisory committee for their support and guidance throughout my graduate studies and for volunteering their time to serve on my committee. Particular thanks are owed to my advisors, Dr. Zahed Siddique and Dr. M. Cengiz Altan, whose encouragement and insight has been invaluable.

I would also like to acknowledge several colleagues who have supported me and been a resource when I had questions. Dr. Landon Grace for developing the framework of the hindered diffusion model and his assistance throughout my doctoral program. Gorkem E. Guloglu assistance with programming and model development has been very helpful. Over the years, Dr. Levent Aktas and Dr. Jacob Anderson have assisted me significantly with experimental research methods and training me on proper use of the various tools and equipment available to the research group.

Finally, I would like to recognize several undergraduate and graduate research assistants who have assisted me with several projects, including Kevin Cox, Andres Romero Vasquez, Davis Crane, Benjamin Lobaugh and Sergio Ceballos.

TABLE OF CONTENTS

LIST OF TABLES ..... **XI**

LIST OF FIGURES ..... **XIII**

ABSTRACT ..... **XVIII**

CHAPTER 1: INTRODUCTION AND OVERVIEW **1**

1.1 Effect of Process-Induced Defects on High-Performance Composite Materials 1

1.2 Composite Degradation due to Environmental and Operational Effects 4

1.3 Research Motivation 5

1.4 Organization of Dissertation 6

PART A: CHARACTERIZATION OF COMPOSITE LAMINATES **8**

CHAPTER 2: COUPLED EFFECT OF VARYING PREPREG HUMIDITY EXPOSURE AND FABRICATION PRESSURE ON LAMINATE MICROSTRUCTURE **9**

2.1 Prepreg Material Overview 9

2.2 Prepreg Conditioning at Varying Relative Humidity Exposure Levels 11

2.2.1 Equipment Used and Experimental Procedure for Prepreg Conditioning *11*

2.2.2 Measuring Prepreg Moisture Content before Laminate Fabrication *12*

2.3 Laminate Fabrication at Varying Cure Pressures 14

2.3.1 Equipment Used and Experimental Procedure for Laminate Fabrication *14*

2.3.2 Initial Assessment of Fabricated Laminate Thickness *17*

2.4 Specimen Preparation and Allocation to Address the Research Objectives 18

2.5 Laminate Fiber Volume Fraction and Void Volume Fraction 22

2.5.1 Experimental Procedure to Determine Fiber Volume Fraction and Void Volume Fraction 22

2.5.2 Development of Trend Line Analysis of Effect of Humidity and Pressure on Laminate Properties 23

2.5.3 Laminate Fiber Volume Fraction Results 24

2.5.4 Laminate Void Volume Fraction Results 27

2.5.5 Effect of Prepreg Humidity Exposure on Laminate Fiber Volume Fraction 30

2.5.6 Effect of Fabrication Pressure on Laminate Fiber Volume Fraction 32

2.5.7 Effect of Prepreg Humidity Exposure on Void Volume Fraction 35

2.5.8 Effect of Fabrication Pressure on Void Volume Fraction 38

2.6 Scanning Electron Microscope Evaluation 40

2.6.1 Humidity and Processing Effect on Void Size and Spatial Distribution for Quartz/BMI Prepregs 40

2.6.2 Humidity and Processing Effect on Void Size and Spatial Distribution for Quartz/Epoxy Prepreg 43

2.6.3 Humidity and Processing Effect on Void Size and Distribution for Carbon / Epoxy Prepreg 45

2.7 Summary of Laminate Microstructure and SEM Analysis Chapter ... 47

CHAPTER 3: COUPLED EFFECT OF PREPREG MOISTURE CONTENT AND FABRICATION PRESSURE ON LAMINATE FLEXURAL PROPERTIES 50

3.1 Background and Literature Review of Processing Conditions Affects on Mechanical Properties 50

3.2 Laminate Flexural Stiffness and Strength 53

3.2.1 Experimental Procedure to Determine Laminate Mechanical Properties .. 54

3.2.2 Laminate Flexural Stiffness Results 55

3.2.3 Laminate Flexural Strength Results 57

3.2.4 Effect of Prepreg Humidity Exposure on Laminate Flexural Stiffness 59

3.2.5 Effect of Fabrication Pressure on Laminate Flexural Stiffness 61

3.2.6 Effect of Prepreg Humidity Exposure on Laminate Flexural Strength 64

3.2.7 Effect of Fabrication Pressure on Laminate Flexural Strength 67

3.3 SUMMARY OF LAMINATE MECHANICAL PROPERTIES CHAPTER 70

CHAPTER 4: CONTOUR PLOTS FOR LAMINATE MICROSTRUCTURE AND MECHANICAL PROPERTIES – COUPLED EFFECT OF PREPREG HUMIDITY EXPOSURE AND FABRICATION PRESSURE 71

4.1 LITERATURE REVIEW OF MODELING TECHNIQUES FOR CONTOUR PLOT ANALYSIS 71

4.2 FORMATION OF PROPERTY FUNCTION EQUATIONS TO GENERATE CONTOUR PLOTS 72

4.3 IDENTIFICATION OF PROPERTY FUNCTIONAL EQUATIONS FOR NORMALIZED LAMINATE PROPERTIES 74

4.3.1 Contour Plots for Normalized Fiber Volume Fraction 74

4.3.2 Contour Plots for Normalized Void Volume Fraction 76

4.3.3 Contour Plots for Normalized Flexural Stiffness 79

4.3.4 Contour Plots for Normalized Flexural Strength 81

4.4 SUMMARY OF CONTOUR PLOT CHAPTER 84

PART B: HYDRAULIC FLUID CONTAMINATION EFFECTS 85

CHAPTER 5: HYDRAULIC FLUID ABSORPTION BEHAVIOR OF AEROSPACE-GRADE LAMINATES: COUPLED EFFECT OF PREPREG HUMIDITY EXPOSURE AND FABRICATION PRESSURE 86

5.1 LITERATURE REVIEW OF MODELING TECHNIQUES FOR FLUID ABSORPTION IN COMPOSITE MATERIALS 86

5.2 EXPERIMENTAL PROCEDURE FOR LIQUID ABSORPTION STUDY 88

5.3 LONG-TERM HYDRAULIC FLUID ABSORPTION 89

5.3.1 Quartz/BMI (AQIII/BMI) Absorption 89

5.3.2 Quartz/Epoxy (AQIII/EX-1522) Absorption 92

5.3.3 Carbon/Epoxy (IM7/EX-1522) Absorption 93

5.4 FOUNDATION FOR APPLYING THE HINDERED DIFFUSION MODEL TO HYDRAULIC FLUID ABSORPTION 95

5.5 HINDERED DIFFUSION MODEL PREDICTION 98

5.5.1 Quartz/BMI (AQIII/BMI) Absorption Model and Equilibrium Fluid Content 98

5.5.2 Quartz/Epoxy (AQIII/EX-1522) Absorption Model and Equilibrium Fluid Content 101

5.5.3 Carbon/Epoxy (IM7/EX-1522) Absorption Model and Equilibrium Fluid Content 103

5.6 COMPARISON OF EQUILIBRIUM FLUID CONTENT FOR QUARTZ-REINFORCED LAMINATES 105

5.6.1 Effect of Humidity Exposure on Equilibrium Fluid Content 105

5.6.2 Effect of Fabrication Pressure on Equilibrium Fluid Content 107

5.7 SUMMARY OF LIQUID ABSORPTION BEHAVIOR CHAPTER 108

CHAPTER 6: THE EFFECT OF LONG-TERM HYDRAULIC FLUID CONTAMINATION ON FLEXURAL PROPERTIES FOR QUARTZ-REINFORCED LAMINATES 110

6.1 EXPERIMENTAL PROCEDURE FOR HYDRAULIC FLUID ABSORPTION OF QUARTZ-REINFORCED FLEXURAL SPECIMENS 111

6.2 HYDRAULIC FLUID ABSORPTION FOR QUARTZ-REINFORCED LAMINATES 113

6.2.1 Long-term Hydraulic Fluid Absorption for Quartz/BMI (AQIII/BMI) Flexural Specimens 113

6.2.2 Long-term Hydraulic Fluid Absorption for Quartz/Epoxy (AQIII/EX-1522) Flexural Specimens 115

6.3 EVALUATION OF HYDRAULIC FLUID CONTAMINATION ON LAMINATE FLEXURAL PROPERTY 117

6.3.1 Effect of Humidity Exposure, Processing Pressure, and Hydraulic Fluid on Laminate Flexural Stiffness 117

6.3.2 Effect of Humidity Exposure, Processing Pressure, and Hydraulic Fluid on Laminate Flexural Strength 118

6.4 PERCENT REDUCTION OF FLEXURAL PROPERTIES DUE TO LONG-TERM HYDRAULIC FLUID CONTAMINATION 121

6.4.1 Effect of Prepreg Humidity Exposure on Flexural Stiffness Percent Reduction 121

6.4.2 Effect of Fabrication Pressure on Flexural Stiffness Percent Reduction .. 122

6.4.3 Effect of Prepreg Humidity Exposure on Flexural Strength Percent Reduction 123

6.4.4 Effect of Fabrication Pressure on Flexural Strength Percent Reduction 124

6.5 CONTRIBUTION OF EQUILIBRIUM FLUID CONTENT ON FLEXURAL PROPERTIES OF QUARTZ-REINFORCED LAMINATES 125

6.5.1 Effect of Equilibrium Fluid Content on Flexural Stiffness Percent Reduction 125

6.5.2 Effect of Equilibrium Fluid Content on Flexural Strength Percent Reduction 127

6.6 SUMMARY OF HYDRAULIC FLUID CONTAMINATION EFFECT ON LAMINATE FLEXURAL PROPERTIES CHAPTER 129

CHAPTER 7: CONCLUDING REMARKS AND RECOMMENDATIONS 131

7.1 SUMMARY OF DISSERTATION 131

7.2 ADDRESSING RESEARCH OBJECTIVE 1 145

7.2.1 Limitations and Future Work Associated with Research Objective 1 148

7.3 ADDRESSING RESEARCH OBJECTIVE 2 149

7.3.1 Limitations and Future Work Associated with Research Objective 2 154

7.4 ADDRESSING RESEARCH OBJECTIVE 3 155

7.4.1 Limitations and Future Work Associated with Research Objective 3 157

REFERENCES 159

APPENDIX A: SPECIMEN AVERAGES FOR PROPERTY FUNCTIONS 165

LIST OF TABLES

TABLE 2.1 PRODUCT SPECIFICATIONS FOR PREPREG MATERIALS 11

TABLE 2.2 PREPREG MOISTURE CONTENT AFTER 24 HOURS EXPOSURE IN ENVIRONMENTAL CHAMBER FOR VARYING LEVELS OF RELATIVE HUMIDITY EXPOSURE. INTERVALS ASSOCIATED WITH 95% CONFIDENCE FOR N=5 SAMPLES 13

TABLE 2.3 MODEL OF BEST FIT TREND LINE FOR PREPREG MOISTURE CONTENT AFTER 24 HOURS 14

TABLE 2.4 MODEL OF BEST FIT TREND LINE FOR LAMINATE THICKNESS 18

TABLE 2.5 SPECIMEN ALLOCATION AND DIMENSIONS USED FOR EACH RESEARCH TASK. NOTE: SPECIMEN QUANTITIES ARE FOR A SINGLE LAMINATE (I.E. ONE HUMIDITY EXPOSURE AND ONE CURE PRESSURE) 20

TABLE 2.6 TREND LINE EQUATIONS FOR PREPREG HUMIDITY CONDITIONING EFFECT ON LAMINATE FIBER VOLUME FRACTION 32

TABLE 2.7 TREND LINE EQUATIONS FOR FABRICATION PRESSURE EFFECT ON LAMINATE FIBER VOLUME FRACTION 35

TABLE 2.8 TREND LINE EQUATIONS FOR PREPREG HUMIDITY CONDITIONING EFFECT ON VOID VOLUME FRACTION 38

TABLE 2.9 TREND LINE EQUATIONS FOR FABRICATION PRESSURE EFFECT ON VOID VOLUME FRACTION 40

TABLE 3.1 TREND LINE EQUATIONS FOR PREPREG HUMIDITY CONDITIONING EFFECT ON FLEXURAL STIFFNESS 61

TABLE 3.2 TREND LINE EQUATIONS FOR FABRICATION PRESSURE EFFECT ON FLEXURAL STIFFNESS 64

TABLE 3.3 TREND LINE EQUATIONS FOR PREPREG HUMIDITY CONDITIONING EFFECT ON FLEXURAL STRENGTH 67

TABLE 3.4 TREND LINE EQUATIONS FOR FABRICATION PRESSURE EFFECT ON FLEXURAL STRENGTH 70

TABLE 5.1 EQUILIBRIUM FLUID CONTENT FOR AQIII/BMI HYDRAULIC FLUID ABSORPTION 100

TABLE 5.2 EQUILIBRIUM FLUID CONTENT FOR AQIII/EX-1522 HYDRAULIC FLUID ABSORPTION 102

TABLE 5.3 EQUILIBRIUM FLUID CONTENT FOR IM7/EX-1522 HYDRAULIC FLUID ABSORPTION 104

TABLE 5.4 TREND LINE EQUATIONS FOR EFFECT OF HUMIDITY EXPOSURE ON EQUILIBRIUM FLUID CONTENT OF QUARTZ-REINFORCED LAMINATES 106

TABLE 5.5 TREND LINE EQUATIONS FOR EFFECT OF FABRICATION PRESSURE ON EQUILIBRIUM FLUID CONTENT OF QUARTZ-REINFORCED LAMINATES 108

TABLE A.1 AVERAGE FIBER VOLUME FRACTION AND 95% CONFIDENCE INTERVAL FOR THE THREE PREPREG MATERIALS 165

TABLE A.2 AVERAGE VOID CONTENT AND 95% CONFIDENCE INTERVAL FOR THREE COMPOSITE PREPREG MATERIALS 166

TABLE A.3 AVERAGE FLEXURAL STIFFNESS AND 95% CONFIDENCE INTERVAL FOR THE THREE COMPOSITE PREPREG MATERIALS 167

TABLE A.4 AVERAGE FLEXURAL STRENGTH AND 95% CONFIDENCE INTERVAL FOR THREE COMPOSITE PREPREG MATERIALS 168

TABLE A.5 AVERAGE FLEXURAL STIFFNESS FOR HYDRAULIC FLUID CONTAMINATED SPECIMENS AND 95% CONFIDENCE INTERVAL FOR TWO QUARTZ-REINFORCED PREPREGS. PERCENT REDUCTION DETERMINED FROM DRY FLEXURAL RESULTS 169

TABLE A.6 AVERAGE FLEXURAL STRENGTH FOR HYDRAULIC FLUID CONTAMINATED SPECIMENS AND 95% CONFIDENCE INTERVAL FOR TWO QUARTZ-REINFORCED PREPREGS. PERCENT REDUCTION DETERMINED FROM DRY FLEXURAL RESULTS 170

LIST OF FIGURES

FIGURE 2.1 REPRESENTATIVE QUARTZ/BMI PREPREG SHEET PRIOR TO CONDITIONING PROCEDURE 10

FIGURE 2.2 THERMOTRON 8200 ENVIRONMENTAL CHAMBER USED FOR CONDITIONING PREPREG SHEETS AT VARYING RELATIVE HUMIDITY LEVELS 12

FIGURE 2.3 PREPREG MOISTURE CONTENT AFTER 24 HOUR EXPOSURE FOR VARYING RELATIVE HUMIDITY CONDITIONING LEVELS FOR THE (A) BMI RESIN AND (B) EPOXY RESIN PREPREGS. THE MODEL OF BEST FIT FOR EACH TREND LINE IS PROVIDED IN TABLE 2.3. INTERVALS ASSOCIATED WITH 95% CONFIDENCE FOR N=5 SAMPLES 14

FIGURE 2.4 CARVER HOT PRESS USED FOR FABRICATING LAMINATES FROM CONDITIONED PREPREGS 16

FIGURE 2.5 MANUFACTURER SUGGESTED TEMPERATURE CURE CYCLE FOR (A) BMI PREPREG MATERIAL AND (B) EPOXY PREPREG MATERIAL 16

FIGURE 2.6 LAMINATE THICKNESS FOR VARYING FABRICATION PRESSURES FOR EACH PREPREG MATERIAL 17

FIGURE 2.7 FINISHED QUARTZ/BMI LAMINATE THAT IS REPRESENTATIVE OF OTHER LAMINATES IN STUDY 18

FIGURE 2.8 LOCATION AND SPECIMEN ALLOCATION FOR EACH RESEARCH TASK 21

FIGURE 2.9 AVERAGE FIBER VOLUME FRACTION AS PREPREG MOISTURE CONTENT (M_P) AND FABRICATION PRESSURE CHANGED FOR (A) QUARTZ/BMI, (B) QUARTZ/EPOXY, AND (C) CARBON/EPOXY. ERROR BARS ARE ASSOCIATED WITH 95% CONFIDENCE FOR N=8 SAMPLES 26

FIGURE 2.10 AVERAGE VOID FRACTION AS PREPREG MOISTURE CONTENT (M_{PP}) AND FABRICATION PRESSURE CHANGED FOR (A) QUARTZ/BMI, (B) QUARTZ/EPOXY, AND (C) CARBON/EPOXY. ERROR BARS ARE ASSOCIATED WITH 95% CONFIDENCE FOR N=8 SAMPLES 29

FIGURE 2.11 EFFECT OF VARYING PREPREG HUMIDITY CONDITIONING ON LAMINATE FIBER VOLUME FRACTION FOR (A) QUARTZ/EPOXY, (B) QUARTZ/BMI, AND (C) CARBON/EPOXY 31

FIGURE 2.12 EFFECT OF VARYING FABRICATION PRESSURE ON LAMINATE FIBER VOLUME FRACTION FOR (A) QUARTZ/EPOXY, (B) QUARTZ/BMI, AND (C) CARBON/EPOXY PREPREGS 34

FIGURE 2.13 EFFECT OF VARYING PREPREG HUMIDITY CONDITIONING ON VOID VOLUME FRACTION FOR (A) QUARTZ/EPOXY, (B) QUARTZ/BMI, AND (C) CARBON/EPOXY ... 37

FIGURE 2.14 EFFECT OF VARYING FABRICATION PRESSURE ON VOID VOLUME FRACTION FOR (A) QUARTZ/EPOXY, (B) QUARTZ/BMI, AND (C) CARBON/EPOXY 39

FIGURE 2.15 SEM IMAGES OF QUARTZ/BMI LAMINATES FABRICATED FROM PREPREGS CONDITIONED AT 2% RELATIVE HUMIDITY AND CURED AT A) 69 KPA, B) 207 KPA, C) 345 KPA, AND D) 483 KPA 41

FIGURE 2.16 SEM IMAGES OF QUARTZ/BMI LAMINATES FABRICATED AT 483 KPA FROM PREPREGS CONDITIONED AT A) 2% RELATIVE HUMIDITY, B) 40% RELATIVE HUMIDITY, C) 70% RELATIVE HUMIDITY, AND D) 99% RELATIVE HUMIDITY 43

FIGURE 2.17 SEM IMAGES OF QUARTZ/EPOXY LAMINATES FABRICATED FROM PREPREGS CONDITIONED AT 2% RELATIVE HUMIDITY AND CURED AT A) 69 KPA, B) 207 KPA, C) 345 KPA, AND D) 483 KPA 44

FIGURE 2.18 SEM IMAGES OF QUARTZ/EPOXY LAMINATES FABRICATED AT 483 KPA FROM PREPREGS CONDITIONED AT A) 2% RELATIVE HUMIDITY, B) 40% RELATIVE HUMIDITY, C) 70% RELATIVE HUMIDITY, AND D) 99% RELATIVE HUMIDITY 45

FIGURE 2.19 SEM IMAGES OF CARBON/EPOXY LAMINATES FABRICATED FROM PREPREGS CONDITIONED AT 2% RELATIVE HUMIDITY AND CURED AT A) 69 KPA, B) 207 KPA, C) 345 KPA, AND D) 483 KPA 46

FIGURE 2.20 SEM IMAGES OF CARBON/EPOXY LAMINATES FABRICATED AT 483 KPA FROM PREPREGS CONDITIONED AT A) 2% RELATIVE HUMIDITY, B) 40% RELATIVE HUMIDITY, C) 70% RELATIVE HUMIDITY, AND D) 99% RELATIVE HUMIDITY 47

FIGURE 3.1 AVERAGE FLEXURAL STIFFNESS FOR VARYING PREPREG HUMIDITY CONDITIONING AND FABRICATION PRESSURE FOR (A) QUARTZ/BMI, (B) QUARTZ/EPOXY, AND (C) CARBON/EPOXY. ERROR BARS ARE ASSOCIATED WITH 95% CONFIDENCE FOR N=6 SAMPLES 56

FIGURE 3.2 AVERAGE FLEXURAL STRENGTH FOR VARYING PREPREG HUMIDITY CONDITIONING AND FABRICATION PRESSURE FOR (A) QUARTZ/BMI, (B) QUARTZ/EPOXY, AND (C) CARBON/EPOXY. ERROR BARS ARE ASSOCIATED WITH 95% CONFIDENCE FOR N=6 SAMPLES 58

FIGURE 3.3 EFFECT OF PREPREG HUMIDITY EXPOSURE ON THE FLEXURAL STIFFNESS FOR (A) QUARTZ/EPOXY, (B) QUARTZ/BMI, AND (C) CARBON/EPOXY LAMINATES 60

FIGURE 3.4 EFFECT OF FABRICATION PRESSURE ON THE FLEXURAL STIFFNESS FOR (A) QUARTZ/EPOXY, (B) QUARTZ/BMI, AND (C) CARBON/EPOXY 63

FIGURE 3.5 EFFECT OF PREPREG HUMIDITY EXPOSURE ON THE FLEXURAL STRENGTH FOR (A) QUARTZ/EPOXY, (B) QUARTZ/BMI, AND (C) CARBON/EPOXY 66

FIGURE 3.6 EFFECT OF FABRICATION PRESSURE ON THE FLEXURAL STRENGTH FOR (A) QUARTZ/EPOXY, (B) QUARTZ/BMI, AND (C) CARBON/EPOXY 69

FIGURE 4.1 COLORBAR SCALE USED FOR CONTOUR PLOTS OF NORMALIZED PROPERTY FUNCTION VALUES 73

FIGURE 4.2 CONTOUR PLOTS OF NORMALIZED FIBER VOLUME FRACTION FOR (A) QUARTZ/EPOXY, (B) QUARTZ/BMI, AND (C) CARBON/EPOXY 76

FIGURE 4.3 CONTOUR PLOTS OF NORMALIZED VOID VOLUME FRACTION FOR (A) QUARTZ/EPOXY, (B) QUARTZ/BMI, AND (C) CARBON/EPOXY 78

FIGURE 4.4 CONTOUR PLOTS OF NORMALIZED FLEXURAL STIFFNESS FOR (A) QUARTZ/EPOXY, (B) QUARTZ/BMI, AND (C) CARBON/EPOXY 81

FIGURE 4.5 CONTOUR PLOTS OF NORMALIZED FLEXURAL STRENGTH FOR (A) QUARTZ/EPOXY, (B) QUARTZ/BMI, AND (C) CARBON/EPOXY 83

FIGURE 5.1 THERMO SCIENTIFIC CONSTANT TEMPERATURE WATER BATH USED FOR HYDRAULIC FLUID ABSORPTION OF COMPOSITE LAMINATES 88

FIGURE 5.2 LONG-TERM (24 MONTHS) HYDRAULIC FLUID ABSORPTION FOR CONDITIONED AQIII/BMI PREPREGS CURED AT FABRICATION PRESSURES OF (A) 69 KPA, (B) 207 KPA, (C) 345 KPA, AND (D) 483 KPA. ERROR BARS ASSOCIATED WITH 95% CONFIDENCE FOR N=6 SAMPLES 91

FIGURE 5.3 LONG-TERM (24 MONTHS) HYDRAULIC FLUID ABSORPTION FOR CONDITIONED AQIII/EX1522 PREPREGS CURED AT FABRICATION PRESSURES AT (A) 69 KPA, (B) 207 KPA, (C) 345 KPA, AND (D) 483 KPA. ERROR BARS ASSOCIATED WITH 95% CONFIDENCE FOR N=6 SAMPLES 93

FIGURE 5.4 LONG-TERM (18 MONTHS) HYDRAULIC FLUID ABSORPTION FOR CONDITIONED IM7/EX1522 PREPREGS CURED AT FABRICATION PRESSURES OF (A) 69 KPA, (B) 207 KPA, (C) 345 KPA, AND (D) 483 KPA. ERROR BARS ASSOCIATED WITH 95% CONFIDENCE FOR N=6 SAMPLES 95

FIGURE 5.5 FIVE-YEAR HINDERED DIFFUSION MODEL PREDICTION FOR CONDITIONED AQIII/BMI PREPREGS CURED AT FABRICATION PRESSURES OF (A) 69 KPA, (B) 207 KPA, (C) 345 KPA, AND (D) 483 KPA 100

FIGURE 5.6 FIVE-YEAR HINDERED DIFFUSION MODEL PREDICTION FOR CONDITIONED AQIII/EX-1522 PREPREGS CURED AT FABRICATION PRESSURES OF (A) 69 KPA, (B) 207 KPA, (C) 345 KPA, AND (D) 483 KPA 102

FIGURE 5.7 FIVE-YEAR HINDERED DIFFUSION MODEL PREDICTION FOR CONDITIONED IM7/EX-1522 PREPREGS CURED AT FABRICATION PRESSURES OF (A) 69 KPA, (B) 207 KPA, (C) 345 KPA, (D) 483 KPA 104

FIGURE 5.8 EFFECT OF HUMIDITY EXPOSURE ON EQUILIBRIUM FLUID CONTENT FOR QUARTZ-REINFORCED (AQIII) LAMINATES WITH EITHER (A) BMI RESIN OR (B) EX-1522 EPOXY RESIN 106

FIGURE 5.9 EFFECT OF FABRICATION CURE PRESSURE ON EQUILIBRIUM FLUID CONTENT FOR QUARTZ-REINFORCED (AQIII) LAMINATES WITH EITHER (A) BMI RESIN OR (B) EX-1522 EPOXY RESIN 108

FIGURE 6.1 LONG-TERM (21 MONTHS) HYDRAULIC FLUID ABSORPTION FOR FLEXURAL SPECIMENS OF CONDITIONED AQIII/BMI PREPREGS CURED AT FABRICATION PRESSURES OF (A) 69 KPA, (B) 207 KPA, (C) 345 KPA, AND (D) 483 KPA. ERROR BARS ASSOCIATED WITH 95% CONFIDENCE FOR N=6 SAMPLES 114

FIGURE 6.2 LONG-TERM (21 MONTHS) HYDRAULIC FLUID ABSORPTION FOR FLEXURAL SPECIMENS OF CONDITIONED AQIII/EX-1522 PREPREGS CURED AT FABRICATION PRESSURES OF (A) 69 KPA, (B) 207 KPA, (C) 345 KPA, AND (D) 483 KPA. ERROR BARS ASSOCIATED WITH 95% CONFIDENCE FOR N=6 SAMPLES 116

FIGURE 6.3 EFFECT OF LONG-TERM (21 MONTHS) HYDRAULIC FLUID CONTAMINATION ON FLEXURAL STIFFNESS FOR QUARTZ-REINFORCED LAMINATES WITH EITHER (A) BMI RESIN OR (B) EX-1522 EPOXY RESIN. ERROR BARS ARE ASSOCIATED WITH 95% CONFIDENCE FOR N=6 SAMPLES 118

FIGURE 6.4 EFFECT OF LONG-TERM (21 MONTHS) HYDRAULIC FLUID CONTAMINATION ON FLEXURAL STRENGTH FOR QUARTZ-REINFORCED LAMINATES WITH EITHER (A) BMI RESIN OR (B) EX-1522 EPOXY RESIN. ERROR BARS ARE ASSOCIATED WITH 95% CONFIDENCE FOR N=6 SAMPLES 120

FIGURE 6.5 EFFECT OF PREPREG HUMIDITY EXPOSURE ON THE FLEXURAL STIFFNESS PERCENT REDUCTION FOR (A) QUARTZ/BMI, AND (B) QUARTZ/EX-1522 EPOXY .. 122

FIGURE 6.6 EFFECT OF FABRICATION PRESSURE ON THE FLEXURAL STIFFNESS PERCENT REDUCTION FOR (A) QUARTZ/BMI, AND (B) QUARTZ/EX-1522 EPOXY 123

FIGURE 6.7 EFFECT OF PREPREG HUMIDITY EXPOSURE ON THE FLEXURAL STRENGTH PERCENT REDUCTION FOR (A) QUARTZ/BMI, AND (B) QUARTZ/EX-1522 EPOXY .. 124

FIGURE 6.8 EFFECT OF FABRICATION CURE PRESSURE ON THE FLEXURAL STRENGTH PERCENT REDUCTION FOR (A) QUARTZ/BMI, AND (B) QUARTZ/EX-1522 EPOXY .. 125

FIGURE 6.9 COMPARISON OF HUMIDITY EXPOSURE AND HYDRAULIC FLUID CONTENT ON THE FLEXURAL STIFFNESS PERCENT REDUCTION FOR (A) QUARTZ/BMI, AND (B) QUARTZ/EX-1522 EPOXY 126

FIGURE 6.10 COMPARISON OF FABRICATION PRESSURE AND HYDRAULIC FLUID CONTENT ON THE FLEXURAL STIFFNESS PERCENT REDUCTION FOR (A) QUARTZ/BMI, AND (B) QUARTZ/EX-1522 EPOXY 127

FIGURE 6.11 COMPARISON OF HUMIDITY EXPOSURE AND HYDRAULIC FLUID CONTENT ON THE FLEXURAL STRENGTH PERCENT REDUCTION FOR (A) QUARTZ/BMI, AND (B) QUARTZ/EX-1522 EPOXY 128

FIGURE 6.12 COMPARISON OF FABRICATION PRESSURE AND HYDRAULIC FLUID CONTENT ON THE FLEXURAL STRENGTH PERCENT REDUCTION FOR (A) QUARTZ/BMI, AND (B) QUARTZ/EX-1522 EPOXY 129

ABSTRACT

Research and technological enhancements over the past several decades have yielded vast improvements in the area of fabricating high quality composite laminates. Process-induced defects, such as microvoids, however remain a critical concern and are often formed by multiple variables simultaneously. The research presented in this dissertation examines two such processing conditions, the moisture content of prepreg sheets prior to laminate fabrication, and the cure pressure. In particular, the coupled and synergistic effects of these two processing conditions on the laminate microstructure, mechanical properties, and the laminates' propensity to absorb liquid contaminants are investigated. With regards to the prepreg moisture content, changes in humidity levels of storage conditions or the fabrication environment can alter the overall prepreg moisture content, which in turn affects the formation of microvoids during laminate cure. Additionally, the fabrication pressure also play a critical role in the formation of voids, fiber volume fraction, and mechanical performance of composite laminates. Three high-performance commercial prepregs, including quartz/Bismaleimide, quartz/epoxy, and carbon/epoxy, that are commonly used in aerospace applications were included in this research study.

To alter the moisture content of composite prepregs, prepreg sheets were exposed to four different relative humidity levels of 2%, 40%, 70%, or 99%. The conditioned prepreg sheets were then subsequently used to fabricate eight-ply laminates cured at four different cure pressures of 68.9, 206.8, 344.7, or 482.6 kPa. This procedure resulted in 16 unique laminates for each prepreg system, thus yielding a number of laminates with a wide range of process-induced void fractions at a particular fiber volume fraction. Property functions were illustrated as contour plots and used to analyze the coupled

effect of prepreg moisture content and fabrication pressure on the resulting fiber volume fraction, void volume fraction, flexural stiffness, and flexural strength for the three prepreg materials. For all three prepregs, the fiber volume fraction and flexural stiffness was primarily dependent on the fabrication pressure, whereas flexural strength and void volume fraction exhibited more complex and coupled dependency on both the cure pressure and prepreg moisture content. Higher local gradients of the property contour plots at lower fabrication pressures indicated stronger dependency and fluctuations of the laminate properties, such as fiber volume fraction, void volume fraction, and flexure properties due to changes in prepreg moisture content and fabrication pressure.

It is well known that liquid contamination is detrimental to composite laminates as the contamination commonly causes irreversible damage. Water absorption remains the most common type of liquid contamination for composite materials. However, the aerospace-grade composite prepregs are frequently used in structures subjected to a variety of liquid contaminants, including hydraulic fluids. Additionally, changes in the laminate fiber volume fraction and void volume fraction contribute to the composite laminates varying propensity to absorb liquid penetrants. The level of fluid saturation, or equilibrium fluid content, due to variations in the prepreg moisture and fabrication pressure was analyzed for the three commercial aerospace-grade prepregs.

Quartz-reinforced and carbon fiber-reinforced laminate specimens were fully immersed in an aerospace-grade hydraulic fluid for a period of 24 months and 18 months, respectively. Generally, the equilibrium fluid content decreased as relative humidity decreased and fabrication pressure increased. However, each prepreg material had unique absorption behaviors and uptake profiles. Finally, the effect of long-term

hydraulic fluid contamination on the flexural stiffness and flexural strength of quartz-reinforced laminates (BMI and epoxy) was discussed. Both matrix materials (i.e., BMI and epoxy) were fairly resilient to long-term hydraulic fluid contamination, in that the flexural properties were reduced by no more than 15% after nearly two years of hydraulic fluid contamination.

CHAPTER 1

INTRODUCTION AND OVERVIEW

1.1 EFFECT OF PROCESS-INDUCED DEFECTS ON HIGH-PERFORMANCE COMPOSITE MATERIALS

Process-induced defects of composite laminates are often complex in nature and can have a detrimental and varying effect on the laminates. Two variables that drive process-induced defects, such as microvoids, that will be examined in this research include 1) the moisture content present in composite prepregs prior to laminate cure, and 2) the applied cure pressure used to fabricate laminates. Numerous operational procedures can be utilized so as to minimize process-induced defects. First, prepregs stored and manufactured in a dry environment will limit the prepreg moisture level. Another operational procedure is utilizing fabrication methods with a substantially high cure pressure so as to expel volatiles during the curing process. However maintaining such restrictive requirements on the laminate fabrication procedure can often be impractical due to a variety of reasons, such as financial implications, equipment capability, or product needs.

Storing prepregs in a vacuum-sealed barrier and low temperature environment often minimizes the moisture content of composite prepregs. However, the prepreg moisture content can vary due to changes in the ambient humidity of the storage or fabrication environment. Because components fabricated using prepregs are cured at high temperatures, any moisture within the prepreg sheets vaporize during the curing process

and can result in the formation of microvoids. This is particularly true for fabrication methods utilizing low cure pressures or without vacuum-assistance, as laminates produced under these scenarios are more susceptible to remaining volatiles, such as microvoids. Additionally, the fabrication pressure can have a significant effect on the laminate fiber volume fraction and mechanical properties.

Composite structures are being implemented into new and diverse products as technology improves. Examples of structural components for aerospace include fuselages, spars, and airfoil supports. Composite materials are also being utilized at an increasing rate for a variety of applications in the oil/gas and electronics industries. In addition to the structural components, composites are being used in many non-structural applications due to their customization and lightweight potential, such as engine cowlings, panels, and radomes. Understandably, structural components commonly have stringent requirements on the laminate microstructure and minimal void formation. Non-structural components, on the other hand, can have flexibility in the manufacturing process by utilizing less costly, low-pressure methods such as vacuum-bagging or heated compression. Low-pressure fabrication methods may increase variability of the laminate microstructure, but they have the significant benefit of reduced production costs when compared to higher-pressure fabrication alternatives, such as autoclave cure [1]. Low-pressure fabrication methods are also more susceptible to higher void fraction due to possible presence of moisture absorbed by the prepregs before cure [2]. The relative humidity environment of prepregs in storage or during the lay-up process can contribute to the increased prepreg moisture content. The local humidity environment may not be actively monitored or controlled at composite manufacturing facilities.

Additionally, composite materials are increasingly being utilized in systems that require a long service-life with minimal repair and maintenance downtime. Therefore, it is becoming increasingly important to accurately characterize the effect of process-induced defects and degradation, such as microvoids and liquid contamination.

High-performance composite materials are typically used in a variety of aerospace and space structures, including radomes, antenna reflectors, and low observable radar transparent structures. Bismaleimide (BMI) resin with Quartz (AQ581) fiber reinforcement is one such high-performance composite material that was developed to overcome existing limitations for use on complex structures and ducting in advanced military aircraft, helicopters, and many high temperature applications. Quartz/BMI has a high glass transition temperature, with superior burn characteristics and excellent electrical properties, making it an ideal candidate for radomes and other electronic applications. Another high-performance composite material is EX-1522 epoxy resin system that has been reinforced with either quartz AQIII or carbon IM7 fibers. EX-1522 is a modified and toughened upgrade for high performance applications over traditional epoxy resin systems. This material displays both excellent mechanical and thermal properties, in addition to a low propensity to absorb moisture. EX-1522's has good electrical properties, making it a low cost option for radomes, antenna, and other critical electrical applications.

1.2 COMPOSITE DEGRADATION DUE TO ENVIRONMENTAL AND OPERATIONAL EFFECTS

As mentioned previously, composite materials are increasingly being implemented in products and structures that require a long service life with minimal downtime for repair or maintenance. Therefore, composite degradation due to long-term environmental exposure or routine operation must be considered. Environmental degradation can include ultraviolet radiation, thermo-oxidative degradation, and liquid absorption. Additionally, standard operational procedures can expose composites to a variety of liquid contaminants, such as moisture, oil, de-icing fluid, or hydraulic fluid. The deleterious effects of moisture absorption on fiber-reinforced epoxy laminates have been extensively studied for several decades [3-5]. Moisture in the form of high relative humidity environments, distilled liquid water exposure, or salt water to simulate ocean environments; make up a vast majority of past and current research focuses [3-9].

The characteristics of BMI are significantly different when compared to traditional epoxy-based materials. For aerospace applications, BMI is frequently exposed to liquid water contamination, as well as specialized liquids such as hydraulic fluid. Although not to the same extent as epoxy-based systems, moisture absorption of BMI resin systems have been addressed occasionally in literature [10-14]. This is most likely attributed to the relatively specialized nature of BMI when compared to the more general and broader appeal of epoxy-based polymer systems. Unlike water absorption, the long-term absorption effect of alternative working fluids on fiber-reinforced laminates has not been studied extensively. The most common research topics for

alternative fluids remain nearly exclusively on the effect of aerospace fluids [15], and crude oils [16] on the performance of epoxy-matrix systems.

Therefore, a focus of this research was to examine the effect of hydraulic fluid contamination on the performance of aerospace-grade composite structures. The hydraulic fluid selected (Castrol Brayco Micronic 881) is commonly used in aerospace applications and conforms to the military standard MIL-PRF-87257B. Castrol Brayco is a synthetic hydrocarbon base hydraulic fluid, and is characterized with a kinematic viscosity of 7.2 cSt, measured at 40°C, and a specific gravity of 0.84.

1.3 RESEARCH MOTIVATION

The research presented in this dissertation was formulated to address the following gaps identified in literature. First, was to examine the coupled effect of prepreg humidity exposure and fabrication pressure on the formation of microvoids and laminate mechanical properties. Although the effect of processing conditions on the formation of microvoids and mechanical properties have been studied extensively [2,17-19], a detailed study that independently varies the void volume fraction by varying the moisture in prepregs before cure and the fiber volume fraction by varying the fabrication pressure has not been reported. Second, was to examine the effect of long-term hydraulic fluid contamination on the performance of aerospace-grade composite laminates. Addressing these gaps in a comprehensive way could be useful in the design or manufacturing stage and assist in understanding the effect of processing conditions and hydraulic fluid contamination on high-performance, aerospace-grade composites. Therefore, the following research objectives were identified:

1. *Coupled effect of varying prepreg humidity exposure level and fabrication pressure on the laminate fiber volume fraction and void formation for aerospace-grade composite prepregs*
2. *In addition to fiber volume fraction and void volume fraction, effect of prepreg humidity exposure level and fabrication pressure on the laminate flexural stiffness, flexural strength, and hydraulic fluid absorption behavior*
3. *Effect of long-term hydraulic fluid contamination on the flexural properties of aerospace-grade composite laminates*

1.4 ORGANIZATION OF DISSERTATION

This dissertation will first introduce the material specifications for the three aerospace-grade commercial prepregs used in this study. Then the equipment and experimental procedure used to alter the prepreg moisture content via relative humidity exposure and laminate fabrication will be discussed. Two distinct focuses, or Parts, were identified to address the research objectives. The research focus for Part A was characterizing the effect of prepreg humidity exposure and fabrication pressure on the laminate microstructure and mechanical properties. Whereas the research focus for Part B was characterizing the absorption behavior due to long-term hydraulic fluid contamination and subsequent effect on flexural properties.

For Part A, the coupled effect of varying relative humidity exposure and fabrication pressure on the laminate fiber volume fraction and void formation will be discussed in Chapter 2. The size and spatial distribution of voids within the laminates were examined using a Scanning Electron Microscope (SEM). Similarly, the coupled effect of prepreg humidity exposure and fabrication pressure on the laminate flexural stiffness

and flexural strength is examined in Chapter 3. Chapter 4 will conclude research Part A with an examination of the prepreg humidity exposure and fabrication pressure on the laminate fiber volume fraction, void fraction, flexural stiffness, and flexural strength by using property functions and illustrated with contour plots.

For Part B, the coupled effect of varying relative humidity exposure and fabrication pressure on the propensity to absorb hydraulic fluid will be discussed in Chapter 5. Later, Chapter 6 will examine the long-term effect of hydraulic fluid contamination on the laminate flexural properties. Concluding remarks, research contributions, limitations, and future work recommendations will summarize this dissertation in Chapter 7.

PART A: CHARACTERIZATION OF COMPOSITE LAMINATES

Part A of the dissertation will focus on the characterization techniques and results for the three prepreg materials. First, the effect of varying prepreg humidity exposure and fabrication pressure on the laminate fiber volume fraction and void volume fraction will be discussed in Chapter 2. Analysis of the laminate microstructure was performed with (i) experimental methods, such as specimen suspension method or acid digestion, and (ii) visual inspection methods, such as scanning electron microscopy. In Chapter 3, the effect of varying prepreg humidity exposure and fabrication pressure on the laminate flexural stiffness and flexural strength, will be introduced. Finally, property functions that examine the coupled effect of relative humidity and fabrication pressure on the laminate fiber volume fraction, void volume fraction, flexural stiffness, and flexural strength will be introduced in Chapter 4.

Work related to this part of the Dissertation has been published in:

- "Coupled Effect of Prepreg Moisture Content and Fabrication Pressure on Microvoid Formation and Mechanical Properties of Composite Laminate", Manuscript under review (2017).
- "Effects of Processing Conditions on Mechanical Properties of Quartz/BMI Laminates", *American Society of Composites 30th Technical Conference,* (2015). East Lansing, MI, 1744.
- "The Coupled Effect of Microvoids and Hydraulic Fluid Absorption on Mechanical Properties of Quartz/BMI Laminates", *American Society of Composites 29th Technical Conference,* (2014). San Diego, CA, 226.
- "Processing Effects on Formation of Microvoids and Hydraulic Fluid Absorption of Quartz/BMI Laminates", *ASME International Mechanical Engineering Congress & Exposition,* (2015). Houston, TX, IMECE2015-53717.

CHAPTER 2

COUPLED EFFECT OF VARYING PREPREG HUMIDITY EXPOSURE AND FABRICATION PRESSURE ON LAMINATE MICROSTRUCTURE

Introduced in Section 1.1, two variables that can influence process-induced microvoid formation include 1) the moisture content of composite prepregs due to humidity exposure, and 2) the applied cure pressure used to fabricate laminates. The remainder of this Chapter will present the experimental method used to condition prepregs at varying humidity exposure levels and then the laminate cure procedure. The resulting laminate fiber volume fraction and void volume fraction will be analyzed i) experimentally by acid digestion and suspension methods and ii) visually using Scanning Electron Microscopy.

2.1 PREPREG MATERIAL OVERVIEW

This study involves three commercial prepregs that are commonly used in aerospace applications, which were presented in Section 1.1. First, is a Bismaleimide (BMI) resin manufactured by the Hexcel Corporation under the trade name HexPly® F650 with quartz style 581 reinforcement (Figure 2.1). Second, is an epoxy resin manufactured by TenCate® with the trade name EX-1522 that has been reinforced with quartz style 4581 fabric. Third, is the TenCate® EX-1522 epoxy resin with IM-7 carbon fiber plain

weave reinforcement. A summary of the material specifications for the three-prepreg systems is provided in Table 2.1.

It is important to note that high-performance composite materials such as these are commonly used in high pressure manufacturing procedures and may include a vacuum-bag to limit void growth and produce high quality laminates. However, lower-pressure fabrication methods can be utilized for some components. Additionally, the research objectives (Section 1.3) in this study require laminates with a variety of void levels at distinct fiber volume fractions. Therefore, prepreg sheets were exposed to varying relative humidity levels and subsequently cured with a heated compression mold without a vacuum-bag so as to artificially induce varying void contents independently of the laminate fiber volume fraction.

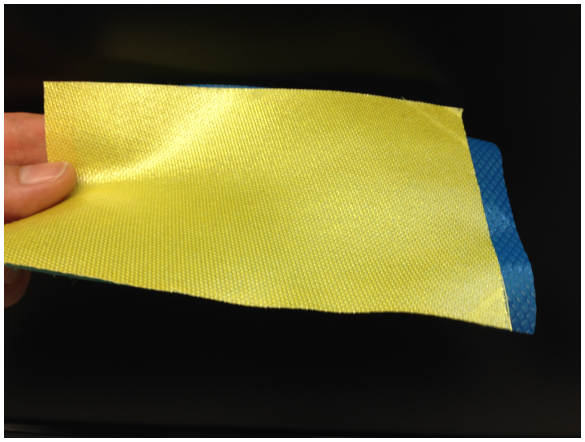

Figure 2.1 Representative quartz/BMI prepreg sheet prior to conditioning procedure

Table 2.1 Product specifications for prepreg materials

	Quartz / BMI	**Quartz / Epoxy**	**Carbon / Epoxy**
Supplier	Hexcel	TenCate	TenCate
Material Designation	F650	EX-1522	EX-1522
Matrix Type	BMI	Epoxy	Epoxy
Matrix Density (g/cc)	1.27	1.35	1.35
Fiber Type	AQIII (Quartz)	AQIII (Quartz)	IM-7 (Carbon)
Fiber Density (g/cc)	2.20	2.20	1.78
Fabric Weave Type	581	4581	Plain

2.2 PREPREG CONDITIONING AT VARYING RELATIVE HUMIDITY EXPOSURE LEVELS

2.2.1 Equipment Used and Experimental Procedure for Prepreg Conditioning

A wide range of void fractions at a specific laminate fiber volume fraction was required to address the research objectives posed in Section 1.3. Therefore, a procedure for conditioning prepreg sheets prior to laminate fabrication was developed that would artificially induce varying levels of prepreg moisture content and in turn induce varying void fractions in the finished laminate. In the context of this research study, prepreg conditioning is the procedure of exposing prepreg sheets at a specific relative humidity exposure level using a Thermotron 8200 environmental chamber (Figure 2.2). The prepreg sheets were conditioned at room temperature (25°C) for a period of 24 hours at the relative humidity set points of (i) 2%, (ii) 40%, (iii) 70%, or (iv) 99%. Prepreg sheets absorb moisture based on the humidity level, which in turn vaporizes during the heated cure process and generate microvoids. Therefore, prepreg moisture content

increases as humidity exposure increases. Subsequently, the void fraction of laminates increases as prepreg moisture content increases.

Figure 2.2 Thermotron 8200 environmental chamber used for conditioning prepreg sheets at varying relative humidity levels

2.2.2 Measuring Prepreg Moisture Content before Laminate Fabrication

A CompuTrac® Vapor Pro® moisture specific analyzer was used to measure the prepreg moisture content after prepreg conditioning. The resulting prepreg moisture content (wt.%) for the three-prepreg materials after an exposure period of 24 hours is provided in Table 2.2.

Table 2.2 Prepreg moisture content after 24 hours exposure in environmental chamber for varying levels of relative humidity exposure. Intervals associated with 95% confidence for n=5 samples

Relative Humidity (% RH)	Prepreg Moisture Content (wt%) after 24 Hours		
	Quartz / BMI	*Quartz / Epoxy*	*Carbon / Epoxy*
2%	0.076 ± 0.032	0.041 ± 0.020	0.043 ± 0.009
40%	0.160 ± 0.018	0.046 ± 0.014	0.070 ± 0.027
70%	0.323 ± 0.036	0.068 ± 0.010	0.083 ± 0.025
99%	0.569 ± 0.046	0.077 ± 0.008	0.121 ± 0.040

Figure 2.3 clearly illustrates the high sensitivity of the BMI resin prepregs to humidity exposure and highlights the importance of proper storage techniques. Even low levels of humidity exposure resulted in a significant amount of absorbed moisture for BMI. Alternatively, the two epoxy-based TenCate® EX-1522 prepregs were fairly resilient to a variety of humidity exposure levels. According to the TenCate® literature, EX-1522 epoxy material has been modified to restrict moisture absorption, which is clearly supported by the conditioning results. The rate of increase for the trend line equations, shown in Table 2.3, indicate that the moisture content for BMI prepregs increases at a rate approximately double that of the epoxy material.

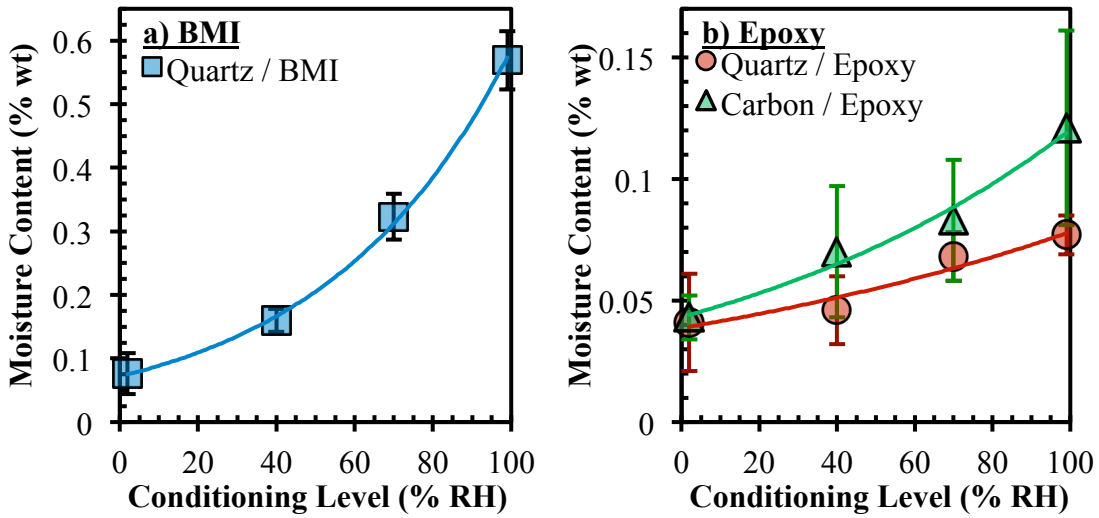

Figure 2.3 Prepreg moisture content after 24 hour exposure for varying relative humidity conditioning levels for the (a) BMI resin and (b) epoxy resin prepregs. The model of best fit for each trend line is provided in Table 2.3. Intervals associated with 95% confidence for n=5 samples

Table 2.3 Model of best fit trend line for prepreg moisture content after 24 hours

	Trend Line Fit	R^2-Value
Quartz/BMI	$0.0719e^{0.021x}$	0.9987
Quartz/Epoxy	$0.0387e^{0.007x}$	0.9315
Carbon/Epoxy	$0.0432e^{0.010x}$	0.9814

2.3 LAMINATE FABRICATION AT VARYING CURE PRESSURES

2.3.1 Equipment Used and Experimental Procedure for Laminate Fabrication

Laminates were fabricated at different applied cure pressures, which in turn would produce different fiber volume fractions. Therefore, a wide range of fiber volume fractions can be achieved simply by controlling the cure pressure. Opposed to varying other processing parameters, varying the cure pressure yields consistent and repeatable fiber volume fraction results. For example, varying the temperature cure cycle can also

have a significant effect on the laminate void volume fraction. Using the conditioned prepreg sheets, eight-ply laminates with a fiber orientation of $[0/90]_{2s}$ and approximate planar dimensions of 25.4 cm by 25.4 cm were fabricated using a Carver heated compression mold (Figure 2.4). Four cure pressures of i) 68.9 kPa (10 psi), ii) 206.8 kPa (30 psi), iii) 344.7 kPa (50 psi), and iv) 482.6 kPa (70 psi) were used along with the material supplier suggested temperature cure profile for each of the four-prepreg conditioning levels. Therefore for each prepreg material, a total of 16 unique laminates were fabricated from a combination of four prepreg conditioning levels and four fabrication pressures

The HexPly® BMI cure cycle, shown in Figure 2.5a, consists of the following procedure:

A. Apply fabrication pressure at room temperature
B. Increase temperature to 38°C at a ramp-rate of 3°C/min and hold for 30 minutes
C. Increase temperature to 191°C at a ramp-rate of 3°C/min
D. Maintain a four-hour isothermal hold at 191°C
E. Cool down to 66°C and remove the finished laminate from the press

Each BMI laminate was then post-cured for eight hours at 232°C in a two-step temperature increase ramp-rate of 6°C/min from ambient to 191°C, followed by a ramp-rate of 1.5°C/min from 191°C to 232°C.

Meanwhile, the TenCate® epoxy cure cycle, shown in Figure 2.5b, consists of the following procedure:

A. Apply fabrication pressure at room temperature
B. Increase temperature to 166°C at a ramp-rate of 3°C/min

C. Maintain a two-hour isothermal hold at 166°C

D. Cool down to 66°C and remove the finished laminate from the press

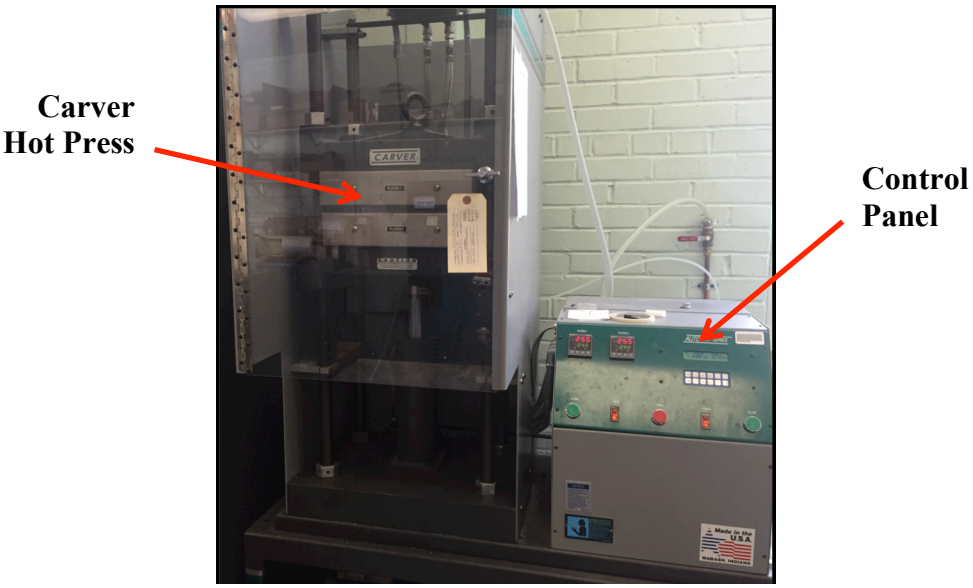

Figure 2.4 Carver hot press used for fabricating laminates from conditioned prepregs

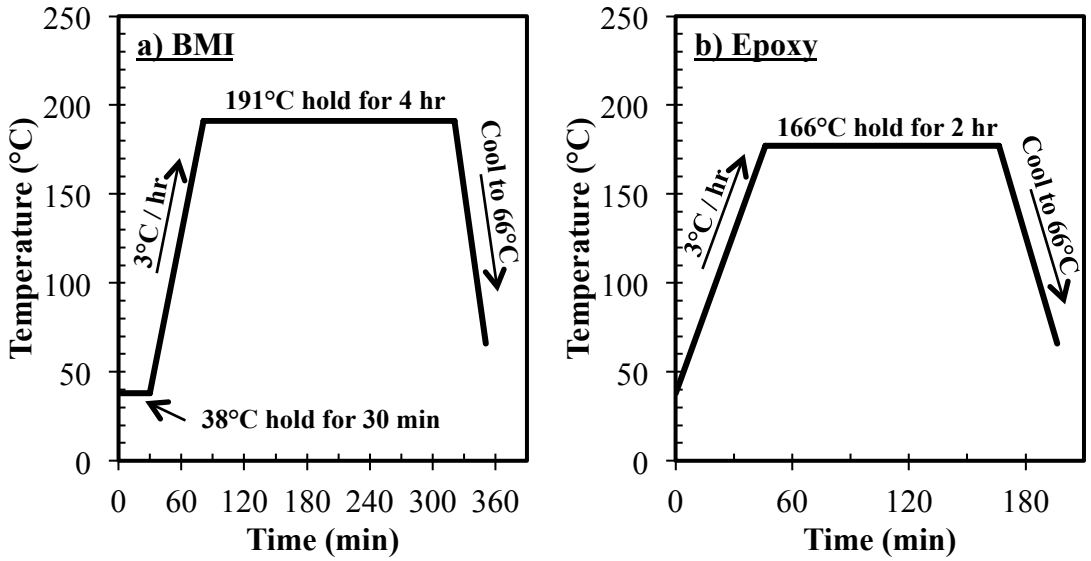

Figure 2.5 Manufacturer suggested temperature cure cycle for (a) BMI prepreg material and (b) epoxy prepreg material

2.3.2 Initial Assessment of Fabricated Laminate Thickness

The average laminate thickness for varying fabrication pressures is shown in Figure 2.6. The laminate thickness decreased for all three-prepreg materials, with the largest incremental decreases occurring at low initial fabrication pressures. The trend line fits shown in Table 2.4 indicate that both quartz-reinforced prepregs (BMI and Epoxy) have similar decaying slopes as the fabrication pressure increases. Additionally, the zero-intercept value is significantly higher when compared to the IM7 carbon-fiber fabric. This behavior was expected because the fiber diameter for the AQIII quartz fibers is nearly four times larger than the IM-7 carbon fiber reinforcement. After the initial thickness assessment was completed, each fabricated laminate, similar to the one shown in Figure 2.7, was categorized and prepared for specimen extraction to address the research objectives pertaining to laminate microstructure, flexural properties, and absorption behavior.

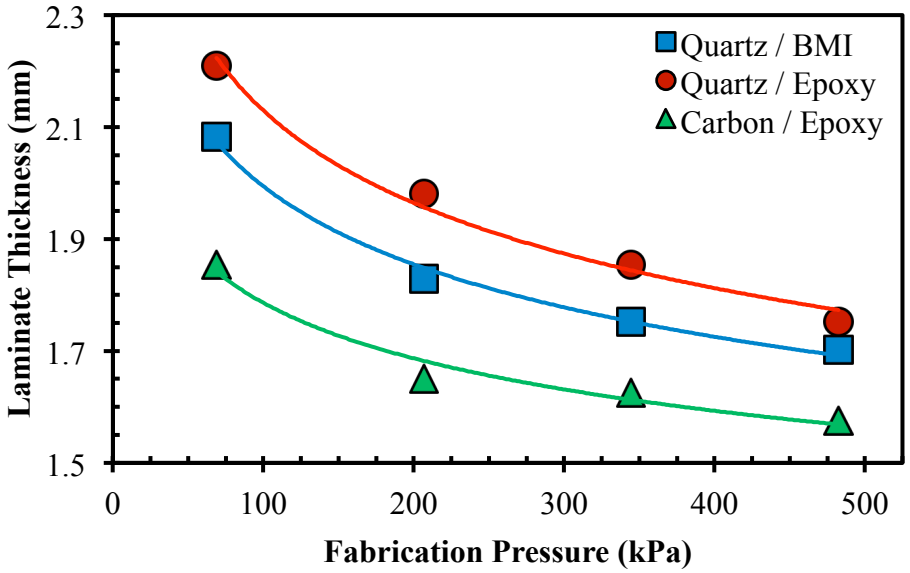

Figure 2.6 Laminate thickness for varying fabrication pressures for each prepreg material

Table 2.4 Model of best fit trend line for laminate thickness

	Trend Line Fit	R^2-Value
Quartz/BMI	$3.2258x^{-0.104}$	0.9929
Quartz/Epoxy	$3.6396x^{-0.116}$	0.9879
Carbon/Epoxy	$2.6111x^{-0.082}$	0.9689

Figure 2.7 Finished quartz/BMI laminate that is representative of other laminates in study

2.4 SPECIMEN PREPARATION AND ALLOCATION TO ADDRESS THE RESEARCH OBJECTIVES

Section 1.3 introduced three primary research objectives that were posed to investigate the coupled effect of varying prepreg humidity exposure and fabrication pressure on several laminate properties. In brevity, the research objectives were:

1. *Humidity exposure and fabrication pressure effects on laminate fiber volume fraction and void volume fraction*

2. *Humidity exposure and fabrication pressure effects on laminate flexural stiffness, flexural strength, and hydraulic fluid absorption*
3. *Effect of long-term hydraulic fluid contamination on flexural properties*

Several Research Tasks were developed to investigate the research objectives. Research Task 1 would be a complete characterization of the laminate microstructure for the three prepregs due to variations in the humidity exposure and fabrication pressure. Laminate fiber volume fractions and void volume fractions would be investigated on two distinct fronts. First, would be a comprehensive assessment of the fiber volume fraction and void volume fraction using experimental methods including specimen suspension, acid digestion, and pycnometer studies. Second, would be a visual inspection of the void shape and spatial distribution using images from scanning electron microscopy. Results from Research Task 1 would be used to address the first research objective. Research Task 2 would be an assessment of the laminate mechanical properties, specifically the flexural stiffness and flexural strength. Flexural specimens would be prepared and experimental testing performed in accordance with ASTM Standards for fiber-reinforced polymers. The first study for Task 2 would be an assessment of the laminates after fabrication. This study would serve as a comparative baseline for any future environmental degradation, i.e. hydraulic fluid contamination. The first study for Task 2 would be used to partially address the second research objective. The second study for Task 2 would be an assessment of the flexural performance after long-term hydraulic fluid contamination, which would be used to address the third research objective. Research Task 3 would be an investigation of the

long-term absorption behavior. The emphasis for this research task was investigating the effect of prepreg humidity exposure and fabrication pressure on the equilibrium fluid content. Results from Research Task 3, along with the aforementioned Research Task 2, will be used to address the second research objective.

Utilizing ASTM Standards and prior experience with experimental testing, the specimen allocations and dimensions shown in Table 2.5 were deemed appropriate for each Research Task.

Table 2.5 Specimen allocation and dimensions used for each Research Task. Note: Specimen quantities are for a single laminate (i.e. one humidity exposure and one cure pressure)

	Study	**Dimension** *(mm)*	**Quantity**
Task 1: Laminate Microstructure Characterization	Experimental analysis of fiber volume fraction and void fraction	57.2 x 12.7	8
	SEM image analysis	31.8 x 12.7	6
Task 2: Laminate Mechanical Property Assessment	Baseline flexural property analysis before degradation	57.2 x 12.7	6
	Flexural property analysis after long-term hydraulic fluid exposure	57.2 x 12.7	6
Task 3: Laminate Absorption Behavior	Long-term hydraulic fluid contamination	31.8 x 31.8	6

Therefore, a total of 32 specimens from each laminate were required to satisfy the Research Tasks. Randomization of the specimen location within the laminate is an important criterion to ensure that any local defects or variations would not significantly influence a specific research study. Therefore, no two samples from the same research study shared a common edge, i.e. at least one specimen from another research study separates two specimens from the same study. Additionally, each fabricated laminate

for each prepreg material had identical cut patterns. The global location for each specimen and study assignment is shown in Figure 2.8.

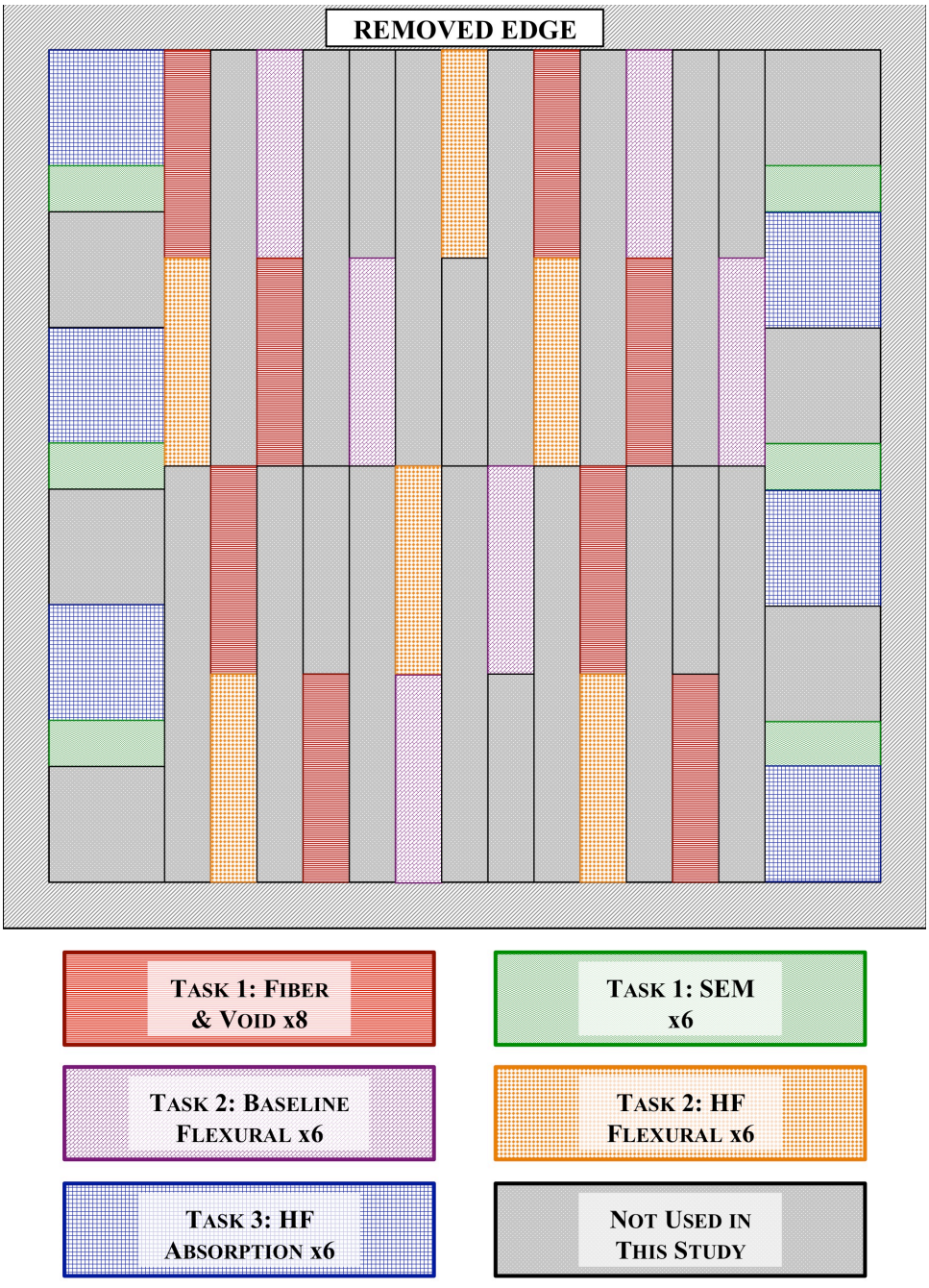

Figure 2.8 Location and specimen allocation for each Research Task

2.5 LAMINATE FIBER VOLUME FRACTION AND VOID VOLUME FRACTION

Process-induced microvoids remain one of the most common defects associated with composites, regardless of the laminate manufacturing technique. It is well known that microvoids have a deleterious effect on mechanical properties [1,2,20-23] and contribute to anomalous absorption behavior. Therefore, the void content of composite materials is often used to judge the quality of a finished product [22]. The average fiber volume fraction and void volume fraction presented in Section 2.5.2 was determined from specimens prepared and tested (i.e. specimen suspension, acid digestion) by Jacob P. Anderson.

2.5.1 Experimental Procedure to Determine Fiber Volume Fraction and Void Volume Fraction

As mentioned previously in Section 2.4, eight rectangular specimens with planar dimensions of 31.8 mm by 12.7 mm were cut from each laminate to determine the average void volume fraction (V_v) and fiber volume fraction (V_f). The experimental procedure involved a combination of specimen suspension-method and acid-digestion method outlined by ASTM D2734-09 and ASTM D3171-15, respectively. These procedures are reported by Anderson and Altan [1,2] to be capable of resolving microvoid contents to within ±0.22%. Acid digestion method was used as opposed to the resin burn-off method. Resin burn-off is not recommended for carbon fiber reinforcement as it may cause oxidation damage and lead to erroneous results. The acid digestion method was used for all prepreg materials to maintain consistency. The experimental procedure involves determining the density of the bulk composite (ρ_c) by

suspending each specimen in a Cargill Labs 2490 kg/m^3 Heavy Liquid and water solution. The density of the matrix solution (ρ_m) is similarly determined by suspending void-free matrix specimens in glycerol (1260 kg/m^3) diluted with water. Matrix specimens were ensured to be void-free through a visual inspection using an optical microscope at high resolution. A liquid pycnometer was then used to measure the density of the solution after sample suspension had been achieved. The density of the fiber reinforcement (ρ_f) was determined through the use of a helium pycnometer. The weight contents of the matrix (W_m) and fiber (W_f) were determined for each specimen using the acid digestion method. Once the composite density, constituent densities, and weight contents are known, the microvoid content (V_v) and fiber volume fraction (V_f) of each specimen was calculated using Equations (1) and (2), respectively.

$$V_V = 100 - \rho_c \left(\frac{W_f}{\rho_f} + \frac{W_m}{\rho_m} \right) \tag{1}$$

$$V_f = \frac{\rho_c W_f}{\rho_f} \tag{2}$$

2.5.2 Development of Trend Line Analysis of Effect of Humidity and Pressure on Laminate Properties

The effect of humidity exposure and fabrication pressure on the laminate fiber volume fraction and void volume fraction was explored using trend line analysis of each parameter individually. This preliminary analysis was useful in identifying general trends as a result of varying humidity exposure or fabrication pressure, and would subsequently be used as a major contributor in developing contour plots that represented the dependent variables (e.g. fiber volume fraction or void volume fraction). All trend

line analysis was restricted to only consider 1st or 2nd-order functions so as to not over-constrain the solution. This restriction was placed because some properties may have local minimums or maximums due to varying humidity or pressure, which would be captured through the use of 2nd-order functions. Although utilizing higher order functions (3rd-order and higher) would result in better level of fits when considering R^2-values, these fits would not be conducive to the actual laminate behavior and therefore would be a misrepresentation of the experimental data. For each laminate property (i.e. fiber volume fraction, void volume fraction, flexural properties, etc.) a comparison of linear, power-type, or 2nd-order polynomial representations of the processing conditions of either humidity exposure and fabrication pressure was performed for each case. The selected trend line representation for each laminate property was determined by comparing both level of fit (R^2-value) and the standard deviations between the experimental data for each trend line representation. In subsequent Sections, the final trend line selected for each laminate property will be presented and discussed. The effect of humidity and pressure on laminate fiber volume fraction and void volume fraction will be discussed in Sections 2.5.5 through 2.5.8. Later, a similar approach will be performed to explore the effect of humidity and pressure on laminate flexural stiffness and strength, which will be presented in Sections 3.2.4 through 3.2.7. The effect of humidity and pressure on the hydraulic fluid equilibrium fluid content will be addressed in Sections 5.6.1 and 5.6.2.

2.5.3 Laminate Fiber Volume Fraction Results

The average fiber volume fraction for the three prepregs for varying humidity exposure and fabrication pressure is shown in Figure 2.9. For reporting purposes, the

average fiber volume fraction with 95% confidence intervals for each fabricated laminate is provided in Appendix A. Typically, the fiber volume fraction for each prepreg material ranged from about 50% to 66%. It is important to note that although there is some small variations in the average fiber volume fraction at a specific fabrication pressure, the error bars, which indicate 95% confidence interval, generally always overlap the mean. Therefore, regardless of the level of humidity exposure or prepreg moisture content, the fiber volume fractions are statistically similar for laminates fabricated at the same cure pressure. Both quartz-reinforced laminates, shown in Figure 2.9a and b, the fiber volume fraction gradually increased from about 50.6% to 61.1% as fabrication pressure increased from 69 to 345 kPa. At higher fabrication pressures, the rate of fiber volume fraction increase declines, which may be due to fibers' increased role in supporting the applied pressure. On the other hand, at lower fabrication pressures, smaller increases in fabrication pressure would have a higher effect in increasing the fiber volume fraction. Similarly, for the carbon fiber-reinforced laminates shown in Figure 2.9c, the largest increase in fiber volume fraction from 53.3% to 60.2% was achieved at the lowest fabrication pressures, from 69 to 207 kPa. While further increases in fabrication pressure yielded fiber volume fraction increases at a reduced rate.

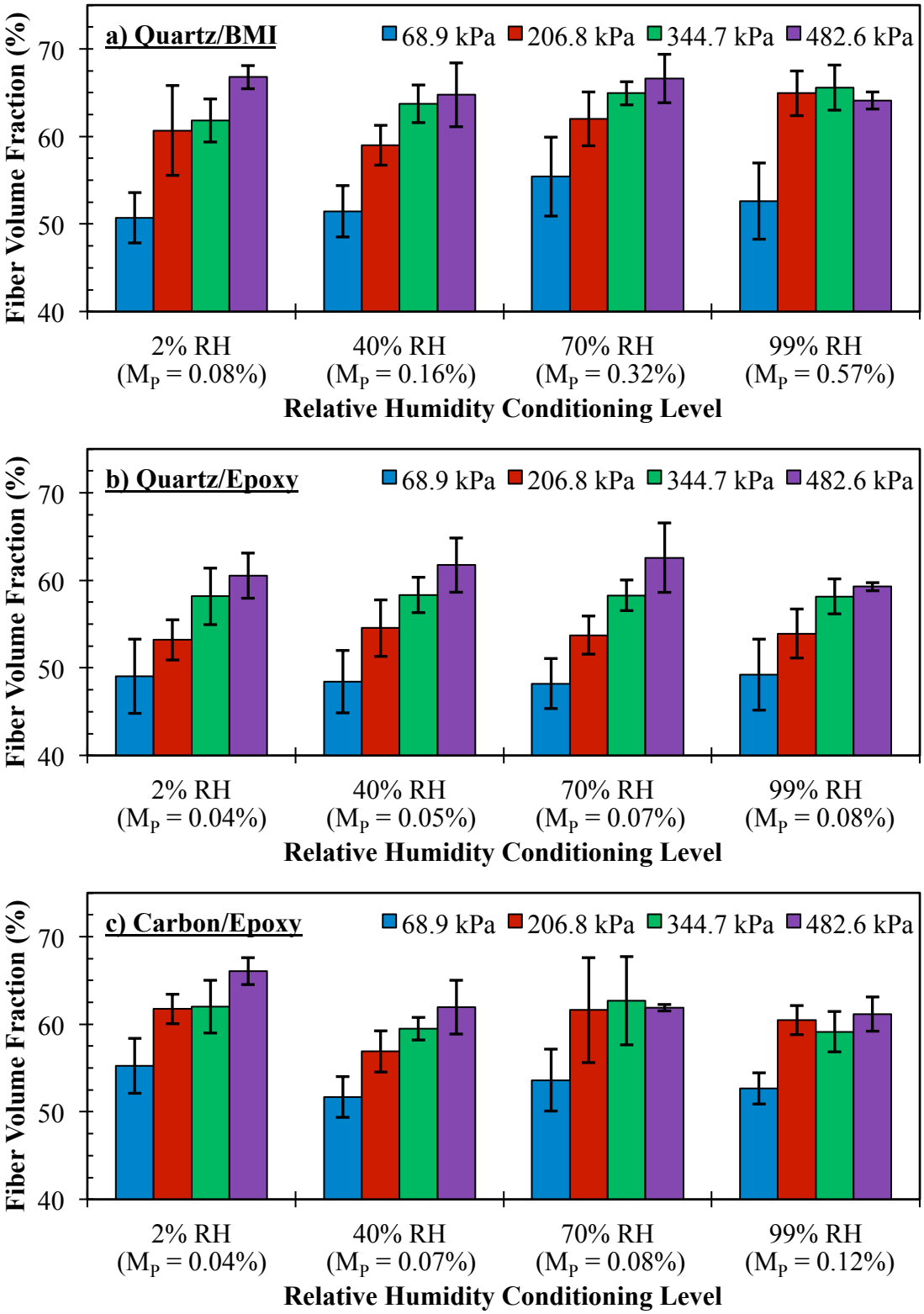

Figure 2.9 Average fiber volume fraction as prepreg moisture content (M_P) and fabrication pressure changed for (a) Quartz/BMI, (b) Quartz/Epoxy, and (c) Carbon/Epoxy. Error bars are associated with 95% confidence for n=8 samples

2.5.4 Laminate Void Volume Fraction Results

The average void volume fraction for the three-prepreg material systems is shown in Figure 2.10. For reporting purposes, the average void volume fraction with 95% confidence intervals for each fabricated laminate is provided in Appendix A. The range of void fractions was significantly different for each prepreg material. As expected, for all prepreg materials, the void volume fraction increased as relative humidity exposure level increased and as the fabrication pressure decreased. The artificially induced high levels of voids and how the void fraction changes among the different material systems clearly illustrate the importance of: (a) removing volatiles and trapped micro-voids during cure by a vacuum bag, (b) proper storage of prepregs in a low humidity environment, and (c) applying proper level of fabrication pressure. Overall, the quartz/BMI laminates contained the highest void levels. Therefore, BMI is more susceptible to a high level of voids when tools used to remove volatiles (i.e. vacuum-bag) are not utilized. The volatiles that are typically expelled during cure seem to have been trapped, thus forming voids without the presence of vacuum. The increase in fabrication pressure only helped to marginally reduce the void volume fraction, possibly by only reducing the size of the trapped voids.

The effect of the resin in dictating the void levels becomes clear when Figure 2.10a and b are compared. Since the quartz fibers are used in both cases, the resin primarily influences the difference in the void volume fraction. It is interesting to note that the void volume fraction of quartz/epoxy laminates are much more susceptible to the prepreg storage conditions as shown in Figure 2.10b. For example, if the quartz/epoxy prepregs are stored in a low humidity environment of 2% RH, a high processing

pressure of 482.6 kPa almost totally eliminates all voids, whereas a high humidity storage environment may lead to more than 5% voids.

The carbon/epoxy laminates had a void volume fraction range of about 1% to 5%, which is much lower than the other two prepregs with the quartz fiber and similar to other void levels reported for carbon/epoxy material systems in literature. For example, Muller de Almeida et al. [24] reported a void fraction range of 1.3-5.9% for carbon/epoxy laminates with a fiber volume fraction of approximately 61%. Liu et al. [17] reported a reduction in void fraction from 3.2 to 0.6% as the autoclave applied cure pressure increased from 0.0 to 0.6 MPa. The results shown in Figure 2.10c indicate that the IM7/EX-1522 prepreg is much less susceptible to prepreg storage conditions compared to AQIII/EX-1522, which has the same epoxy resin but has the quartz fiber, AQIII, reinforcement instead of the carbon IM7. The fiber/resin interphase or the sizing used in the AQIII/EX-1522 prepregs may act as storage sites for the moisture if the prepreg is stored in a highly humid environment. Therefore, the expelled moisture during cure forms higher levels of microvoids in quartz/epoxy laminates compared to carbon/epoxy laminates. The epoxy resin EX-1522 seems to have less volatiles and a high quality laminate can be produced even without the vacuum bag if the prepreg is stored properly in a dry environment and a sufficiently high fabrication pressure is applied.

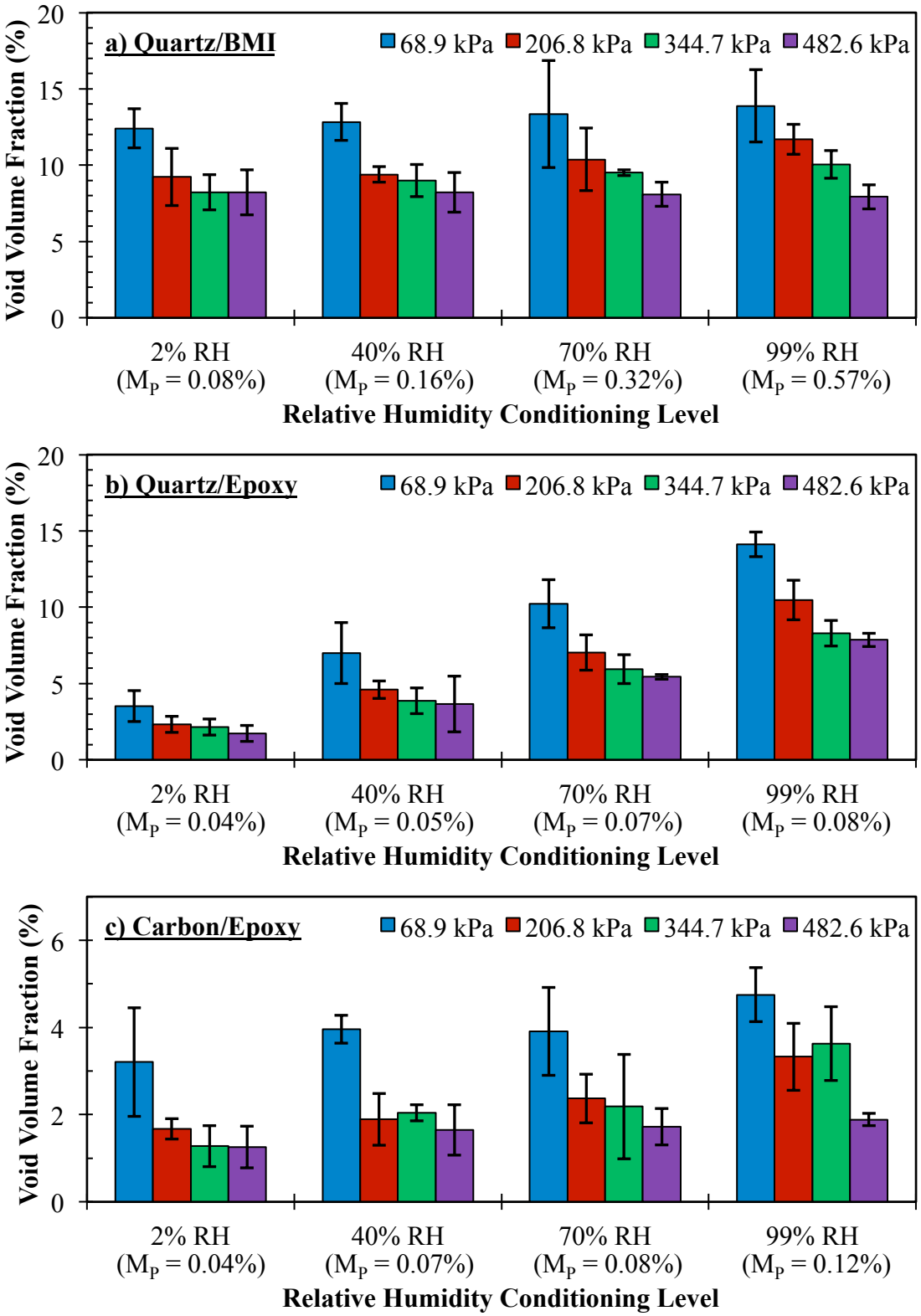

Figure 2.10 Average void fraction as prepreg moisture content (M_{PP}) and fabrication pressure changed for (a) Quartz/BMI, (b) Quartz/Epoxy, and (c) Carbon/Epoxy. Error bars are associated with 95% confidence for n=8 samples

2.5.5 Effect of Prepreg Humidity Exposure on Laminate Fiber Volume Fraction

The effect of varying humidity exposure on the laminate fiber volume fraction for each prepreg material is shown in Figure 2.11. The linear trend line fits for each prepreg conditioning and fabrication pressure specimen is provided in Table 2.6. For comparative purposes, power-function trend lines resulted in R^2-values of 0.20-0.30 as opposed to the R^2-values of 0.60-0.97 for the selected linear trend line fits. Additionally, the experimental data clearly exhibited very limited effects of humidity exposure on the fiber volume fraction. Therefore, higher order trend line representations (i.e. polynomial) would not be an accurate representation of the fiber volume fraction. The laminate fiber volume fraction was not influenced greatly by varying levels of humidity exposure for all prepreg materials. For example, in the most extreme case, the fiber volume fraction for BMI (Figure 2.11b) increased by less than 4.7% when humidity exposure increased from 0% RH to 100% RH. Therefore, this behavior corroborates the hypothesis that exposing prepregs to varying humidity levels will primarily affect the laminate void volume fraction without significantly affecting the laminate fiber volume fraction. Both epoxy-resin systems, Figure 2.11a and c, were influenced less to varying humidity levels. The fiber volume fraction for quartz/epoxy was nearly exclusively varied by fabrication pressure, which is indicated by the near-horizontal trend lines in Figure 2.11a. Meanwhile, the carbon fiber reinforced epoxy laminates in Figure 2.11c demonstrated slight decreases in fiber volume fraction as humidity exposure increased.

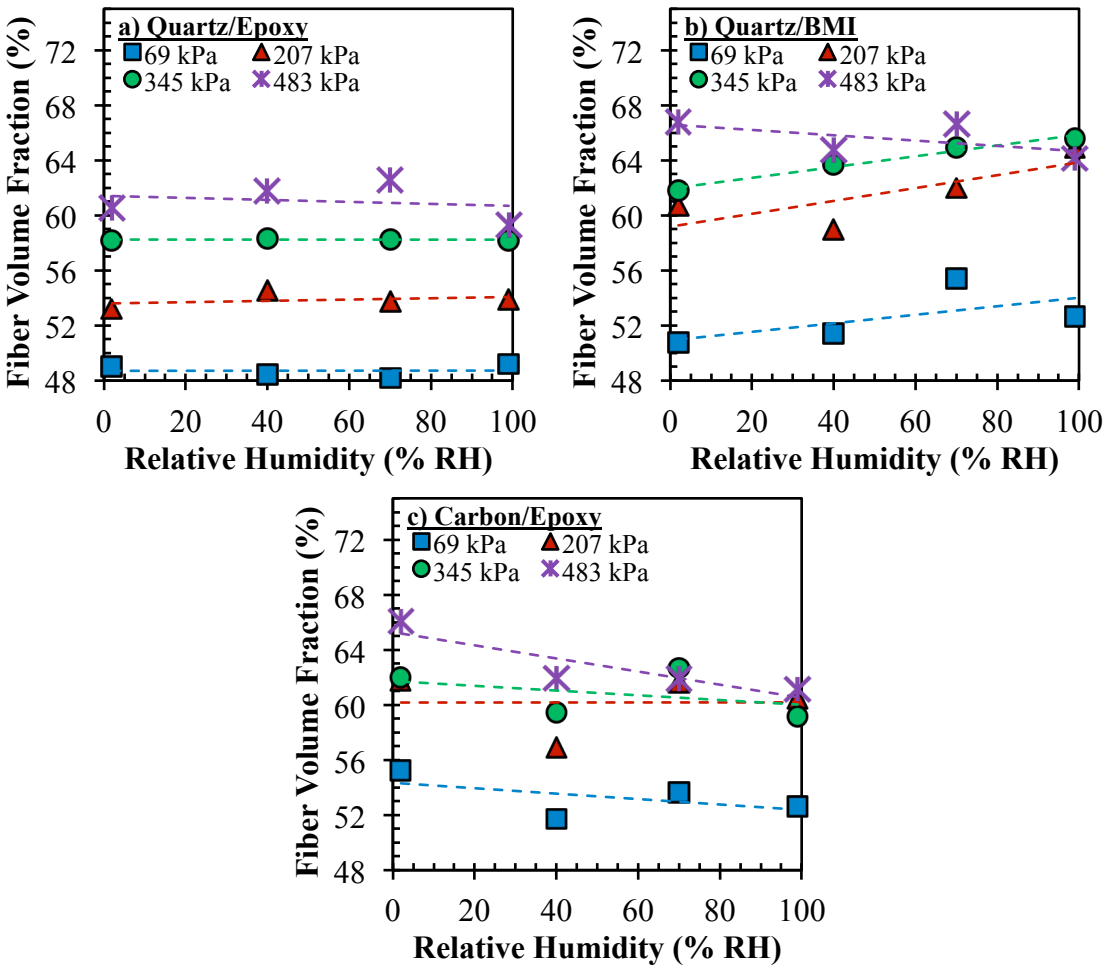

Figure 2.11 Effect of varying prepreg humidity conditioning on laminate fiber volume fraction for (a) Quartz/Epoxy, (b) Quartz/BMI, and (c) Carbon/Epoxy

Table 2.6 Trend line equations for prepreg humidity conditioning effect on laminate fiber volume fraction

a) Quartz/Epoxy	Trend Line Equation	R^2 Value
69 kPa	0.0002x + 48.712	0.0003
207 kPa	0.0048x + 53.602	0.1269
345 kPa	-8E-05 + 58.244	0.0017
483 kPa	-0.0073x + 61.417	0.0441
b) Quartz/BMI		
69 kPa	0.0310x + 50.925	0.3871
207 kPa	0.0467x + 59.181	0.5926
345 kPa	0.0391x + 61.944	0.9748
483 kPa	-0.0193x + 66.590	0.3633
c) Carbon/Epoxy		
69 kPa	-0.0197x + 54.344	0.2965
207 kPa	0.0001x + 60.172	4.3E-06
345 kPa	-0.0172x + 61.729	0.1619
483 kPa	-0.0476x + 65.278	0.7888

2.5.6 Effect of Fabrication Pressure on Laminate Fiber Volume Fraction

Generally, increasing fabrication pressure yielded similar trends of increasing the laminate fiber volume fraction for all three prepreg materials, as shown in Figure 2.12. However, there are a few distinct differences among the three prepregs. By comparing the two quartz-reinforced laminates in Figure 2.12a and b, it was observed that the BMI resin yields higher fiber volume fractions at the same cure pressure. Additionally, the BMI resin type had a slightly larger range of fiber volume fractions, 50.7-66.6%, when compared to the range for epoxy resin, 48.2-62.6%. Excluding high pressures of 483 kPa, the fiber volume fraction for quartz/epoxy laminates, shown in Figure 2.12a, was very consistent at a specific cure pressure and typically did not vary by more than ±1.3%. Comparing the two epoxy-resin prepregs in Figure 2.12a and c, both prepregs had identical delta changes (between the maximum and minimum observed values) in

the fiber volume fraction of 14.4%. The magnitude for carbon fiber reinforcement was higher for a specific cure pressure when compared to the quartz reinforcement. Additionally, the carbon fiber laminates had slightly more variations in the fiber volume fraction at a specific cure pressure. Figure 2.12a-c also reiterate the effect of humidity exposure on the fiber volume fraction presented in Section 2.5.5. Generally, as humidity exposure increased, the fiber volume fraction slightly increases for quartz-reinforcement and slightly decreases for carbon fiber-reinforcement. There was a good deal of randomness at some fabrication pressures that did not follow the general trends. Table 2.7 contains the power-function trend line equations that were selected to represent each specimen series. The power-function trend lines selected for quartz/epoxy resulted in R^2-values of 0.96-0.99 as opposed to linear R^2-values of 0.90-0.97. Therefore, a power-function trend line representation of the effect of fabrication pressure was selected to represent the laminate fiber volume fraction for each prepreg material.

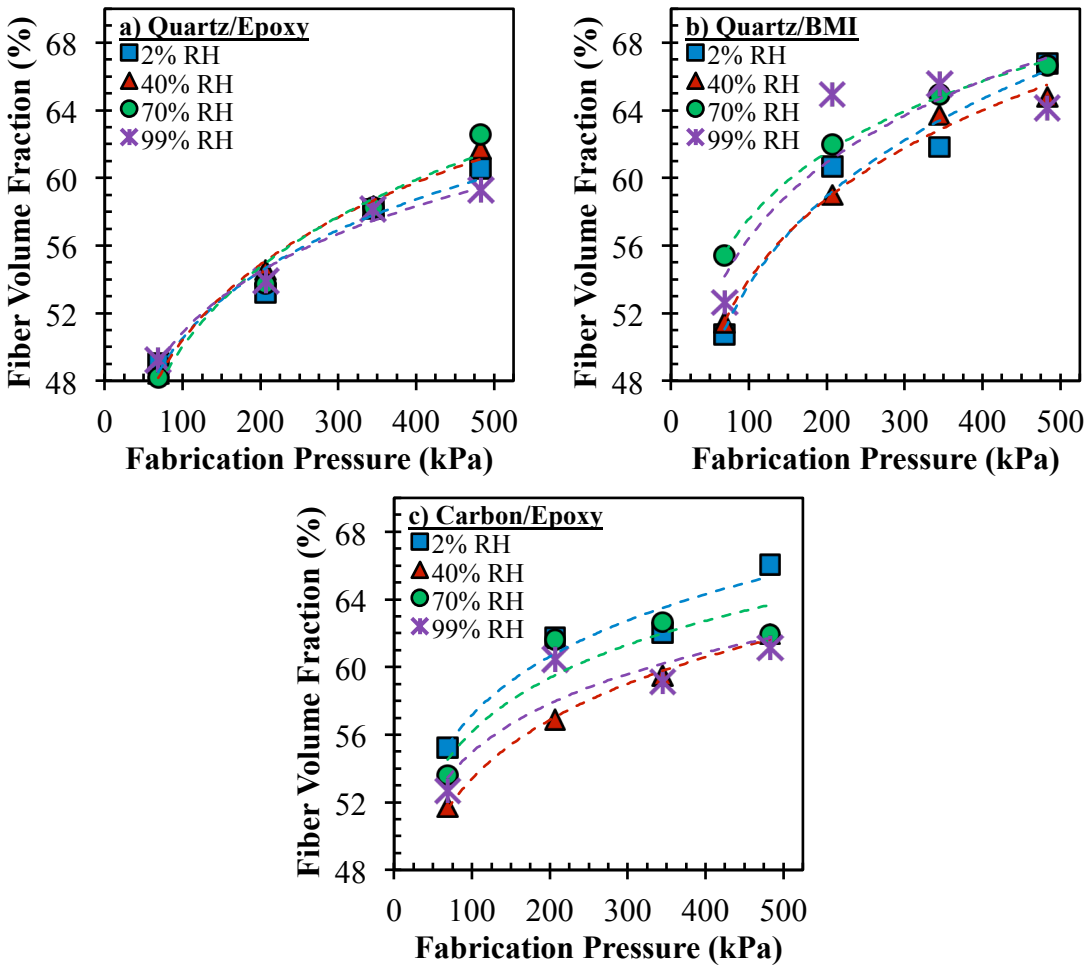

Figure 2.12 Effect of varying fabrication pressure on laminate fiber volume fraction for (a) Quartz/Epoxy, (b) Quartz/BMI, and (c) Carbon/Epoxy prepregs

Table 2.7 Trend line equations for fabrication pressure effect on laminate fiber volume fraction

a) Quartz/Epoxy	Trend Line Equation	R^2 Value
2% RH	$30.649x^{0.1085}$	0.9628
40% RH	$28.722x^{0.1222}$	0.9919
70% RH	$27.506x^{0.1299}$	0.9712
99% RH	$32.265x^{0.0988}$	0.9839
b) Quartz/BMI		
2% RH	$28.891x^{0.1345}$	0.9671
40% RH	$30.660x^{0.1228}$	0.9903
70% RH	$37.080x^{0.0955}$	0.9975
99% RH	$33.997x^{0.1100}$	0.7959
c) Carbon/Epoxy		
2% RH	$38.647x^{0.0850}$	0.9442
40% RH	$35.101x^{0.0911}$	0.9966
70% RH	$38.906x^{0.0797}$	0.8516
99% RH	$39.157x^{0.0736}$	0.8312

2.5.7 Effect of Prepreg Humidity Exposure on Void Volume Fraction

The effect of varying humidity exposure on the void volume fraction for each prepreg material is shown in Figure 2.13. The linear trend line equations for each prepreg conditioning and fabrication pressure specimen are provided in Table 2.8. For all prepreg materials and fabrication pressures, the R^2-values associated with the selected linear trend lines were greater than 0.85. Conversely, the R^2-values associated for power functions ranged from 0.47-0.91. All prepregs observed an increase in void volume fraction as the prepreg humidity exposure level increased. The BMI resin laminates, shown in Figure 2.13b, had the highest void fractions of any of the prepreg materials, with the y-intercept of the average void fraction trend lines ranging from 8.2 to 12.3%. Meanwhile, both epoxy-matrix prepregs (Figure 2.13a and c) had approximate void fraction y-intercept values of 1.1 to 3.2%. However, utilizing quartz

reinforcement can cause a rate of increasing void fraction due to increasing humidity over five times that of carbon fiber-reinforcement. For all materials, the void volume fraction decreased as fabrication pressure increased. The quartz/BMI laminates had a reasonably low rate of increasing void volume fraction as humidity exposure increased, in that the largest rate of increasing void volume fraction was 2.5% per 100% relative humidity increase. Recall from Section 2.2.2, BMI also had a wide range of prepreg moisture contents of 0.08-0.57%. It appears that BMI is susceptible to a high void fraction when high-pressure fabrication procedures or vacuum-bag assistance is not utilized. However, BMI is very resistant to further increases in the void volume fraction due to high humidity exposures.

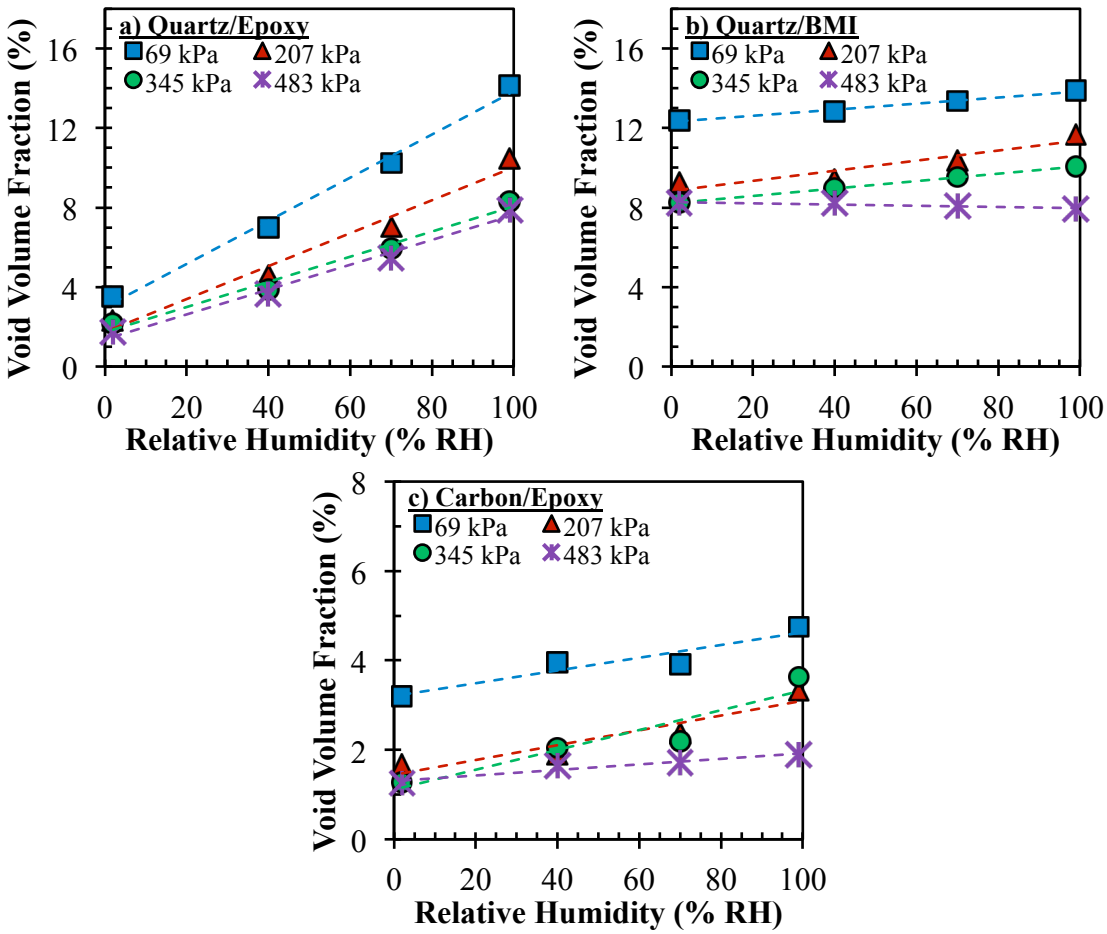

Figure 2.13 Effect of varying prepreg humidity conditioning on void volume fraction for (a) Quartz/Epoxy, (b) Quartz/BMI, and (c) Carbon/Epoxy

Table 2.8 Trend line equations for prepreg humidity conditioning effect on void volume fraction

a) Quartz/Epoxy	Trend Line Equation	R^2 Value
69 kPa	0.1085x + 2.992	0.9920
207 kPa	0.0829x + 1.7369	0.9749
345 kPa	0.0633x + 1.7278	0.9822
483 kPa	0.0625x + 1.3722	0.9858
b) Quartz/BMI		
69 kPa	0.0153x + 12.311	0.9854
207 kPa	0.0254x + 8.834	0.8702
345 kPa	0.0187x + 8.209	0.9993
483 kPa	-0.0030x + 8.271	0.8497
c) Carbon/Epoxy		
69 kPa	0.0143x + 3.2054	0.8830
207 kPa	0.0166x + 1.4424	0.8783
345 kPa	0.0222x + 1.1123	0.8786
483 kPa	0.0062x + 1.3031	0.9357

2.5.8 Effect of Fabrication Pressure on Void Volume Fraction

The effect of fabrication cure pressure on the void volume fraction for each prepreg material is shown in Figure 2.14. The selected power function trend line equations for each prepreg conditioning and fabrication pressure specimen are provided in Table 2.9 had R^2-values greater than 0.88 for most cases. The high R^2-values for power function trend lines clearly illustrate that this analysis method represents the void volume fraction well. Alternatively, a linear function analysis for BMI results in an R^2-value range of 0.78-0.93. The quartz reinforced laminates had similar power-reduction slopes for each humidity exposure level. The rate of increase for epoxy matrix was slightly higher (0.31-0.34) than the BMI matrix material (0.22-0.26). The zero y-intercept value for quartz/epoxy, shown in Figure 2.14a, varied significantly due to humidity exposure. Meanwhile, utilizing carbon fiber as the reinforcement material results in much more

consistent values regardless of humidity exposure. The carbon fiber-reinforced prepregs, shown in Figure 2.14c, had a much smaller range of void volume fractions. This may be due to the smaller diameter carbon fiber threads allowing the epoxy-matrix to fully wet the fabric and expel more microvoids.

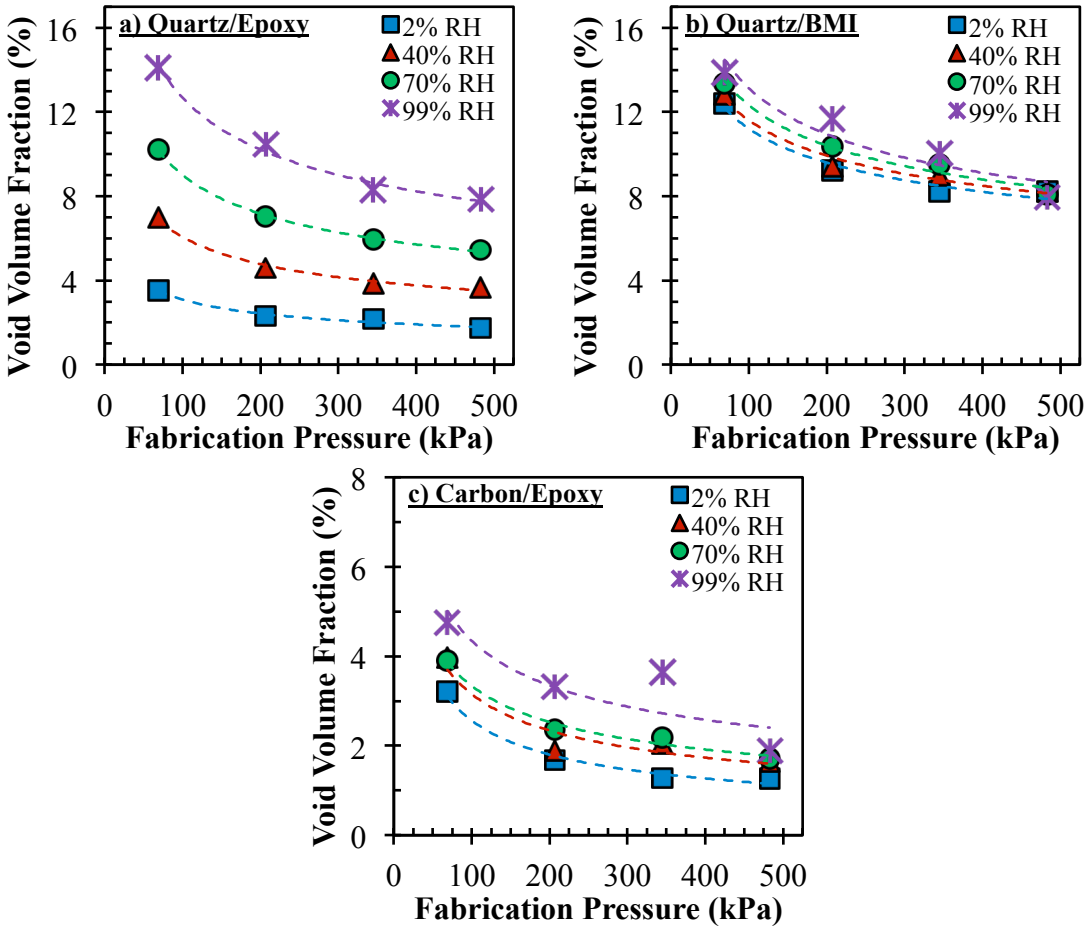

Figure 2.14 Effect of varying fabrication pressure on void volume fraction for (a) Quartz/Epoxy, (b) Quartz/BMI, and (c) Carbon/Epoxy

Table 2.9 Trend line equations for fabrication pressure effect on void volume fraction

a) Quartz/Epoxy	Trend Line Equation	R^2 Value
2% RH	$15.175x^{-0.346}$	0.9736
40% RH	$29.619x^{-0.344}$	0.9903
70% RH	$40.760x^{-0.328}$	0.9987
99% RH	$53.274x^{-0.312}$	0.9862
b) Quartz/BMI		
2% RH	$31.445x^{-0.224}$	0.9635
40% RH	$32.659x^{-0.225}$	0.9723
70% RH	$37.689x^{-0.243}$	0.9741
99% RH	$44.183x^{-0.263}$	0.8880
c) Carbon/Epoxy		
2% RH	$26.452x^{-0.507}$	0.9701
40% RH	$22.872x^{-0.430}$	0.8824
70% RH	$21.036x^{-0.400}$	0.9756
99% RH	$24.706x^{-0.377}$	0.6837

2.6 SCANNING ELECTRON MICROSCOPE EVALUATION

It was also of interest to examine the effect humidity exposure and fabrication pressure had on the size and spatial distribution of voids for the laminates. Two specimens from each laminate was embedded in a quick cure acrylic resin with a cross-section of the through-the-thickness oriented vertically up and polished with grit sizes ranging from 15μm to 1.9μm in three successive steps. The samples were then sputter coated with gold/palladium to mitigate sample charging and cross-sectional images were acquired using a Zeiss NEON FEG-SEM.

2.6.1 Humidity and Processing Effect on Void Size and Spatial Distribution for Quartz/BMI Prepregs

The SEM images revealed the formation of many large-scale voids, which were primarily located in the intra-tow regions and ply-to-ply interface. Figure 2.15 contains

representative images of prepregs conditioned at the lowest relative humidity level (2% RH) and subsequently cured at each of the four fabrication pressures (68.9, 206.8, 344.7, 482.6 kPa). The low conditioning level resulted in the lowest prepreg moisture content and would therefore produce the lowest microvoid content for a given cure pressure. Each fabrication pressure for BMI matrix laminates featured several elongated voids that were located between plies and fiber bundles. Some of the larger voids measured over 1 mm in length, which equates to about 50% of the through-the-thickness measurement.

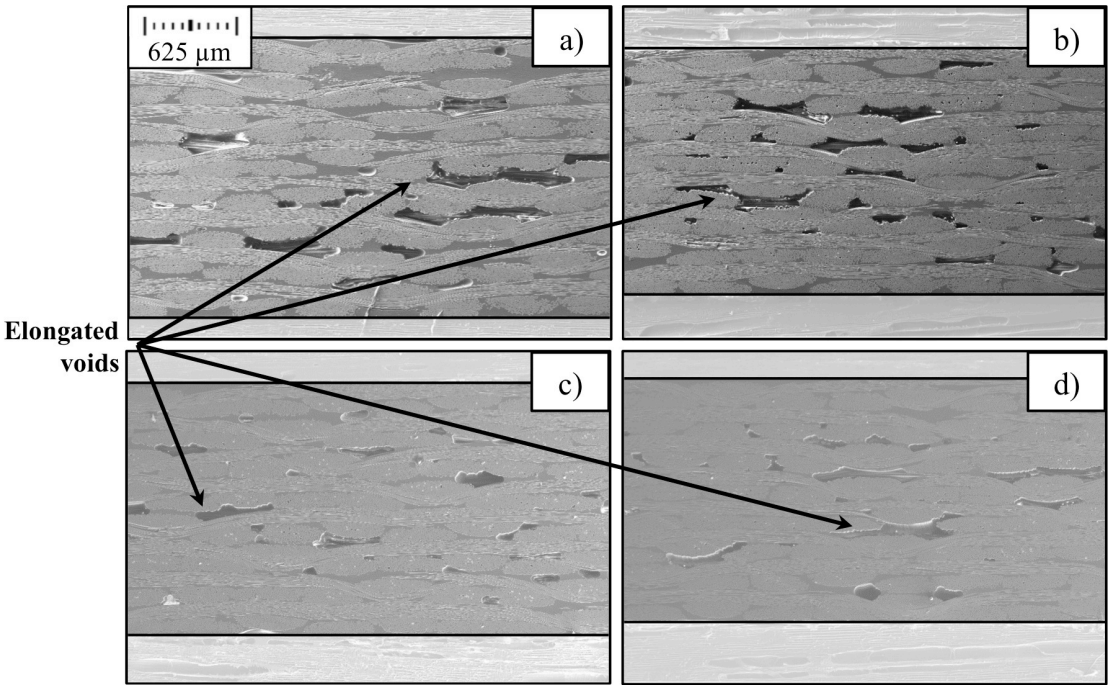

Figure 2.15 SEM images of Quartz/BMI laminates fabricated from prepregs conditioned at 2% relative humidity and cured at a) 69 kPa, b) 207 kPa, c) 345 kPa, and d) 483 kPa

Figure 2.16 contains representative images of laminates cured at the highest fabrication pressure (482.6 kPa) from each of the four prepreg conditioning levels (2%, 40%, 70%, 99% RH). Generally, the spatial distribution throughout the thickness of the laminate did not change as a result of increasing prepreg conditioning level or fabrication pressure. As fabrication pressure increased, the void morphology became more elongated, or void aspect ratio increased. In addition to the many large-scale voids, the laminates exhibited many microscale voids with diameters equivalent to the fiber diameter. These microscale voids were predominantly located within the fiber tows. The laminate thickness reduced by approximately 20% as fabrication pressure increased from 68.9 kPa to 482.6 kPa. Varying prepreg moisture content with different relative humidity levels did not have a discernible effect on the void morphology or distribution for the laminates. The average void content increased in a near-linear fashion as relative humidity conditioning increased. Laminates fabricated at lower cure pressures had a larger range of microvoid contents due to variations in the prepreg relative humidity exposure level.

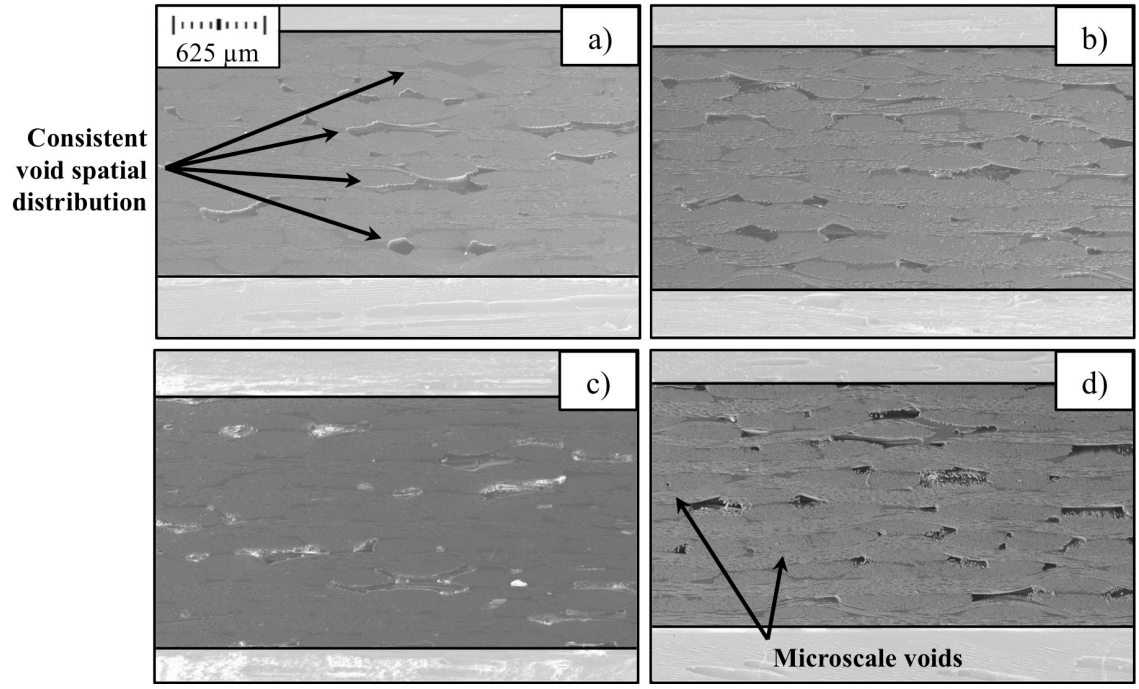

Figure 2.16 SEM images of Quartz/BMI laminates fabricated at 483 kPa from prepregs conditioned at a) 2% relative humidity, b) 40% relative humidity, c) 70% relative humidity, and d) 99% relative humidity

2.6.2 Humidity and Processing Effect on Void Size and Spatial Distribution for Quartz/Epoxy Prepreg

The SEM images for Quartz/Epoxy laminates revealed more spherical shaped voids, which were primarily located in resin-rich regions and the ply-to-ply interface. Figure 2.17 contains representative images of prepregs conditioned at the lowest relative humidity level (2% RH) and subsequently cured at each of the four fabrication pressures (68.9, 206.8, 344.7, 482.6 kPa). The largest voids occurred at the lowest fabrication pressure, and measured up to 0.5 mm in length and had aspect ratios ranging from 1 to 3. As fabrication pressure increased, the effective area of the voids

significantly decreased with voids having diameters on the microscale level and being of a similar scale to the quartz fiber reinforcement.

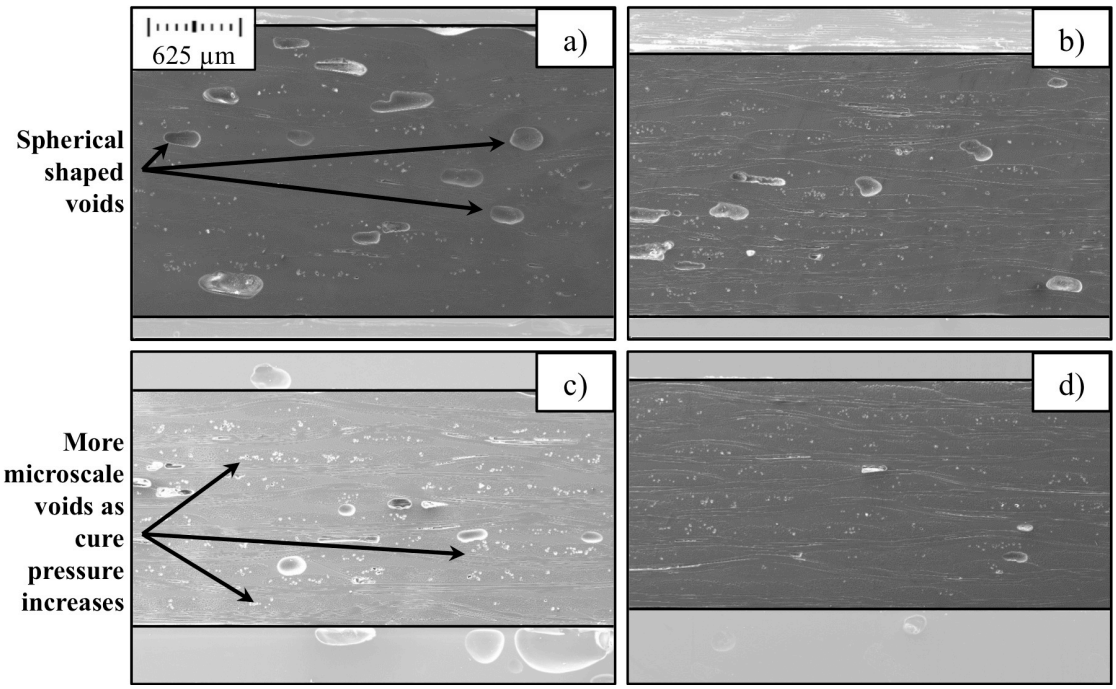

Figure 2.17 SEM images of Quartz/Epoxy laminates fabricated from prepregs conditioned at 2% relative humidity and cured at a) 69 kPa, b) 207 kPa, c) 345 kPa, and d) 483 kPa

Figure 2.18 contains representative images of laminates cured at the highest fabrication pressure (482.6 kPa) from each of the four prepreg conditioning levels (2%, 40%, 70%, 99% RH). Similar to the BMI matrix laminates, the spatial distribution throughout the thickness of the laminate did not change as a result of increasing prepreg conditioning level or fabrication pressure. Increasing prepreg relative humidity conditioning levels resulted in the void effective diameter and aspect ratios increasing substantially. The average void fraction increased in a near-linear fashion as relative

humidity conditioning increased. Laminates fabricated at lower cure pressures had a larger range of microvoid contents due to variations in the prepreg relative humidity exposure level.

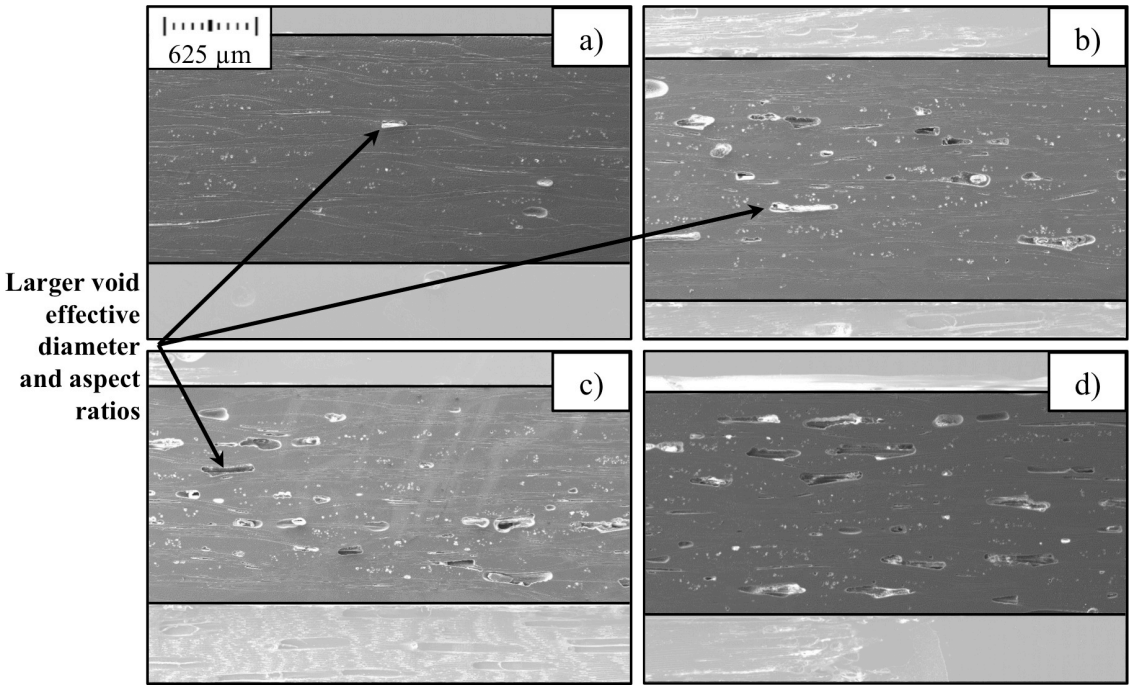

Figure 2.18 SEM images of Quartz/Epoxy laminates fabricated at 483 kPa from prepregs conditioned at a) 2% relative humidity, b) 40% relative humidity, c) 70% relative humidity, and d) 99% relative humidity

2.6.3 Humidity and Processing Effect on Void Size and Distribution for Carbon / Epoxy Prepreg

The microvoid content for carbon-reinforced laminates was significantly lower than the other two prepreg materials in this study. The SEM images for Carbon/Epoxy laminates revealed sporadic, slightly elongated voids, which were primarily located in

resin-rich regions and the ply-to-ply interface. Figure 2.19 contains representative images of prepregs conditioned at the lowest relative humidity level (2% RH) and subsequently cured at each of the four fabrication pressures (68.9, 206.8, 344.7, 482.6 kPa). As fabrication pressure increased, the effective area of the voids significantly decreased and the void aspect ratio increased.

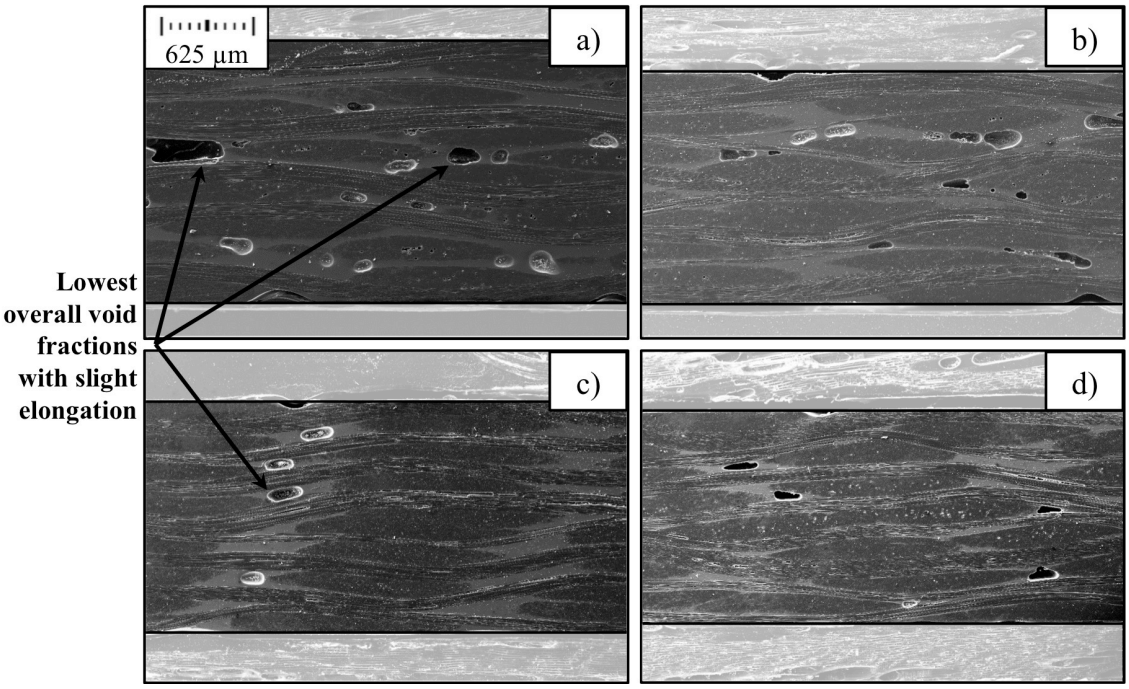

Figure 2.19 SEM images of Carbon/Epoxy laminates fabricated from prepregs conditioned at 2% relative humidity and cured at a) 69 kPa, b) 207 kPa, c) 345 kPa, and d) 483 kPa

Figure 2.20 contains representative images of laminates cured at the highest fabrication pressure (482.6 kPa) from each of the four prepreg conditioning levels (2%, 40%, 70%, 99% RH). It appears that the larger microvoids by effective area were predominantly located within plies close to the laminate midplane. Increasing prepreg relative humidity conditioning levels did not have a significant effect on overall

microvoid content, however the microvoids did become more spherical in shape and slightly larger in diameter. All laminate fabrication pressures for carbon-reinforced prepregs had a smaller range of microvoid contents when compared to the two quartz-reinforced prepreg materials.

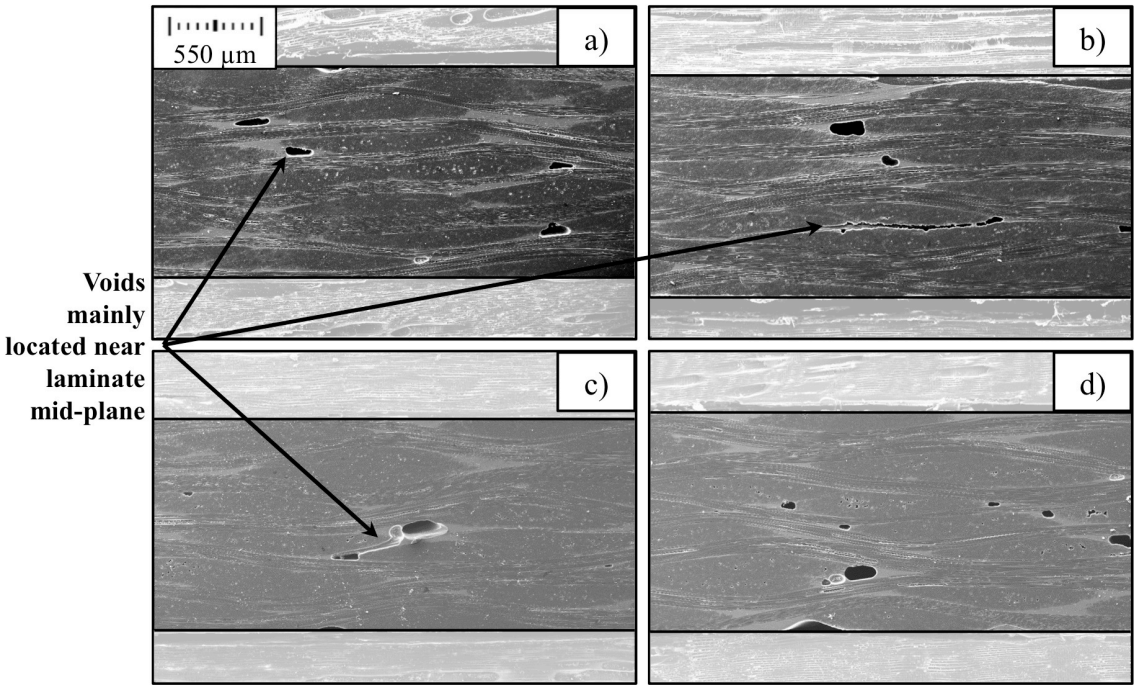

Figure 2.20 SEM images of Carbon/Epoxy laminates fabricated at 483 kPa from prepregs conditioned at a) 2% relative humidity, b) 40% relative humidity, c) 70% relative humidity, and d) 99% relative humidity

2.7 SUMMARY OF LAMINATE MICROSTRUCTURE AND SEM ANALYSIS CHAPTER

Three aerospace-grade composite prepregs that are typically used in high-performance applications were introduced. These composite prepregs included a Hexcel HexPly® F650 Bismaleimide (BMI) resin with quartz style 581 reinforcement,

and two variations of a TenCate® EX-1522 epoxy resin with either quartz style 4581 reinforcement or IM-7 carbon fiber plain weave reinforcement. A procedure for altering the prepreg moisture content using an environmental chamber at varying relative humidity exposure levels was described in Section 2.2. It is expected that varying levels of prepreg moisture content will result in laminates with different void volume fractions. Eight-ply thick laminates were fabricated from the conditioned prepregs using a Carver hot press and the manufacturer suggested temperature cure cycle, as described in Section 2.3. A total of 32 specimens were extracted from each fabricated laminate to address the research objectives associated with this Dissertation

The experimental procedure for determining the laminate fiber volume fraction and void volume fraction was presented in Section 2.5. Section 2.5.2 contained the resulting fiber volume fraction and void volume fraction due to variations in prepreg relative humidity conditioning level, which caused unique prepreg moisture contents, and variations in fabrication pressure. Generally, the fiber volume fraction did not change significantly due to varying prepreg moisture contents and increased as fabrication pressure increased, with the largest incremental improvement occurring when at low initial fabrication pressures. The void volume fraction increased as relatively humidity conditioning increased and fabrication pressure decreased. SEM image analysis of each prepreg material for varying processing conditions was presented in Section 2.6. BMI matrix prepregs (Section 2.6.1) featured numerous large-scale voids, which were primarily located in the intra-tow regions and ply-to-ply interface; as well as several micro-scale voids primarily located within the fiber tows. Quartz/Epoxy prepregs (Section 2.6.2) had voids that were more spherically shaped and

were primarily located in resin-rich regions or the ply-to-ply interface. Carbon fiber-reinforced prepregs (Section 2.6.3) had much lower void contents than the quartz-reinforced materials and had sporadic, slightly elongated voids primarily located in resin-rich regions and were generally closer to the laminate mid-plane.

CHAPTER 3

COUPLED EFFECT OF PREPREG MOISTURE CONTENT AND FABRICATION PRESSURE ON LAMINATE FLEXURAL PROPERTIES

3.1 BACKGROUND AND LITERATURE REVIEW OF PROCESSING CONDITIONS AFFECTS ON MECHANICAL PROPERTIES

Variations in the prepreg moisture content due to humidity changes in prepreg storage or fabrication environment as well as variations in the fabrication pressure can have a significant effect on the laminate fiber volume fraction and void volume fraction. This in turn can contribute to significant variations in the resulting laminate mechanical properties. Low-pressure fabrication methods, such as vacuum-bag or composite hot-press, are generally desirable for many secondary structures due to the significant benefit of reduced operating costs when compared to high-pressure alternatives such as autoclave. However, low-pressure fabrication methods are also more susceptible to a higher void fraction due to an inability to fully remove volatiles during laminate cure. It is therefore useful to accurately characterize the extent of detrimental behavior due to variations in prepreg humidity exposure and fabrication cure pressure on the laminate mechanical performance. As it would allow components with a high void volume fraction but still mechanically suitable for their desired application to be fully vetted and approved. The remainder of this Chapter will examine the synergistic relationship

and interaction between prepreg humidity exposure and laminate fabrication pressure on the mechanical flexural stiffness and flexural strength for the three aerospace-grade prepreg materials; quartz/BMI, quartz/epoxy, and carbon/epoxy.

Regardless of the manufacturing technique, process-induced microvoids remain one of the most common defects associated with composites laminates. An increase in laminate void fraction is known to have a deleterious effect on mechanical properties, such as interlaminar shear strength and flexural strength [1,2,20-23], and increase propensity of fiber-reinforced polymers to fluid absorption [2,18,25]. Therefore, the void fraction of composite materials is often used to judge the quality of a finished product. Typically a void fraction less than 1.0% is deemed acceptable for aerospace-grade composite materials. However there are instances where products would be mechanically suitable with a higher void fraction. If a higher void fraction is still acceptable for use, a significant cost-savings could be achieved by utilizing production methods that are less costly than autoclave manufacturing.

Researchers have investigated the effect of process-induced defects, such as microvoids, for several decades [19,27-30]. Since voids primarily influence matrix-dominated phenomena in laminates, a majority of void effect research is focused on interlaminar shear strength [31-33], compressive strength [34], bending strength [17,18,24,35] or fatigue behavior [36]. Research on the physics of void formation and its effect on laminate properties for carbon fiber reinforced polymers remains the most common [17,20,24,27-29,31-33,35,37]. Studies of similar scope for quartz-reinforced polymers, Bismaleimide resin systems, or other high-performance aerospace-grade composites are not as prevalent in literature [18,31,38].

Processing effects on void formation and mechanical strength have been studied in various details. Lundström and Gebart studied the effect of varying processing pressure in a resin transfer molding set-up on the void morphology of a unidirectional carbon reinforced laminate [39]. They concluded that doubling pressure above atmospheric pressure resulted in a 60% reduction in void fraction. Additionally studies have primarily focused on void formation in laminate repair techniques using out-of-autoclave and vacuum-bag only processes [37,40]. Numerous studies exist that examine the effect a range of void fractions may have on the absorption characteristics or mechanical properties of fiber-reinforced laminates. Some common methods of varying the void fraction for similarly prepared laminates include changing autoclave or hot-press pressure [27], modifying cure cycle temperature ramps and holds [28], or by varying the extent of debulking prepregs prior to laminate fabrication [29]. All of these methods carry the drawback of significantly altering the fiber volume fraction of a laminate, some by as much as 20% [30]. Changes in fiber volume fraction also have a significant role on the mechanical performance of the composite laminate. Procedures such as these make it difficult to examine the effect of changing fiber volume fraction and void volume fraction independently.

The consensus among researchers is that an increase in void fraction will reduce mechanical performance and cause laminates to be more susceptible to fluid absorption or fatigue damage. The magnitude of void effect on these parameters is a matter of debate however. Muller de Almeida et al. [24] focused on modeling flexural strength and fatigue life on carbon/epoxy laminates. All laminates had a fiber volume fraction of approximately 60%, and void fractions ranging from 1.3 – 5.8%. Overall, a

reduction in flexural strength of about 18% was observed throughout the void fraction range. However, Liu et al. [17] reported a 22% reduction in flexural strength for carbon/epoxy laminates with a void fraction of just 3.5%. These discrepancies are most likely attributed to the complex nature and interaction with a number of different variables, such as void fraction, void morphology and distribution, and fiber volume fraction. A majority of research is focused on the effect on mechanical performance at discrete levels of fiber volume fraction or void volume fractions. However variations in the prepreg moisture content as a result of relative humidity exposure level and fabrication pressures can also have a significant effect on the laminate microstructure [1].

In summary, the effect of variations of select processing conditions on the formation of microvoids and subsequent mechanical properties has been well documented. However, a detailed study that independently varies two processing conditions of prepreg humidity exposure and fabrication pressure and its subsequent effect on the laminate flexural properties for several aerospace-grade prepreg materials has not been reported.

3.2 LAMINATE FLEXURAL STIFFNESS AND STRENGTH

All laminate flexural property testing was conducted in accordance with the ASTM testing standard for fiber-reinforced polymers D790. Flexural properties were determined from a bar of rectangular cross section resting on two supports and loaded by means of a loading nose located midway between the two supports. The ASTM Standard states the following critical testing criteria for each flexural test:

1) The support span-to-depth ratio should be 16:1, however a larger span-to-depth ratio may become necessary for laminated materials.
2) The specimen should be deflected until rupture occurs in the outer surface or until the maximum strain of 5.0% is reached, whichever occurs first.
3) A strain rate of 0.01 mm/mm/min should be maintained until specimen failure.

With regards to the flexural testing conducted in this study, the support span-to-depth ratio for all prepreg materials was chosen to be 20:1. This value was chosen because (i) it allowed for a larger span-to-depth ratio to account for the laminated composite specimens and (ii) specimen overall lengths were within the range of useable space for the fabricated laminates. All specimens ruptured prior to the 5.0% maximum strain threshold, and loading was conducted at the specified strain rate of 0.01 mm/mm/min.

3.2.1 Experimental Procedure to Determine Laminate Mechanical Properties

Six specimens of each laminate humidity conditioning level and fabrication pressure was prepared for baseline flexural testing. The laminate flexural stiffness (GPa) for a laminate specimen in bending was determined by:

$$E_B = \frac{L^3 m}{4bd^3} \tag{3}$$

where L is the support span length (mm), m is the slope of the tangent to the initial straight-line portion of the load-deflection curve (kN/mm), b is the tested specimen beam width (mm), and d is the specimen beam depth (mm). For all laminate flexural tests, the tangent slope of the initial straight-line portion of the load-deflection curve

was determined between the loads of 50-175 N. The laminate flexural strength (MPa), or the maximum stress in the outer surface of the test specimen at the deflection midpoint, was determined by:

$$\sigma_f = \frac{3P_{max}L}{2bd^2} \tag{4}$$

where P_{max} is the failure load (N), L is the support span length (mm), b is the tested specimen beam width (mm), and d is the depth or thickness of the specimen beam (mm).

3.2.2 Laminate Flexural Stiffness Results

Figure 3.1a and b indicate both quartz-reinforced laminates have similar flexural stiffness values regardless of the matrix material (BMI or epoxy) and were within the range of 22 to 29 GPa. Carbon fiber-reinforced laminates, on the other hand, had the highest flexural stiffness values ranging from 42 to 53 GPa, as shown in Figure 3.1c. Figure 3.1a-c also depict that the quartz-reinforced laminates have slightly larger percentage variation in flexural stiffness of approximately 20 – 25%, while the carbon-reinforced laminates has a variation of 20% throughout the prepreg conditioning and fabrication pressure range. As expected, the flexural stiffness showed a strong dependence on the pressure, while the prepreg moisture content did not seem to yield a discernible effect on the laminate flexural stiffness. A careful analysis of the data show that at a particular fiber volume fraction, the flexural stiffness is often reduced by as much as 10-15% when considering void fractions up to 3%. Similar reduction levels have also been observed previously, where Liu et al. [17] reported a 15% reduction in

flexural stiffness for carbon/epoxy (i.e., T700/TDE85) laminates that had a void fraction increase from 0.6 to 3.2%.

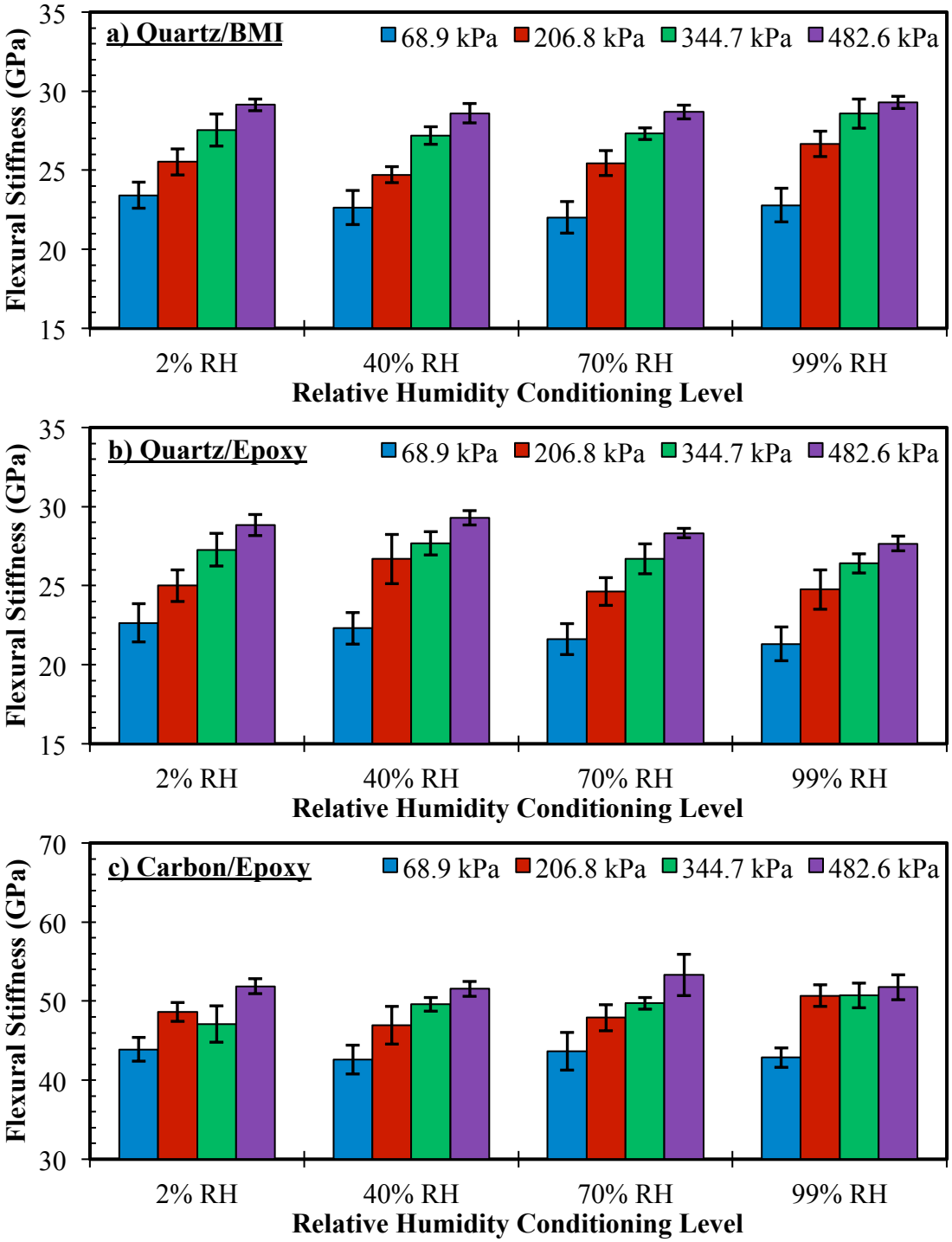

Figure 3.1 Average flexural stiffness for varying prepreg humidity conditioning and fabrication pressure for (a) Quartz/BMI, (b) Quartz/Epoxy, and (c) Carbon/Epoxy. Error bars are associated with 95% confidence for n=6 samples

3.2.3 Laminate Flexural Strength Results

Figure 3.2a-c indicate that the quartz/BMI laminates have the lowest flexural strength values of the three prepreg material systems used in this study, with strength values ranging from 425 to 600 MPa. The two epoxy-matrix laminates have higher flexural strength values, both with a maximum of about 950 MPa. The flexural strength of quartz/epoxy laminates shown in Figure 3.2b varied from 562 to 967 MPa, or approximately by 40%, which is most likely due to these laminates having the highest variation in void volume fraction. The carbon-reinforced laminates (Figure 3.2c) had a flexure strength reduction of 23% as void volume fraction increased from 1.3 to 4.8%. This is very similar to the reduction levels reported by Liu et al. [17], where a strength reduction of nearly 20% was observed as void fraction increased from 0.6 to 3.2%. Typically, reducing the relative humidity level of the prepreg conditioning level and increasing fabrication pressure achieved the largest improvement in flexural strength. For example, for quartz/epoxy laminates cured at 68.9 kPa, decreasing the relative humidity level from 99% to 2% improved the flexural strength by nearly 30% (i.e., from 562.2 to 721.9 MPa). Increasing the fabrication pressure to 482.6 kPa for these laminates improved the flexural strength further by more than 13% to 818.1 MPa. Thus, by only controlling the storage environment at a low humidity level and applying a higher processing pressure, one can increase the flexural strength by 45%. It is interesting to note that for all three material systems, the flexural strength values observed at the highest relative humidity exposure and fabrication pressure were 50-80 MPa higher than the strength values obtained at the lowest relative humidity and

fabrication pressure. Thus, the importance of applying higher fabrication pressure is validated, particularly if the prepregs are stored in a highly humid environment.

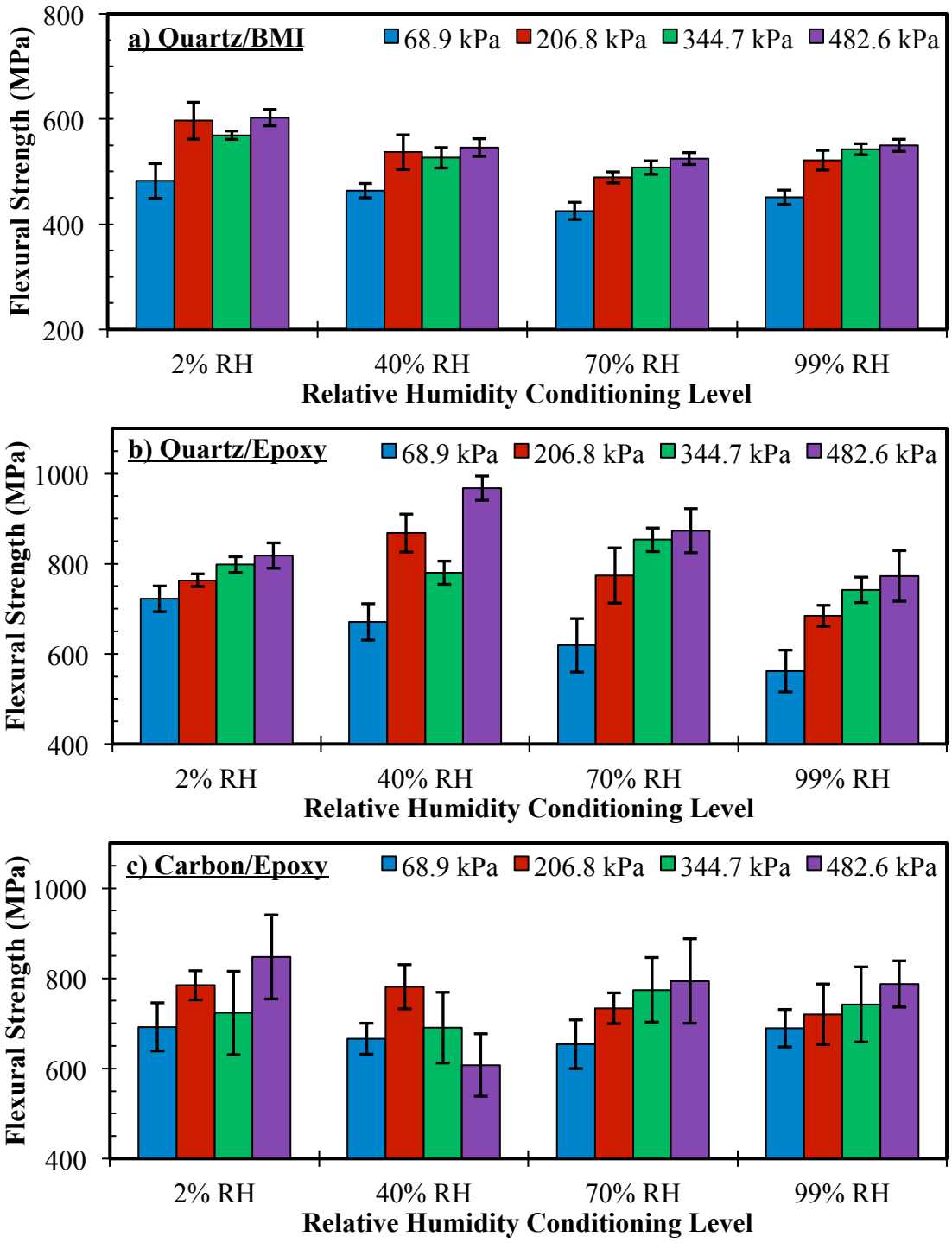

Figure 3.2 Average flexural strength for varying prepreg humidity conditioning and fabrication pressure for (a) Quartz/BMI, (b) Quartz/Epoxy, and (c) Carbon/Epoxy. Error bars are associated with 95% confidence for n=6 samples

3.2.4 Effect of Prepreg Humidity Exposure on Laminate Flexural Stiffness

The effect of prepreg humidity conditioning on the laminate flexural stiffness is shown in Figure 3.3. The linear trend line equations for each prepreg conditioning and fabrication pressure specimen are provided in Table 3.1. The experimental data clearly exhibited very limited effects of humidity exposure on the flexural stiffness. Therefore, higher order trend line representations (i.e. polynomial) would not be an accurate representation of the flexural stiffness. For each prepreg material, varying humidity exposure did not significantly change the flexural stiffness, illustrated by each material having low increasing rates. For example, the most extreme case was observed with carbon fiber reinforced epoxy laminates (Figure 3.3c) fabricated at 345 kPa, which had a slope of 0.035 GPa / % relative humidity. Additionally, carbon fiber reinforcement has high baseline stiffness values of 43.6 GPa and greater. Therefore, considering both the low increasing slope and high baseline stiffness, the laminate stiffness increased by less than 7.5% when humidity exposure was increased from zero to 100% relative humidity. Quartz-reinforced laminates, shown in Figure 3.3a and b, had even lower stiffness slopes due to humidity exposure, of no more than 0.015 GPa / % relative humidity for all fabrication levels. Regardless of the matrix material (BMI and epoxy), both quartz-reinforced laminates had similar stiffness offsets at the same fabrication pressure, which ranged from 22.7 to 29.2 GPa. Flexural stiffness increased as fabrication pressure increased for each prepreg material. This was expected because stiffness is predominantly a fiber-dominated phenomenon, and increasing pressure results in an increase in fiber volume fraction. The effect of fabrication pressure on flexural stiffness will be discussed in more detail in the next Section.

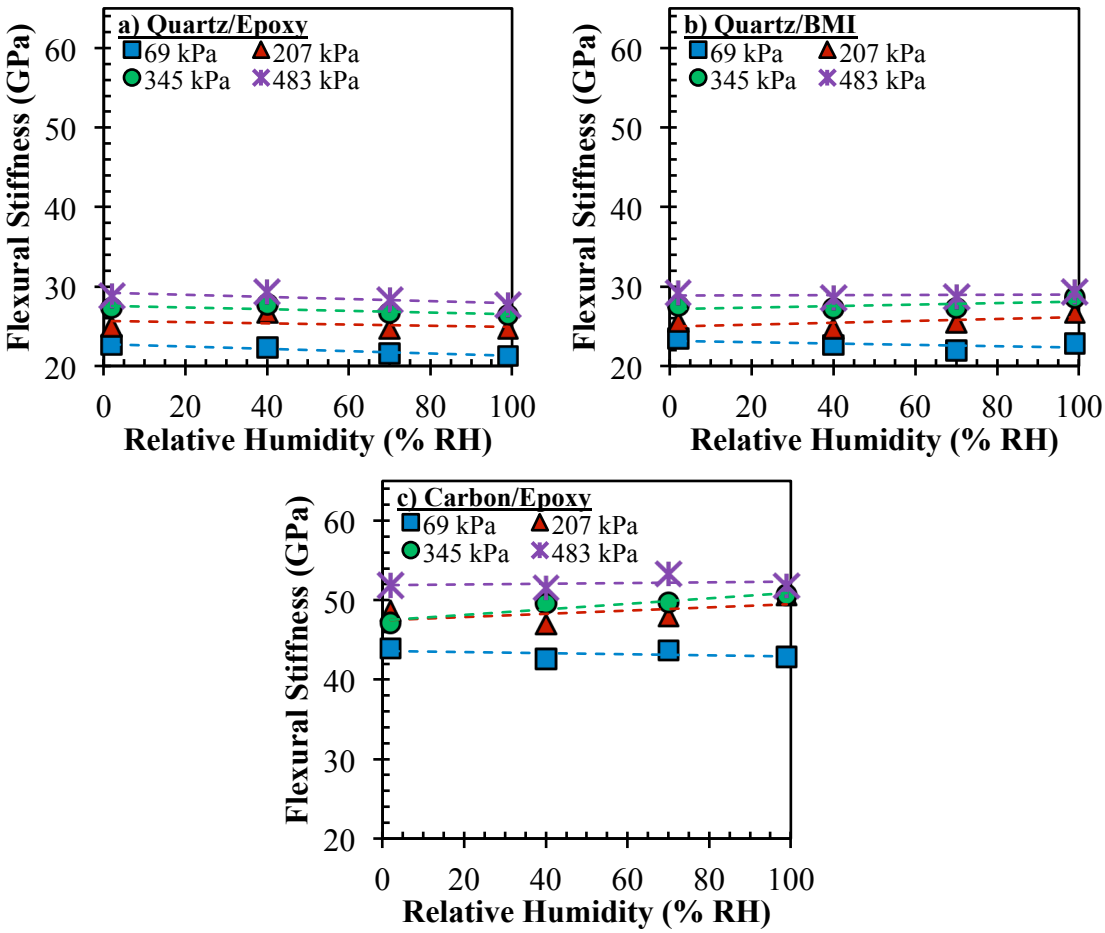

Figure 3.3 Effect of prepreg humidity exposure on the flexural stiffness for (a) Quartz/Epoxy, (b) Quartz/BMI, and (c) Carbon/Epoxy laminates

Table 3.1 Trend line equations for prepreg humidity conditioning effect on flexural stiffness

a) Quartz/Epoxy	Trend Line Equation	R^2 Value
69 kPa	-0.0146x + 22.74	0.9693
207 kPa	-0.0076x + 25.67	0.1090
345 kPa	-0.0107x + 27.57	0.5996
483 kPa	-0.0133x + 29.22	0.6197
b) Quartz/BMI		
69 kPa	-0.0084x + 23.16	0.3666
207 kPa	0.0119x + 24.96	0.3763
345 kPa	0.0095x + 27.16	0.3851
483 kPa	0.0012x + 28.87	0.0218
c) Carbon/Epoxy		
69 kPa	-0.0069x + 43.60	0.2056
207 kPa	0.0203x + 47.47	0.2814
345 kPa	0.0347x + 47.45	0.8846
483 kPa	0.0045x + 51.88	0.0547

3.2.5 Effect of Fabrication Pressure on Laminate Flexural Stiffness

The effect of applied cure pressure on the flexural stiffness for each laminate material is shown in Figure 3.4. The linear trend line equations for each prepreg conditioning and fabrication pressure specimen are provided in Table 3.2. For most prepreg materials and humidity exposure, the R^2-values associated with the selected linear trend lines were greater than 0.90. Conversely, the R^2-values associated for power function trend lines were also reasonable good representations of the flexural stiffness, although not to the same level as a linear trend line representation. As fabrication pressure increased, all materials demonstrated near linear flexural stiffness increases. Regardless of the humidity exposure, the rate of stiffness increase and offset was similar for quartz/epoxy and quartz/BMI laminates, as indicated by the trend line equations for Figure 3.4a and b, respectively. The rate of stiffness increase for quartz-

reinforcement was within the range of 0.014-0.016 GPa/kPa. The stiffness offset for quartz-reinforcement was between 20.9 and 22.6 GPa. Comparing the two epoxy matrix materials in Figure 3.4a and c, it was observed that the flexural stiffness for carbon fiber reinforced laminates was slightly more sensitive to changes in pressure than laminates fabricated with quartz-reinforcement. This is indicated by the larger increasing slopes of carbon fiber (0.016-0.023 GPa/kPa) as opposed to that of quartz fiber (0.015-0.016 GPa/kPa). This may be due to differences in the fabric weave architecture, in that carbon fiber is assembled as a plain weave and quartz fiber is assembled as a satin weave. Additionally, Figure 3.4 clearly indicates the limited effect that prepreg humidity exposure had on the flexural stiffness, in that all conditioning treatments are in close proximity for a given prepreg material. Therefore, it can be concluded that flexural stiffness is predominantly dependent on fiber reinforcement type, which defines the initial stiffness value, and fabrication pressure.

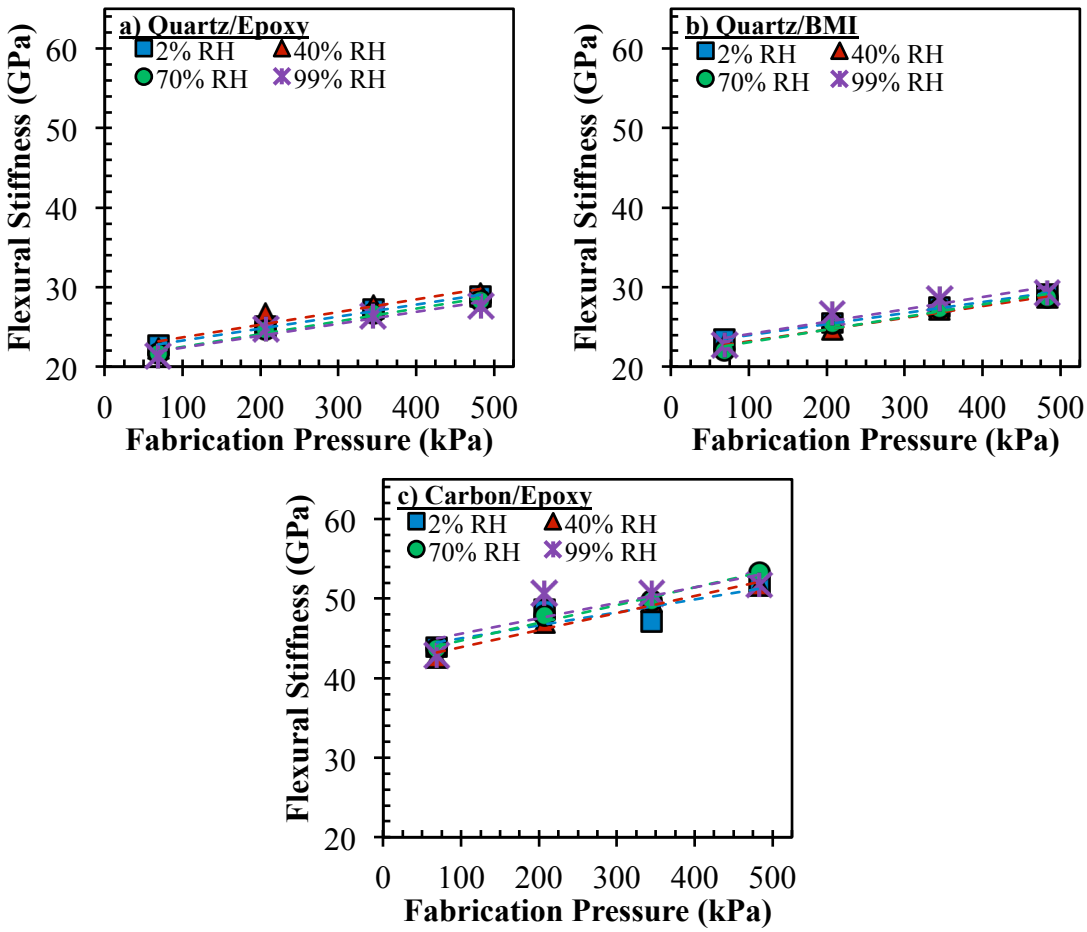

Figure 3.4 Effect of fabrication pressure on the flexural stiffness for (a) Quartz/Epoxy, (b) Quartz/BMI, and (c) Carbon/Epoxy

Table 3.2 Trend line equations for fabrication pressure effect on flexural stiffness

a) Quartz/Epoxy	Trend Line Equation	R^2 Value
2% RH	0.0151x + 21.78	0.9917
40% RH	0.0159x + 22.10	0.8986
70% RH	0.0161x + 20.89	0.9805
99% RH	0.0150x + 20.89	0.9427
b) Quartz/BMI		
2% RH	0.0139x + 22.57	0.9963
40% RH	0.0148x + 21.72	0.9896
70% RH	0.0159x + 21.49	0.9550
99% RH	0.0155x + 22.55	0.9007
c) Carbon/Epoxy		
2% RH	0.0163x + 43.38	0.7633
40% RH	0.0214x + 41.76	0.9665
70% RH	0.0223x + 42.49	0.9795
99% RH	0.0194x + 43.65	0.6987

3.2.6 Effect of Prepreg Humidity Exposure on Laminate Flexural Strength

The effect of prepreg conditioning on the laminate flexural strength for each material is shown in Figure 3.5. The polynomial trend line equations for each prepreg conditioning and fabrication pressure specimen are provided in Table 3.3. Each material demonstrated complex, polynomial-like behavior on flexural strength when considering humidity exposure. Therefore, 1st-order trend line representations (i.e. linear or power-function) of the flexural strength due to varying humidity exposure would not be as accurate an representation of flexural strength when compared to a polynomial function. Strength was lower when BMI resin (Figure 3.5b) was used instead of epoxy resin (Figure 3.5a). However, strength for BMI was not influenced to the same degree by changes in humidity. This is indicated by the tighter data groupings in Figure 3.5b, which represent an overall flexure strength delta of 178 MPa. Compared to the flexural strength delta of 405 MPa for epoxy resin. Additionally, utilizing BMI

for the resin material resulted in a local minimum for flexural strength near 70% relative humidity. Epoxy resin on the other hand generally had a local maximum near 50% relative humidity or an overall decline when fabrication pressure was low (i.e. 69 kPa). Both epoxy resin systems (Figure 3.5a and c) had initial strength values between 700-840 MPa that were in close proximity to each other at a specific fabrication pressure. However, the effect of humidity exposure was distinctly different for each fiber reinforcement type. Quartz reinforcement, shown in Figure 3.5a, was influenced by humidity to a larger degree. Meanwhile the flexural strength for carbon fiber reinforcement, shown in Figure 3.5c, declined slightly as humidity increased with a local minimum near 50%. There were instances for carbon fiber that was more sporadic and random in nature. For example, samples fabricated at 483 kPa demonstrated a large local minimum near 40% relative humidity, which was caused by the unusually low flexural strength for the specimens conditioned at 40% relative humidity. The overall trend of a slight decline as humidity increased from zero to 100% relative humidity remained true, therefore it is believed that this behavior was more likely due to uncertainties with experimental data.

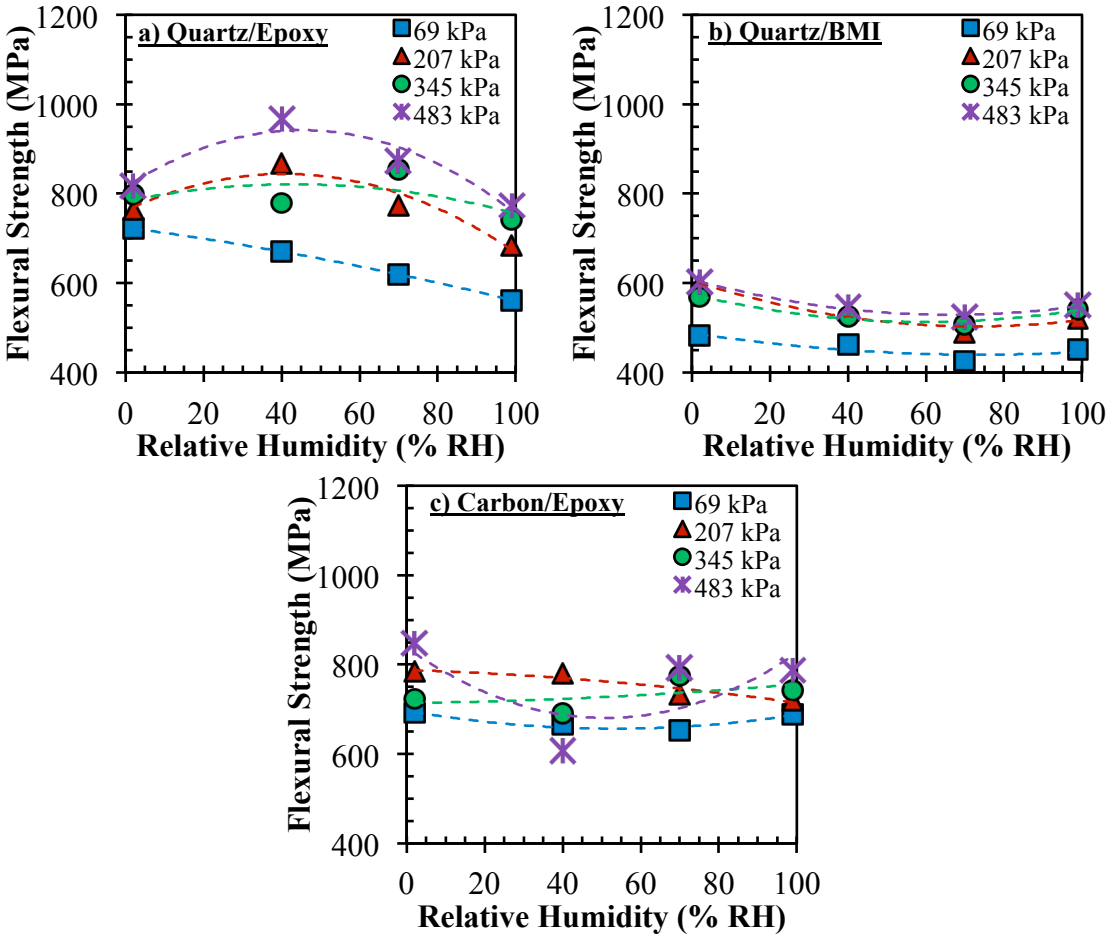

Figure 3.5 Effect of prepreg humidity exposure on the flexural strength for (a) Quartz/Epoxy, (b) Quartz/BMI, and (c) Carbon/Epoxy

Table 3.3 Trend line equations for prepreg humidity conditioning effect on flexural strength

a) Quartz/Epoxy	Trend Line Equation	R^2 Value
69 kPa	$-0.0049x^2 - 1.1531x + 724.37$	0.9999
207 kPa	$-0.0499x^2 + 4.0562x + 761.68$	0.9148
345 kPa	$-0.0201x^2 + 1.7347x + 783.48$	0.3410
483 kPa	$-0.0624x^2 + 5.6440x + 814.28$	0.9119
b) Quartz/BMI		
69 kPa	$0.0089x^2 - 1.3163x + 488.46$	0.7451
207 kPa	$0.0195x^2 - 2.8268x + 605.82$	0.9318
345 kPa	$0.0172x^2 - 2.0571x + 574.62$	0.9490
483 kPa	$0.0181x^2 - 2.3985x + 608.65$	0.9877
c) Carbon/Epoxy		
69 kPa	$0.0143x^2 - 1.5178x + 696.94$	0.8964
207 kPa	$-0.0047x^2 - 0.2647x + 787.93$	0.9013
345 kPa	$0.0031x^2 + 0.1091x + 713.90$	0.2584
483 kPa	$0.0605x^2 - 6.1662x + 837.74$	0.5018

3.2.7 Effect of Fabrication Pressure on Laminate Flexural Strength

The effect of applied cure pressure on the laminate flexural strength for each prepreg material is shown in Figure 3.6. The power-function trend line equations for each prepreg conditioning and fabrication pressure specimen are provided in Table 3.4. The R^2-values for the selected power-function trend lines for quartz/epoxy ranged from 0.71 to 0.99. Comparatively, the R^2-values for a linear representation ranged from 0.67 to 0.91. Therefore, a power-function trend line representation of the effect of fabrication pressure was selected as the best representation of laminate flexural strength for each prepreg material. The flexure strength increased as fabrication pressure increased for each prepreg material. Excluding dry humidity environments (i.e. 2% RH), the flexural strength for quartz/epoxy (Figure 3.6a) increased substantially as fabrication pressure increased. Disregarding the 2% relative humidity quartz/epoxy

prepreg, all quartz-reinforced materials, Figure 3.6a and b, had similar initial strength values ranging from 270-350 MPa. However, the rate of increase for epoxy was nearly double when compared to BMI. Therefore this results in a flexural strength range of 562-967 MPa and 425-602 MPa for quartz/epoxy and quartz/BMI, respectively. The flexural strength for carbon fiber reinforced laminates was influenced the least due to fabrication pressure, which was indicated by the smallest power functions of Figure 3.6c. One unusual characteristic noted in the carbon fiber specimens was a reduction in flexural strength once pressure increased above 207 kPa for prepregs conditioned at 40% relative humidity. This behavior is not observed at any other conditioning level or prepreg material, therefore this may be due to measurement uncertainties and is not believed to be a representation of the actual behavior of flexural strength for carbon fiber laminates.

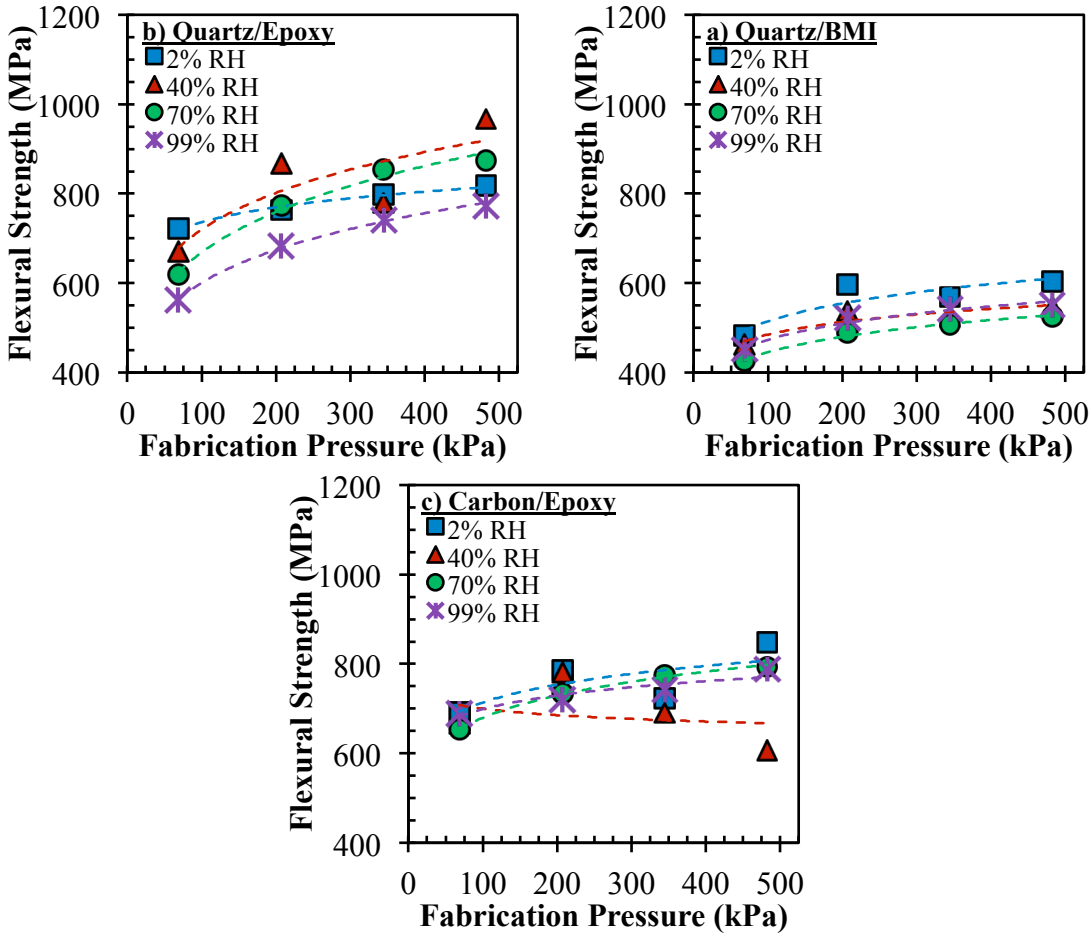

Figure 3.6 Effect of fabrication pressure on the flexural strength for (a) Quartz/Epoxy, (b) Quartz/BMI, and (c) Carbon/Epoxy

Table 3.4 Trend line equations for fabrication pressure effect on flexural strength

a) Quartz/Epoxy	Trend Line Equation	R^2 Value
2% RH	$548.34x^{0.064}$	0.9831
40% RH	$352.19x^{0.155}$	0.7146
70% RH	$287.70x^{0.183}$	0.9865
99% RH	$280.00x^{0.166}$	0.9963
b) Quartz/BMI		
2% RH	$312.95x^{0.108}$	0.7904
40% RH	$334.21x^{0.081}$	0.8506
70% RH	$270.20x^{0.108}$	0.9890
99% RH	$291.76x^{0.105}$	0.9679
c) Carbon/Epoxy		
2% RH	$498.27x^{0.078}$	0.5508
40% RH	$804.55x^{-0.030}$	0.0612
70% RH	$425.32x^{0.102}$	0.9976
99% RH	$525.75x^{0.062}$	0.8848

3.3 SUMMARY OF LAMINATE MECHANICAL PROPERTIES CHAPTER

The experimental procedure for determining the laminate mechanical properties in the form of flexural stiffness and flexural strength along with the associated results for the three aerospace-grade composite prepregs were introduced. Section 3.2.2 contained the resulting flexural stiffness and strength due to variations in prepreg relative humidity conditioning level and fabrication pressure. Generally, the flexural stiffness did not change significantly due to varying prepreg moisture contents and increased near-linearly as fabrication pressure increased. The flexural strength was generally maximized when relatively humidity conditioning decreased and fabrication pressure increased.

CHAPTER 4

CONTOUR PLOTS FOR LAMINATE MICROSTRUCTURE AND MECHANICAL PROPERTIES – COUPLED EFFECT OF PREPREG HUMIDITY EXPOSURE AND FABRICATION PRESSURE

The two processing parameters, prepreg humidity exposure and fabrication pressure, can influence the fiber volume fraction, void volume fraction, laminate flexural stiffness and laminate flexural strength in unique and complex ways. A common method to analyze the coupled contributions of two parameters is by using property function equations illustrated by contour plots. Then, unique behaviors such as local minimums or maximums, and sensitivities can be properly accounted for and documented. The remainder of this Chapter will introduce the property function equations selected to characterize each dependent variable and the associated contour plot analysis.

4.1 LITERATURE REVIEW OF MODELING TECHNIQUES FOR CONTOUR PLOT ANALYSIS

Surface model formation and analysis of two independent variables on the investigated phenomenon is commonly used in a variety of applications and research fields. Shen et al. [41] used multi-variant surface analysis in biomedical applications to investigate protein absorption. Kumar and Reddy [42] investigated the performance of polymer electrolyte membrane fuel cells using surface models with independent

variables of channel dimensions and shapes. Surface models were generated to locate the optimum efficiency values from a 6x6 grid of channel width and depth values. Campanelli et al. [43] studied the effect of various machining parameters (laser power, frequency, scanning speed, etc.) on the surface roughness of aluminum-magnesium alloys machined by laser milling. Contour plots of surface models were useful in illustrating trends and effects due to varying frequency and machining overlap. Yong and Hahn [44] investigated the effect of temperature and humidity on the moisture absorption characteristics of two glass/epoxy laminate systems. Nine unique combinations of temperature (30 to 90°C) and relative humidity level (30 to 90%) were used to generate up to a 2^{nd} order polynomial function of the experimental data to examine the trends and characteristics of moisture absorption.

Therefore, contour plots have been successfully used for a variety of research fields and topics to illustrate the coupled contribution of two parameters on the property of interest. A similar procedure will be used to examine the coupled effect of prepreg humidity conditioning and fabrication pressure on the following laminate properties: i) fiber volume fraction, ii) void volume fraction, iii) flexural stiffness, and iv) flexural strength.

4.2 FORMATION OF PROPERTY FUNCTION EQUATIONS TO GENERATE CONTOUR PLOTS

In order to explore the synergistic effect of prepreg relative humidity conditioning level and fabrication pressure on the laminate microstructure and flexural properties, functional equations were identified to illustrate variations of dependent variables via two-dimensional contour plots. Using these plots, the dependence as well as the

sensitivity of fiber volume fraction, void volume fraction, flexural stiffness and flexural strength due to prepreg humidity exposure and fabrication pressure can be better visualized. Furthermore, the possibility of the presence of local maximum or minimum property values can be better ascertained. For each contour plot, up to a 2^{nd}-order polynomial bivariate model was considered. Considering the identified trends in Chapters 2 and 3, each property function equation was developed to provide the most accurate assessment of the experimental data without over-constraining the solution. Additionally, each property function equation was normalized with respect to the maximum observed value. For example, if the maximum stiffness was 25.0 GPa for a prepreg material, that data point was assigned a normalized stiffness of 1.0. Meanwhile, if the stiffness for a different conditioning and fabrication treatment for the same prepreg material were 20.0 GPa, that data point would be assigned a normalized stiffness of 0.8. Normalization eases identification of similar process-induced property trends between the three-prepreg materials. A distinctive color bar scale was utilized to compare the extent of change among the property functions.

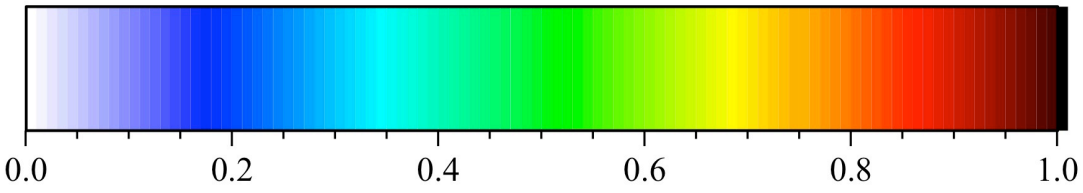

Figure 4.1 Colorbar scale used for contour plots of normalized property function values

4.3 IDENTIFICATION OF PROPERTY FUNCTIONAL EQUATIONS FOR NORMALIZED LAMINATE PROPERTIES

4.3.1 Contour Plots for Normalized Fiber Volume Fraction

The property function equation for normalized fiber volume fraction was developed based on the trends associated with changing prepreg humidity exposure and fabrication pressure, which was introduced in Sections 2.5.5 and 2.5.6. A functional equation that considers a linear contribution for prepreg humidity exposure and a power function contribution for fabrication pressure was selected as the most accurate representation of the dependent variable, normalized fiber volume fraction. Therefore, the functional equation for normalized fiber volume fraction (φ_{NF}) was:

$$\varphi_{NF} = C + C_{10}x^{A} + C_{11}xy + C_{01}y \tag{5}$$

where x is the fabrication pressure in kPa, y is the prepreg relative humidity conditioning level in % RH, and *A and C's* are parameter constants.

Contour plots of normalized fiber volume fraction are shown in Figure 4.2a-c. From Figure 4.2, it was observed that the fiber volume fraction was predominantly dependent on the fabrication pressure for all prepreg materials. The near vertical contour lines in Figure 4.2a indicated that prepreg humidity exposure had very little subsequent effect on the fiber volume fraction for quartz/epoxy laminates. Meanwhile, humidity exposure for quartz/BMI (Figure 4.2b) and carbon/epoxy (Figure 4.2c) prepreg systems had some influence on the laminate fiber volume fraction, particularly when fabrication pressure was high. BMI has been shown to absorb significantly more moisture than the epoxy resin, which may be contributing to the increased dependency on humidity exposure. However, the humidity dependency for carbon/epoxy prepregs

at high fabrication pressures is another issue. Since the epoxy resin is identical to that used with quartz-reinforcement shown in Figure 4.2a, the slight dependency observed with carbon fiber-reinforcement must be due to unique interactions with the fabric material. One possible reason is the weave structure of the two reinforcement materials. The IM7 carbon fiber fabric is constructed in a plain weave style, whereas the AQIII quartz fabric is constructed in a 4-harness satin weave style. Multi-layer plain weave fabric layups can collapse more easily at high cure pressures and can potentially extrude more resin during the fabrication process. This may cause the variations in fiber volume fraction demonstrated at high cure pressures, and also explains the larger fiber volume fraction (66.1%) when compared to that with quartz fiber reinforcement (62.6%). Each material demonstrated the largest rate of increase in fiber volume fraction when fabrication pressure was increased from a low initial level, which was indicated by the tighter contour lines in Figure 4.2. Generally, this trend was expected because the fibers' contribute more to supporting the applied load as fabrication pressure is increased, which results in less resin being squeezed out. Even though the general behavior is similar, the contours revealed that BMI resin varies at a larger rate than the epoxy resin. Therefore, a tighter window of fabrication cure pressure would be required to achieve a specific fiber volume fraction for products produced with BMI resin. The fiber volume fraction for both epoxy resin prepreg materials, shown in Figure 4.2a and c, changed by about 20%. Quartz-reinforcement was generally more consistent throughout the entire fabrication pressure range, whereas carbon fiber-reinforcement was offset with a majority of the change occurring at low cure pressures.

On the other hand, the fiber volume fraction for BMI resin, shown in Figure 4.2b, changed by nearly 30%.

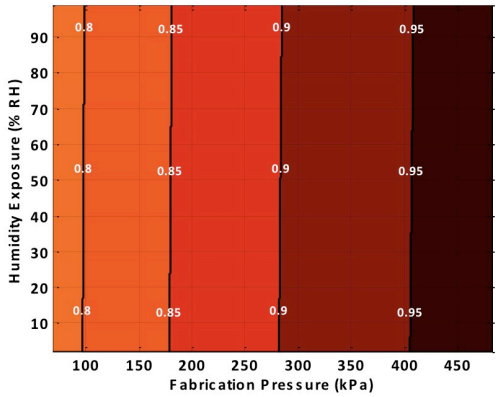

a) Quartz/Epoxy normalized fiber volume fraction (max = 62.6%)

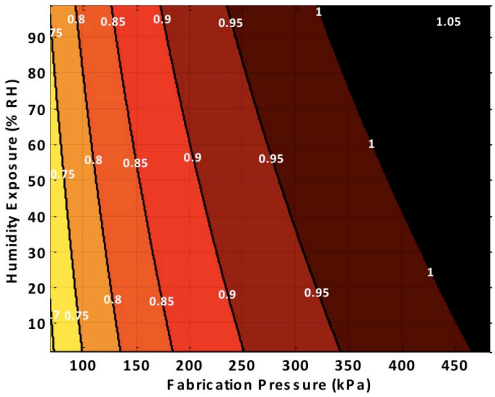

b) Quartz/BMI normalized fiber volume fraction (max = 66.8%)

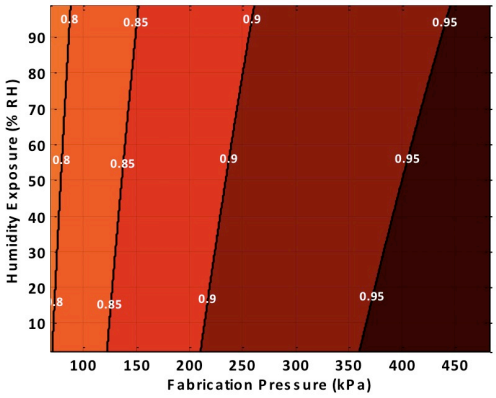

c) Carbon/Epoxy normalized fiber volume fraction (max = 66.1%)

Figure 4.2 Contour plots of normalized fiber volume fraction for (a) Quartz/Epoxy, (b) Quartz/BMI, and (c) Carbon/Epoxy

4.3.2 Contour Plots for Normalized Void Volume Fraction

The property function equation for normalized void volume fraction was developed based on the trends associated with changing prepreg humidity exposure and fabrication cure pressure, which was introduced in Sections 2.5.7 and 2.5.8. A functional equation

that considers a linear contribution for prepreg humidity exposure and a negative power function contribution for fabrication pressure was selected as the most accurate representation of the dependent variable, normalized void volume fraction. Therefore, the functional equation for normalized void volume fraction (φ_{NV}) was:

$$\varphi_{NV} = C + C_{10}x^{-A} + C_{11}xy + C_{01}y \quad (6)$$

where x is the fabrication pressure in kPa, y is the prepreg relative humidity conditioning level in % RH, and *A and C's* are parameter constants.

Contour plots of normalized void volume fraction are shown in Figure 4.3a-c. Unlike the behavior observed with fiber volume fraction, both prepreg humidity exposure and fabrication pressure significantly affected the void volume fraction. For all prepreg materials, the rate of increasing void volume fraction progressively increased as fabrication pressure declined and relatively humidity exposure increased. As expected, the contour plots clearly depict all material systems have the highest observed void fractions when laminates were produced at low pressure from prepregs conditioned at high relative humidity. This particular scenario results in the highest prepreg moisture content, which would vaporize to form voids during the heated cure cycle, and the lowest cure pressure, which would be unable to excrete or eliminate volatiles. Comparing Figure 4.3a and b, both quartz-reinforced laminates had similar maximum void volume fractions, which was 14.1% for epoxy resin and 13.9% for BMI resin. However, the quartz/BMI laminates had the smallest change in void fraction for varying levels of humidity exposure and fabrication pressure. At the minimum, the void fraction for BMI reduced to about 8%, or a normalized percent reduction of about 40%. Alternatively, the void volume fraction for quartz/epoxy was progressively

reduced to 1.7%, which represents a normalized percent reduction of 90%. Even at low humidity exposure levels, BMI absorbed significantly more moisture during the conditioning process. The absorbed moisture is the most likely cause of the high void fractions associated with BMI. The void volume fraction for carbon/epoxy laminates, shown in Figure 4.3c, reduced from 4.8% to 1.3% as pressure increased and humidity exposure decreased, which represents a normalized percentage range of approximately 70%. The lower range of void fractions for carbon fiber reinforcement is most likely attributed to the smaller fiber diameter, which facilitates full wetting of the fabric.

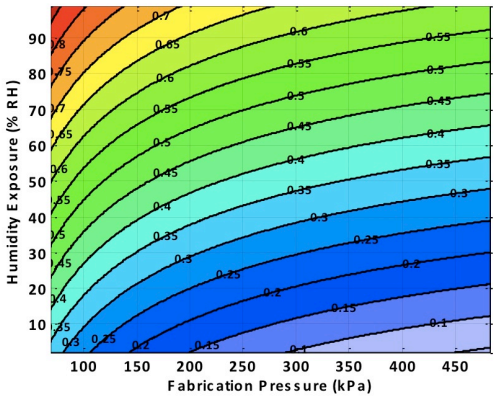

a) Quartz/Epoxy normalized void volume fraction (max = 14.1%)

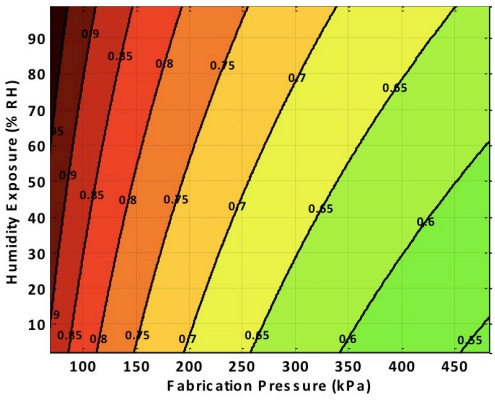

b) Quartz/BMI normalized void volume fraction (max = 13.9%)

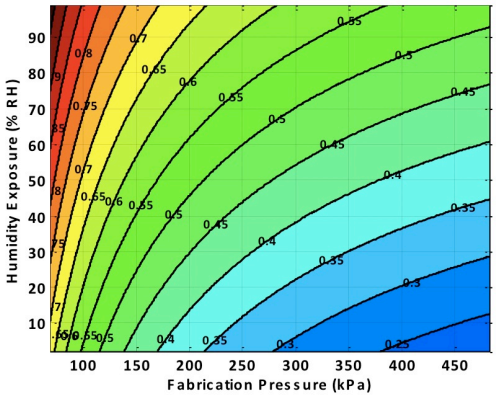

c) Carbon/Epoxy normalized void volume fraction (max = 4.8%)

Figure 4.3 Contour plots of normalized void volume fraction for (a) Quartz/Epoxy, (b) Quartz/BMI, and (c) Carbon/Epoxy

4.3.3 Contour Plots for Normalized Flexural Stiffness

The property function equation for normalized flexural stiffness was developed based on the trends associated with changing prepreg humidity exposure and fabrication pressure, which was introduced in Sections 3.2.4 and 3.2.5. A functional equation that considers a linear contribution for prepreg humidity exposure and a linear contribution for fabrication pressure was selected as the most accurate representation of the dependent variable, normalized flexural stiffness. Therefore, the functional equation for normalized flexural stiffness (φ_{NE}) was:

$$\varphi_{NE} = C + C_{10}x + C_{11}xy + C_{01}y \tag{7}$$

where x is the fabrication pressure in kPa, y is the prepreg relative humidity conditioning level in % RH, and *C's* are parameter constants.

Contour plots of normalized flexural stiffness are shown in Figure 4.4a-c. From Figure 4.4, it was observed that the flexural stiffness was primarily dependent on the fabrication pressure for all prepreg materials. From Section 4.3.1, humidity exposure was shown to not significantly affect the fiber volume fraction. Similarly, it would be expected that humidity exposure would not significantly affect the flexural stiffness, because stiffness is primarily a fiber-dominated phenomenon. This general behavior was confirmed by the near vertical contour lines in Figure 4.4, which indicate that humidity exposure had very little influence on the laminate flexural stiffness. Overall, the spacing between contour lines remained similar throughout the entire fabrication pressure range. The constant contour line spacing indicates near-linear increases in stiffness as fabrication pressure increases. Eventually, It would be expected that the stiffness rate of increase would begin to decline when significantly high cure pressures

are used. This would be caused by either i) fiber crushing damage due to excessive cure pressure or ii) achieving the upper fiber volume fraction limit for a structural-viable laminate. Regardless the resin system, the maximum flexural stiffness was 29.3 GPa for both quartz-reinforced prepreg materials, shown in Figure 4.4a and b. Additionally, each quartz-reinforced prepreg material had a normalized percent reduction of about 25%. Meanwhile, the flexural stiffness for carbon fiber-reinforcement was significantly higher, with a maximum of 53.3 GPa. The load-bearing capability of carbon fiber is well known to be superior when compared to quartz fiber, which is reflected by the higher flexural stiffness values. Carbon fiber-reinforcement also had a much narrower range of flexural stiffness values, as the normalized percent change was less than 20% for all fabricated specimens.

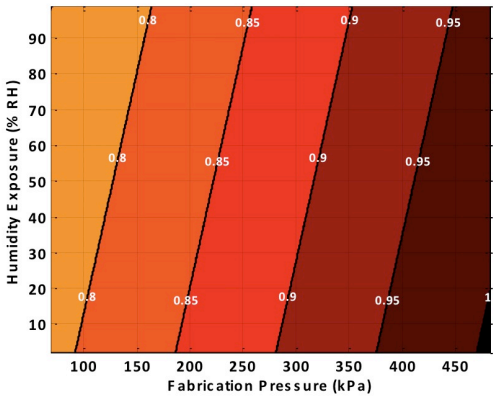

a) Quartz/Epoxy normalized flexural stiffness (max = 29.3 GPa)

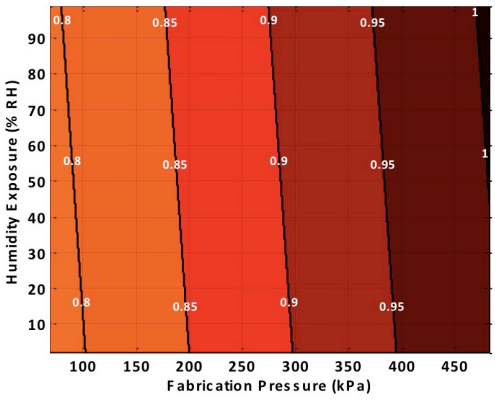

b) Quartz/BMI normalized flexural stiffness (max = 29.3 GPa)

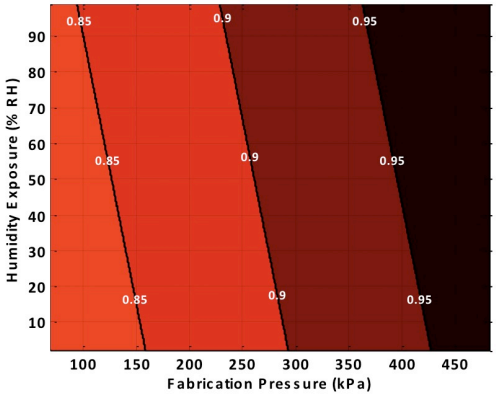

c) Carbon/Epoxy normalized flexural stiffness (max = 53.3 GPa)

Figure 4.4 Contour plots of normalized flexural stiffness for (a) Quartz/Epoxy, (b) Quartz/BMI, and (c) Carbon/Epoxy

4.3.4 Contour Plots for Normalized Flexural Strength

The property function equation for normalized flexural strength was developed based on the trends associated with changing prepreg humidity exposure and fabrication pressure, which was introduced in Sections 3.2.6 and 3.2.7. A functional equation that considers a 2nd-order polynomial contribution for prepreg humidity exposure and a power contribution for fabrication pressure was selected as the most accurate

representation of the dependent variable, normalized flexural strength. Therefore, the functional equation for normalized flexural strength ($\varphi_{N\sigma}$) was:

$$\varphi_{N\sigma} = C + C_{10}x^A + C_{11}xy + C_{02}y^2 + C_{01}y \quad (8)$$

where x is the fabrication pressure in kPa, y is the prepreg relative humidity conditioning level in % RH, and *A and C's* are parameter constants.

Contour plots of normalized flexural strength are shown in Figure 4.5a-c. From Figure 4.5, it was observed that both prepreg humidity exposure and fabrication pressure significantly affected flexural strength. Flexural strength requires a good fiber-matrix interface to transfer loads between plies; therefore any laminate defects can significantly degrade the strength potential of a composite laminate. Thus, an increase in void fraction should decrease the laminate flexural strength. The strength for quartz-reinforced laminates, shown in Figure 4.5a and b, follows this behavior very closely. The highest flexural strength was observed when humidity exposure was minimized and fabrication pressure was maximized, which resulted in the lowest void volume fraction for the prepreg materials. Additionally, the gap between contour lines was the closest in the same region when void fraction similarly had the closest intervals, which was at high humidity exposure and low fabrication pressure. An interesting note is the complex procedure required to improve strength for these laminates. If starting at a low fabrication cure pressure, a majority of improvement can be achieved simply by increasing the cure pressure. However, as pressure increases to higher amounts (greater than 350 kPa), it becomes increasingly necessary to reduce to humidity exposure level to continue improving the flexural strength. Resin type has a significant role on the maximum flexural strength, which is corroborated by BMI being much lower (603

MPa) when compared to epoxy (967 MPa). The normalized strength reduction for carbon/epoxy, shown in Figure 4.5c, was much lower than the two quartz-reinforced laminates. Additionally, the strength for carbon/epoxy laminates demonstrated no significant affect due to humidity changes. This may be due to the relatively low void fraction levels (4.8% maximum) when compared to the quartz-reinforced laminates (14% maximum).

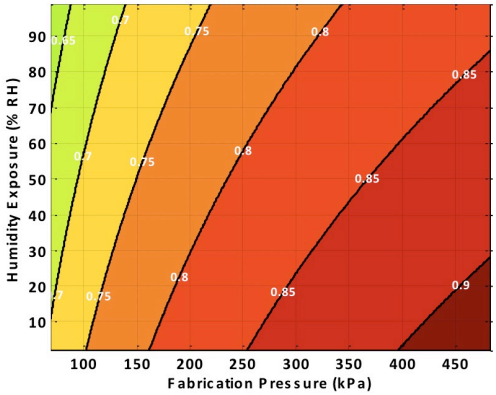

a) Quartz/Epoxy normalized flexural strength (max = 967.3 MPa)

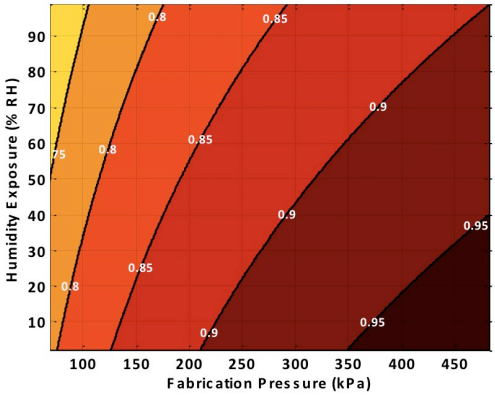

b) Quartz/BMI normalized flexural strength (max = 602.9 MPa)

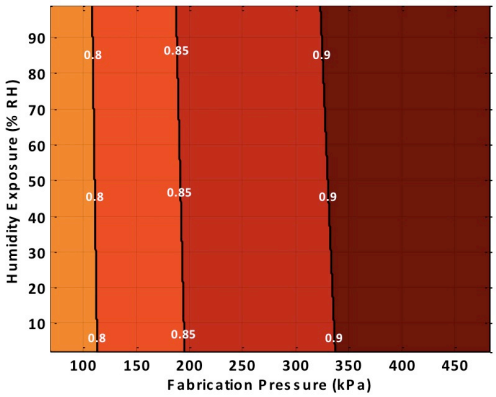

c) Carbon/Epoxy normalized flexural strength (max = 847.2 MPa)

Figure 4.5 Contour plots of normalized flexural strength for (a) Quartz/Epoxy, (b) Quartz/BMI, and (c) Carbon/Epoxy

4.4 SUMMARY OF CONTOUR PLOT CHAPTER

Contour plots were used to examine the synergistic relationship between prepreg humidity conditioning and fabrication pressure on some key laminate characterization properties, including fiber volume fraction, void volume fraction, flexural stiffness, and flexural strength. Sections 4.3.1 and 4.3.2 introduced the property function equations related to the fiber volume fraction and void volume fraction, respectively. Fiber volume fraction was primarily dependent on changing fabrication pressure, whereas the void fraction demonstrated a more complex relationship between pressure and relative humidity. The property function equations associated with flexural stiffness and flexural strength was presented in Sections 4.3.3 and 4.3.4, respectively. Changes in fabrication pressure were the primary influence in varying the laminate flexural stiffness. Meanwhile, a more complex coupled interaction of both prepreg humidity exposure and fabrication pressure was responsible for varying the laminate flexural strength for quartz-reinforced laminates. Flexural strength for carbon fiber-reinforced laminates seemed to be primarily influenced by changing cure pressure.

PART B: HYDRAULIC FLUID CONTAMINATION EFFECTS

In this part, the focus is to characterize the effect that long-term contamination with an aerospace-grade hydraulic fluid has on the performance and durability of the composite prepregs. First, the effect of varying prepreg moisture contents and fabrication pressures on the composite laminates propensity to absorb hydraulic fluid will be discussed. Then, the effect long-term hydraulic fluid contamination on the laminate flexural properties will be compared to the dry baseline condition presented earlier.

Work related to this part of the Dissertation has been published in:

- "Prepreg Moisture Content and Fabrication Pressure Effects on Moisture and Hydraulic Fluid Absorption Behavior of Quartz/BMI Laminates", Manuscript under review (2017).
- "Long-term Liquid Contamination Effects on Flexure Properties of Composite Prepregs with Varying Moisture Contents and Fabrication Pressures", *Composite Structures,* Manuscript in progress (2017).
- "The Coupled Effect of Microvoids and Hydraulic Fluid Absorption on Mechanical Properties of Quartz/BMI Laminates", *American Society of Composites 29th Technical Conference,* (2014). San Diego, CA, 226.
- "Processing Effects on Formation of Microvoids and Hydraulic Fluid Absorption of Quartz/BMI Laminates", *ASME International Mechanical Engineering Congress & Exposition,* (2015). Houston, TX, IMECE2015-53717.
- "Effect of Microvoids on Anomalous Moisture Absorption of Quartz/BMI Composite Laminates", *ASME International Mechanical Engineering Congress & Exposition,* (2014). Montreal, Canada, IMECE2014-38407.
- "Laminate Processing Effect on Microvoids and Hydraulic Fluid Absorption of Quartz/BMI Laminates", *20th International Conference on Composite Materials,* (2015). Copenhagen, Denmark, ICCM/20-5109-4.
- "The Coupled Effect of Fiber Volume Fraction and Void Content on Hydraulic Fluid Absorption of Quartz/BMI Laminates", *31st International Conference of the Polymer Processing Society,* (2015). Jeju Island, Korea, PPS31-S11-325.
- "Experimental and Theoretical Investigation of Non-Fickian Moisture Absorption of Quartz/BMI Laminates Fabricated by Preconditioned Prepregs", *31st International Conference of the Polymer Processing Society,* (2015). Jeju Island, Korea, PPS31-S11-342.

CHAPTER 5

HYDRAULIC FLUID ABSORPTION BEHAVIOR OF AEROSPACE-GRADE LAMINATES: COUPLED EFFECT OF PREPREG HUMIDITY EXPOSURE AND FABRICATION PRESSURE

High-performance aerospace-grade composite materials are frequently exposed to a variety of liquid contaminants through routine operating conditions. Absorbed fluids in polymer structures can have a detrimental effect on the durability or affect the reliability of other subsystems around the structure, such as electronics calibration. Therefore it is necessary to accurately characterize the liquid absorption for a polymer system and to ascertain the extent of damage on the composite material. The remainder of this Chapter will present the experimental procedure used to contaminate the three prepregs with an aerospace-grade hydraulic fluid. A hindered diffusion model approach [45-47] was used to determine the equilibrium fluid content at each humidity conditioning level and fabrication pressure for each prepreg material.

5.1 LITERATURE REVIEW OF MODELING TECHNIQUES FOR FLUID ABSORPTION IN COMPOSITE MATERIALS

Fiber-reinforced composite laminates are well known to be susceptible to fluid intake, which can potentially degrade their performance and reduce their effective service life. Even a relatively low level of moisture absorption in polymers and

composites can result in resin plasticization, swelling, and residual stresses in the material; which are correlated to be the primary sources of material property degradation. Perez-Pacheco et al. [48] reported that 0.75 wt%. moisture absorption for a carbon/epoxy composite resulted in a reduction of tensile strength, elastic modulus and interfacial shear strength by 25%, 38% and 11%, respectively. Pomies and Carlsson [49] reported that 1.21% absorbed water in carbon/epoxy and 0.63% absorbed water in carbon/BMI reduced the transverse tensile strength by 66% and 41%, respectively. Other studies have observed losses in tensile strength [50], interlaminar shear strength [51], and transverse flexural strength [52] of different composite structures as a result of absorbed moisture. Bismaleimide (BMI) is a high-performance resin system commonly used in aerospace applications as a radome or engine cowl material. Moisture absorption behavior and laminate degradation of BMI resin has been addressed occasionally in varying detail [10,11,49] but not as extensively as fiber-reinforced epoxy laminates [5,48,50-55]. This is most likely due to the relatively specialized applications of BMI systems when compared to more universally applicable epoxy-based systems. The effects of hydraulic fluid absorption on BMI systems are even more limited in research [56]. Excessive mechanical property degradation due to moisture or hydraulic fluid absorption limits the design and effectiveness of composites in environmentally harsh conditions. Therefore, it is essential to predict the fluid absorption behavior of a composite laminate so as to account for any losses in performance or durability.

5.2 EXPERIMENTAL PROCEDURE FOR LIQUID ABSORPTION STUDY

From each prepreg conditioning type and fabrication pressure, six specimens with planar dimensions 31.5 mm by 31.5 mm were prepared for absorption testing. Prior to fluid exposure, any initial moisture present in the composite specimens was removed by drying the specimens in a vacuum-oven at 40°C until an equilibrium weight was achieved. The dried specimens were immersed in sealed glass containers filled with hydraulic fluid. The temperature of each glass container was maintained at room temperature (25°C) with a Thermo Scientific water bath, as shown in Figure 5.1. Immersion studies for polymers are routinely conducted at room temperature because it provides a good baseline analysis on the interactions between the polymer and penetrant. Temperatures greater than room temperature will frequently cause more rapid diffusion of the penetrant.

Figure 5.1 Thermo Scientific constant temperature water bath used for hydraulic fluid absorption of composite laminates

The fluid uptake for a given immersion time period was periodically measured with a high-precision analytical balance. A significant amount of hydraulic fluid remains on the laminate surface after removing the specimen from the immersion container. Additionally, the level of applied pressure and duration (i.e. hand drying) used to remove the surface fluid significantly affects the measured fluid content. Therefore, a detailed drying procedure using a lint-free cloth was developed for removing surface fluid that minimizes human contact and was easily repeatable. The time required to remove surface fluid and weigh specimens was subtracted from the total fluid exposure time. Typically, less than 10 minutes was necessary to complete the entire procedure of removal, surface drying, weighing, and re-immersion for each series of six specimens. The percentage mass gain of each specimen was calculated by:

$$M_{exp}(t) = 100\left[\frac{m_i(t) - m_0}{m_0}\right] \tag{9}$$

where $m_i(t)$ is the measured instantaneous mass of the specimen, and m_0 is the initial dried mass of the specimen. Experimental hydraulic fluid mass gain data was collected over a period of 24 months for quartz-reinforced laminates and 18 months for carbon fiber-reinforced laminates. All gravimetric data reported in this Chapter is an average of six specimens for a specific laminate series with uncertainty levels calculated using 95% confidence.

5.3 LONG-TERM HYDRAULIC FLUID ABSORPTION

5.3.1 Quartz/BMI (AQIII/BMI) Absorption

The fluid mass gain for Quartz/BMI laminates subjected to long-term exposure to hydraulic fluid is shown in Figure 5.2. After two years of immersion, the fluid mass

gain ranged from 2.7-8.5 %wt. for laminates fabricated at low pressure (69 kPa) and reduced to 1.4-4.1 %wt. for laminates fabricated at high pressure (483 kPa). The largest reduction in fluid mass gain was observed when fabrication pressure was increased from 69 kPa to 207 kPa. Additional increases in fabrication pressure above 207 kPa did not reduce the fluid content to the same degree. This also correlates closely with the fiber volume fraction at each fabrication pressure, in that the largest delta was observed between 69 and 207 kPa. For an absorption period up to approximately $hr^{0.5} \approx 25.0$, the hydraulic fluid diffusion was very rapid when humidity exposure was greater than 40% relative humidity, regardless of the fabrication pressure. Longer exposure periods (i.e. greater than $hr^{0.5} \approx 25.0$) resulted in a more gradual fluid uptake profile. The rate of fluid uptake for the second range of absorption gradually declined as fabrication pressure increased. After two years of immersion, three distinct regions were observed in the absorption data that correlates with the relative humidity exposure level. Prepregs conditioned in a dry environment (i.e. 2% RH) exhibited the lowest fluid contents, of about 1.2-2.7 %wt. Prepregs conditioned in a mild environment (i.e. 40% RH) exhibited a mid-range fluid content range, of about 3.1-6.1 %wt. Prepregs conditioned in a humid environment (i.e. 70% and 99% RH) exhibited the highest fluid content range, of about 4.1-8.5 %wt. The fluid mass gain was slightly larger for prepregs conditioned at 70% relative humidity when compared to prepregs conditioned at 99% relative humidity. This may be due to uncertainties inherent with experimental measurements. Both of these conditioning levels can be deduced as statistically similar as the 95% confidence intervals intersect the means. Regardless, the overall trend of an increase in fluid absorption as humidity exposure increases is clearly evident at all

fabrication pressures. Higher fabrication pressures resulted in smaller sampling variations, which is indicated by the smaller confidence intervals in Figure 5.2d.

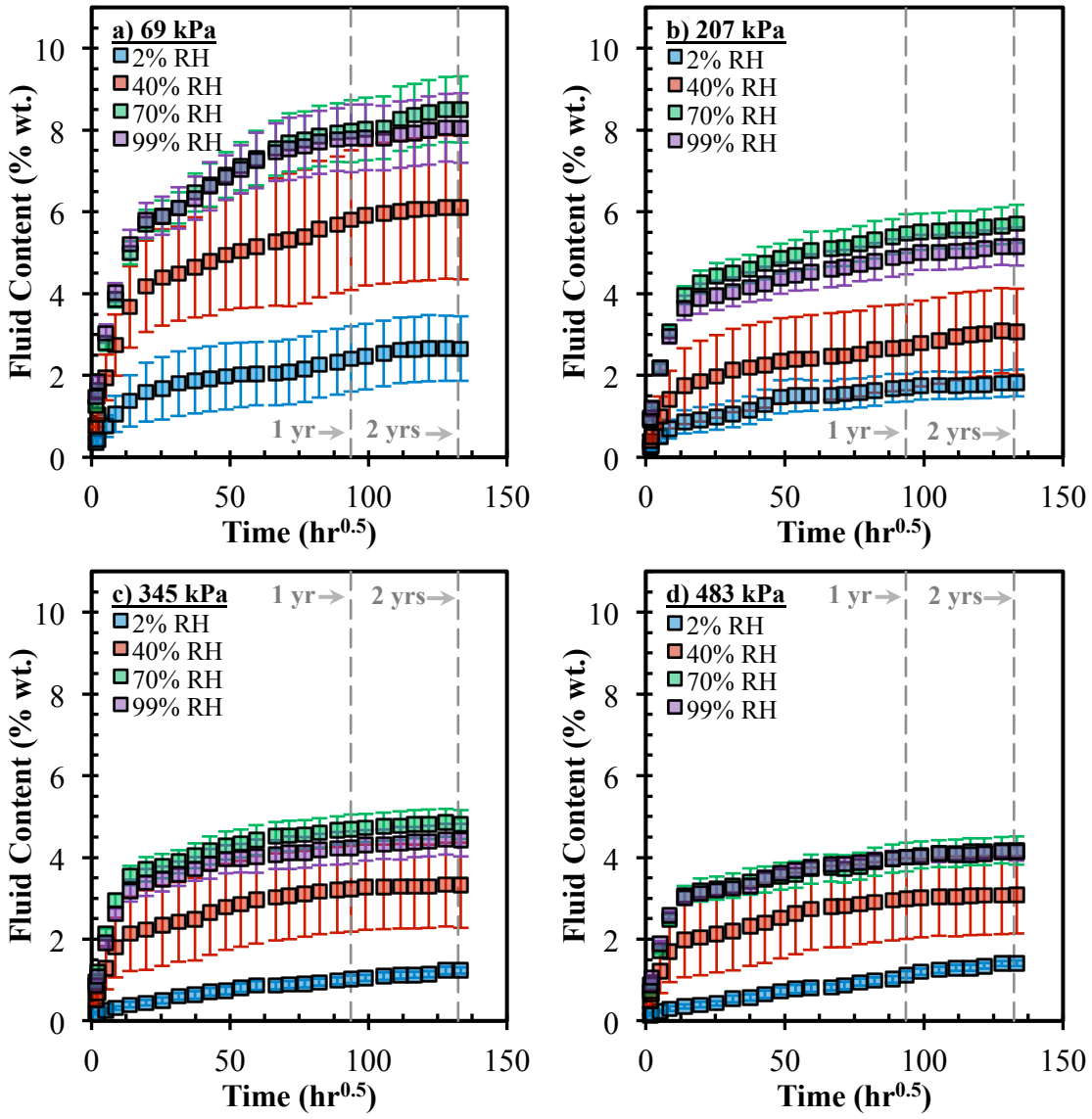

Figure 5.2 Long-term (24 months) hydraulic fluid absorption for conditioned AQIII/BMI prepregs cured at fabrication pressures of (a) 69 kPa, (b) 207 kPa, (c) 345 kPa, and (d) 483 kPa. Error bars associated with 95% confidence for n=6 samples

5.3.2 Quartz/Epoxy (AQIII/EX-1522) Absorption

The fluid mass gain for Quartz/Epoxy laminates subjected to long-term exposure to hydraulic fluid is shown in Figure 5.3. According to the manufacturers' data sheet, EX-1522 epoxy resin was modified specifically to reduce fluid absorption. This is confirmed by the fluid mass gain for epoxy resin being significantly lower than BMI resin presented in Section 5.3.1. The fluid mass gain ranged from 0.5-1.2 %wt. for laminates fabricated at a low pressure (69 kPa) and reduced slightly to 0.4-1.0 %wt. as fabrication pressure increased. Generally, hydraulic fluid uptake was more gradual when compared to the absorption behavior of BMI. Prepregs conditioned at 99% relative humidity had the most apparent two-stage absorption behavior with rapid diffusion up to $hr^{0.5} \approx 20.0$, followed by a more gradual uptake. Additionally, the fluid content for 99% relative humidity specimens was significantly higher than any other conditioning treatment level. This is most likely due to these specimens having the highest void volume fractions. At a given fabrication pressure, the laminate fiber volume fraction was very similar for quartz/epoxy laminates, which was discussed in Section 2.5.6. Therefore, the effect of high void fractions, which serve as storage sites for liquid, is clearly illustrated in this case. Sampling variation increased as prepreg humidity exposure increased, which is indicated by the larger confidence intervals for 99% relative humidity specimens in Figure 5.3.

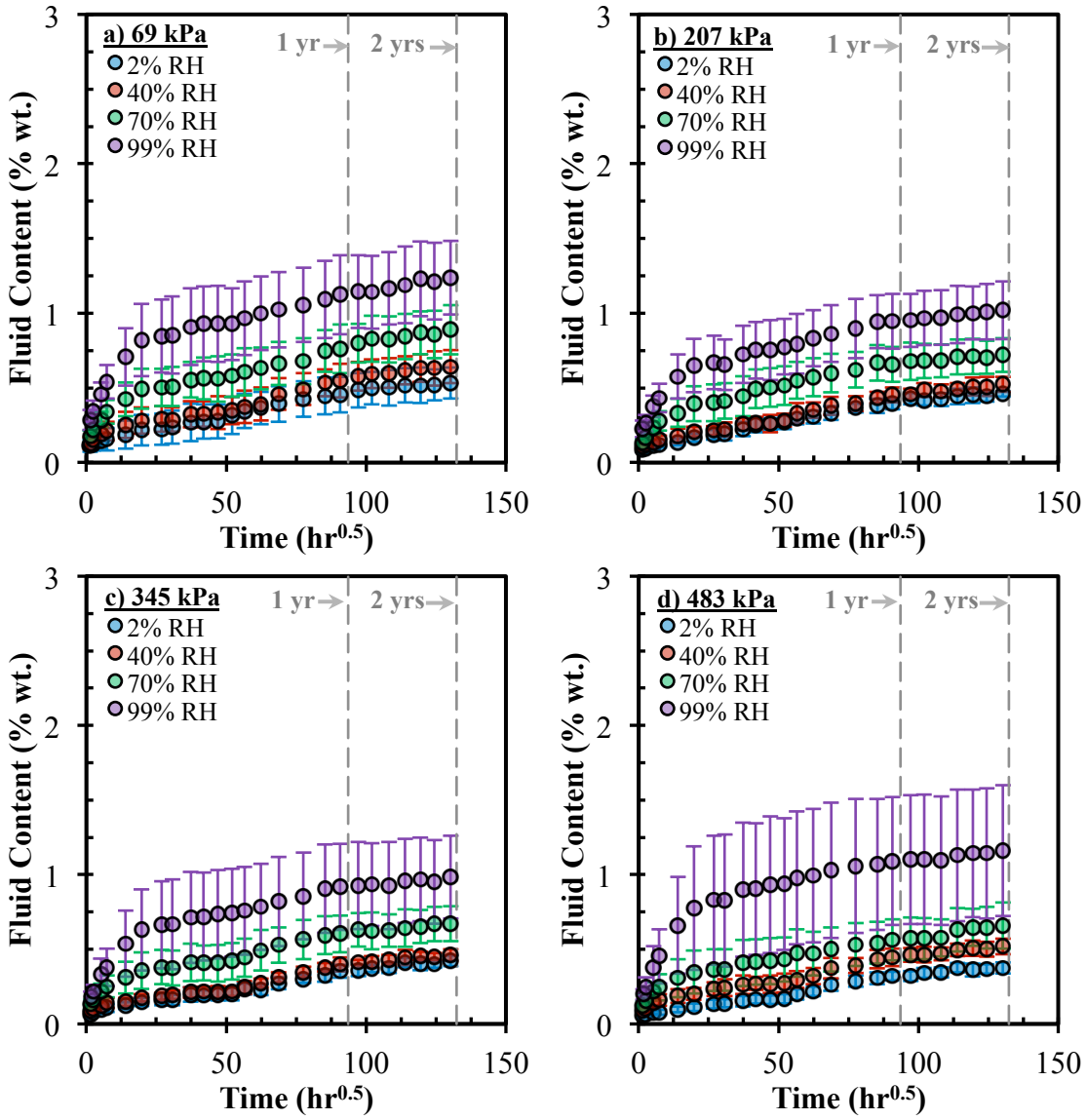

Figure 5.3 Long-term (24 months) hydraulic fluid absorption for conditioned AQIII/EX1522 prepregs cured at fabrication pressures at (a) 69 kPa, (b) 207 kPa, (c) 345 kPa, and (d) 483 kPa. Error bars associated with 95% confidence for n=6 samples

5.3.3 Carbon/Epoxy (IM7/EX-1522) Absorption

The fluid mass gain for Carbon/Epoxy laminates subjected to long-term exposure to hydraulic fluid is shown in Figure 5.4. The fluid mass gain for IM7/EX-1522 laminates

was similar to that for quartz-reinforced epoxy laminates (AQIII/EX-1522). Again, this was expected as the EX-1522 resin was designed to inhibit fluid absorption. When humidity exposure was less than 70% relative humidity, the fluid mass gain ranged from 1.1-1.8 %wt. for laminates fabricated at a low pressure (69 kPa) and reduced to 0.7-1.1 %wt. for laminates fabricated at a high pressure (483 kPa). The fluid mass gain for laminates fabricated from 99% relative humidity prepregs was similar (1.8-2.1 %wt.) and had large sampling variance, regardless of the fabrication pressure. As humidity exposure increased, the two-stage hydraulic fluid absorption behavior became more prevalent. Generally, rapid diffusion took place up to $hr^{0.5} \approx 14.0$, followed by consistent fluid uptake at lower rate. From Figure 5.4, carbon-reinforced epoxy laminates continue to absorb hydraulic fluid after 18 months exposure and does not appear to be approaching saturation.

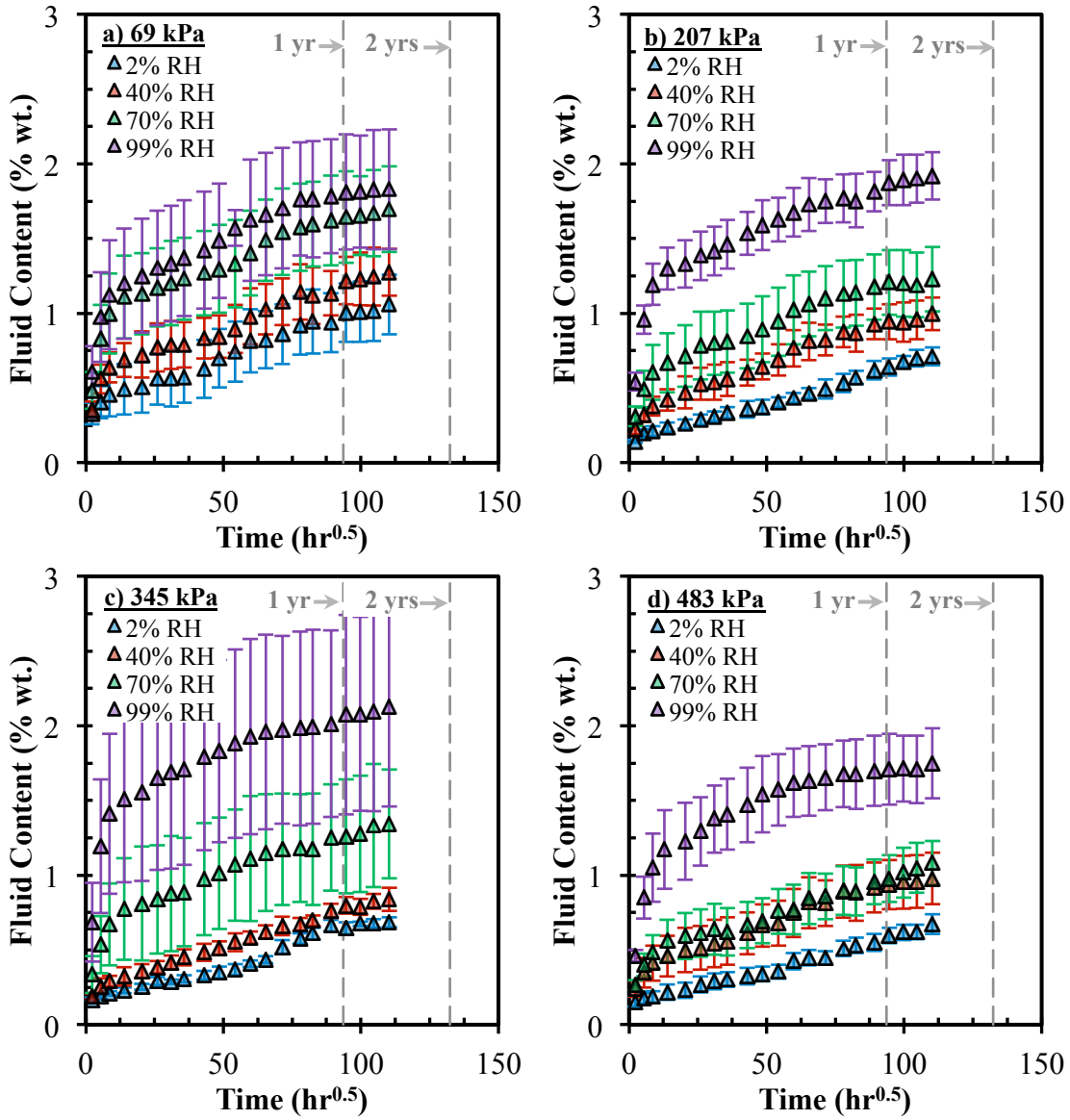

Figure 5.4 Long-term (18 months) hydraulic fluid absorption for conditioned IM7/EX1522 prepregs cured at fabrication pressures of (a) 69 kPa, (b) 207 kPa, (c) 345 kPa, and (d) 483 kPa. Error bars associated with 95% confidence for n=6 samples

5.4 FOUNDATION FOR APPLYING THE HINDERED DIFFUSION MODEL TO HYDRAULIC FLUID ABSORPTION

Significant efforts have been made to accurately model liquid absorption behavior of polymers. The most common absorption model applied to composites laminates is

the one-dimensional case of Fickian second law of diffusion with appropriate correction factors to account for edge effects. The widespread use of Fickian-based models partially stems from their ease of use as the ASTM D30 committee recommends the Fickian-based characterization, outlined in the D5229 standard. This approach is suitable when characterizing through-the-thickness absorption for single-phase, Fickian solid materials. In many cases, these methods can be insufficient when investigating anisotropic materials or samples with finite dimensions [57]. Moisture absorption behavior reported in literature often varies widely among different polymer systems and conditions, which often necessitates the use of non-Fickian diffusion models [45-47,58-61]. Among the most common non-Fickian models are the "Langmuir-type" model of diffusion [59] and time-varying diffusivity models [58,60,61]. Grace and Altan [45,46] recently developed a three-dimensional hindered diffusion model (HDM) that considers material anisotropy by proposing an alternative mechanism for anomalous moisture uptake behavior based on polymer-penetrant interaction. This interaction has the effect of hindering diffusion of mobile molecules. Given the same maximum moisture content, moisture uptake in the presence of diffusion hindrance lags behind the absorption in a purely Fickian diffusion process. Previously, this model has been used successfully to model anomalous moisture uptake for quartz/BMI systems [47].

Fickian second law of diffusion has often been used to characterize the absorption of liquid penetrants into polymers and composites. However, there are several limitations that can affect the accuracy of this approach. Limitations of Fickian diffusion can include considering specimens with finite dimensions, anisotropic materials, variations in laminate microstructural features and possible chemical

interactions between the liquid penetrants and polymer molecules. Therefore, the hindered diffusion model (HDM) proposed by Grace and Altan [45] was developed for applications considering anisotropic, three-dimensional cases of liquid absorption of thermosetting composites. The hindered diffusion model extends the one-dimensional, Langmuir-type diffusion model [59]. Details regarding the formulation of the hindered diffusion model and method for recovering liquid absorption parameters have been investigated in recent publications [45-47]. The following contains a brief overview of the hindered diffusion model approach and its application within this study.

An analytical solution for the hindered diffusion model can be obtained for three-dimensional, anisotropic composite laminates. The analytical solution yields temporal and spatial evolution of unbound and bound moisture concentrations, *n(x, y, z, t)* and *N(x, y, z, t)*, respectively. The total mass gain, *M(t)*, of a three-dimensional composite can be determined by integrating the unbound and bound concentrations over the specimen volume. The hindered diffusion model approach used in this study was a one-dimensional case because one specimen size with an aspect ratio of 1.0 was used. Additionally, the research objective for this study was to evaluate the equilibrium fluid content for varying prepreg humidity exposures and fabrication pressures, which can be determined using a one-dimensional approach. The one-dimensional expression for total mass gain, *M(t)*, is:

$$M(t) = M_{\infty}\left\{\begin{array}{l} 1-\dfrac{8}{\pi^2}\displaystyle\sum_{p=1}^{\infty(odd)}\dfrac{\left[r_p^{+}exp\left(-r_p^{-}t\right)-r_p^{-}exp\left(-r_p^{+}t\right)\right]}{p^2\left(r_p^{+}-r_p^{-}\right)}+ \\ \dfrac{8}{\pi^2}\left(\dfrac{k\beta}{\gamma+\beta}\right)\displaystyle\sum_{p=1}^{\infty(odd)}\dfrac{\left[exp\left(-r_p^{-}t\right)-exp\left(-r_p^{+}t\right)\right]}{r_p^{+}-r_p^{-}} \end{array}\right\} \tag{10}$$

where,

$$r_p^{\pm} = \frac{1}{2}\left[(kp^2 + \gamma + \beta) \pm \sqrt{(kp^2 + \gamma + \beta)^2 - 4k\beta p^2}\right] \quad (11a)$$

$$k = \frac{\pi^2 D_Z}{H^2} \quad (11b)$$

One critical parameter of interest in Equation 10 that describes the absorption behavior of composites is the equilibrium fluid content, M_∞. The equilibrium fluid content can be used to determine the extent of damage due to varying prepreg humidity exposure and fabrication pressure. Absorption parameters were determined by the steepest descent optimization method, which minimizes the least square error function, or the summation of square of the difference between the model prediction that contains the equilibrium fluid content and the experimental mass gain data. The equilibrium fluid content for all hindered diffusion model fits presented in the next Sections will be determined from an absorption period of five years, or $hr^{0.5} \approx 210$.

5.5 HINDERED DIFFUSION MODEL PREDICTION

5.5.1 Quartz/BMI (AQIII/BMI) Absorption Model and Equilibrium Fluid Content

The hindered diffusion absorption prediction and experimental mass gain data for quartz/BMI laminates is shown in Figure 5.5. The equilibrium fluid contents associated with the model fits for quartz/BMI laminates are provided in Table 5.1. The hindered diffusion model had good correlation with the experimental mass gain data for all prepreg humidity exposure levels and fabrication pressures. Generally, the equilibrium fluid content reduced in a power function like behavior as the fabrication pressure increased. This is evident by the largest incremental reduction in equilibrium fluid content occurring when fabrication pressure increased from 69 kPa to 207 kPa. The

hindered diffusion model fits indicate that the experimental mass gain data have achieved near saturation for nearly all humidity exposure levels and fabrication pressures. The lone exceptions was observed for prepregs conditioned at 2% relative humidity and fabricated at 69 kPa, and to a lesser degree at 483 kPa. After two years, the experimental mass gain for 2% RH – 69 kPa specimens was at 2.7 %wt. Meanwhile, the equilibrium fluid content prediction was 3.1 %wt., or a further increase of approximately 13%. However, a closer examination of the experimental mass gain data revealed that the measured fluid contents have been within 0.05 %wt. for over eight months. Therefore, it can be deduced that this specimen series is also nearing equilibrium and a few more months of consistent mass gain data will correct the over-prediction currently being observed with the hindered diffusion model prediction.

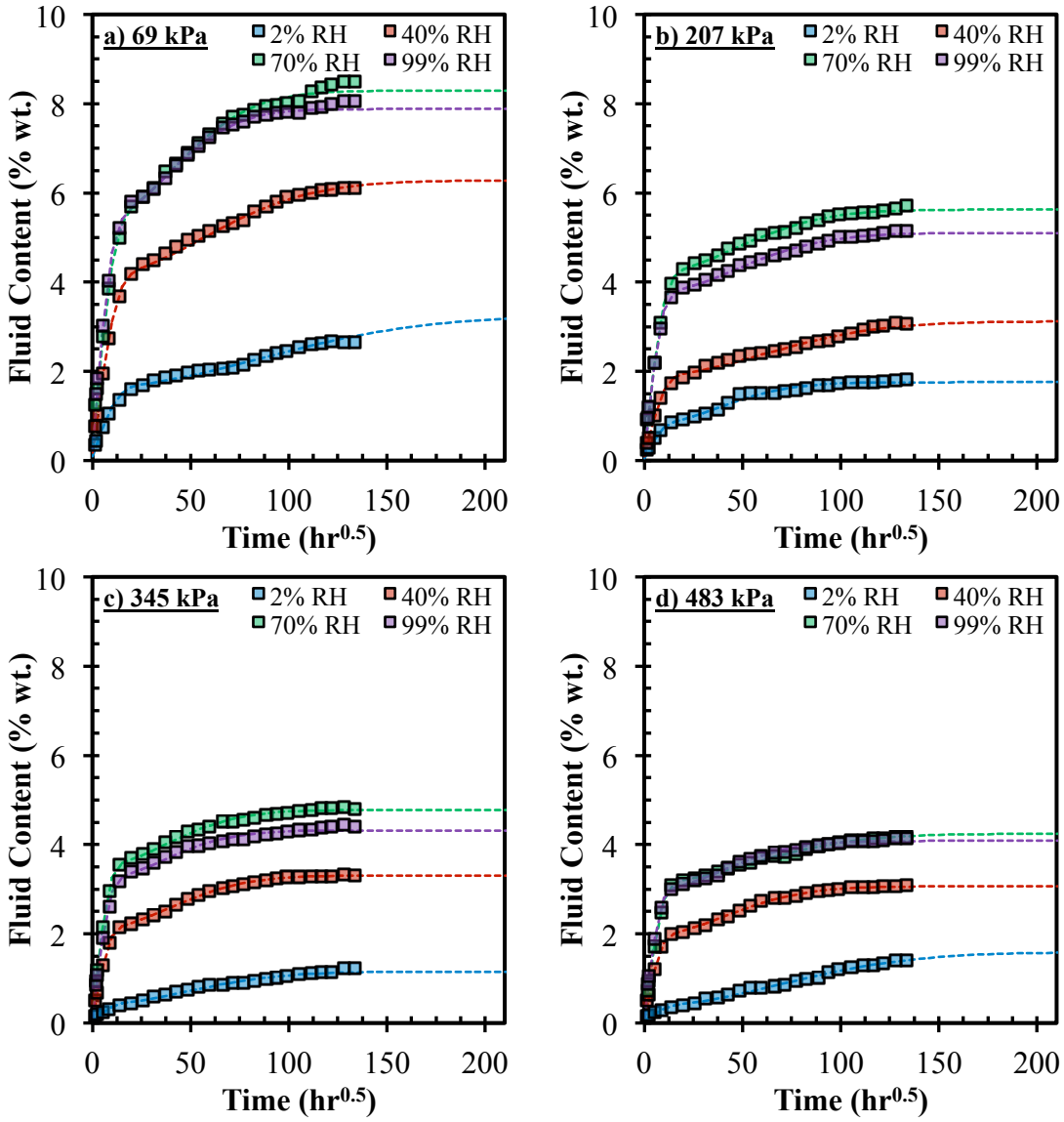

Figure 5.5 Five-year hindered diffusion model prediction for conditioned AQIII/BMI prepregs cured at fabrication pressures of (a) 69 kPa, (b) 207 kPa, (c) 345 kPa, and (d) 483 kPa

Table 5.1 Equilibrium fluid content for AQIII/BMI hydraulic fluid absorption

		Fabrication Pressure			
		69 kPa	*207 kPa*	*345 kPa*	*483 kPa*
Prepreg Humidity Exposure	*2% RH*	3.10	1.76	1.20	1.58
	40% RH	6.19	3.32	3.31	3.07
	70% RH	8.34	5.66	4.79	4.24
	99% RH	7.91	5.14	4.33	4.09

5.5.2 Quartz/Epoxy (AQIII/EX-1522) Absorption Model and Equilibrium Fluid Content

The hindered diffusion absorption prediction and experimental mass gain data for quartz/epoxy laminates is shown in Figure 5.6. The equilibrium fluid contents associated with the model fits for quartz/epoxy laminates are provided in Table 5.2. Similar to the model predictions for BMI, the hindered diffusion model had good correlation with the quartz/epoxy experimental mass gain data for all prepreg humidity exposure levels and fabrication pressures. The equilibrium fluid content reduced slightly as the fabrication pressure increased. Hindered diffusion models indicate that the experimental mass gain data for quartz/epoxy laminates are nearing saturation after two years of contamination. This observation is particularly true as fabrication pressure increased to higher levels. For example, the experimental mass gain data for all specimens fabricated at 69 kPa were within 6.2-15.6% of the equilibrium fluid content. Comparatively, the mass gain data for specimens fabricated at 483 kPa were within 2.0-10.5% of the equilibrium fluid content.

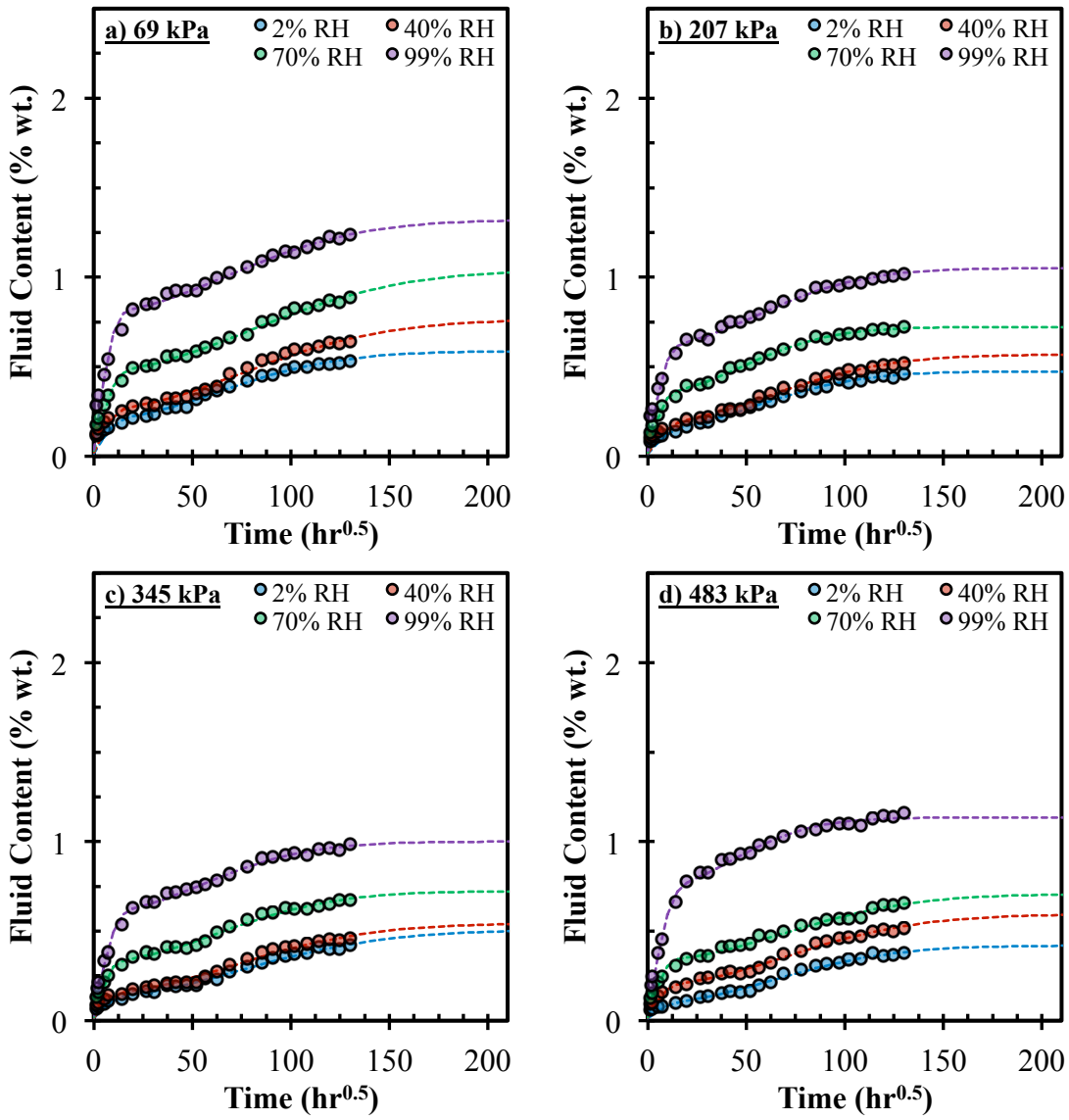

Figure 5.6 Five-year hindered diffusion model prediction for conditioned AQIII/EX-1522 prepregs cured at fabrication pressures of (a) 69 kPa, (b) 207 kPa, (c) 345 kPa, and (d) 483 kPa

Table 5.2 Equilibrium fluid content for AQIII/EX-1522 hydraulic fluid absorption

Prepreg Humidity Exposure	Fabrication Pressure			
	69 kPa	*207 kPa*	*345 kPa*	*483 kPa*
2% RH	0.59	0.47	0.51	0.42
40% RH	0.76	0.57	0.54	0.59
70% RH	1.04	0.72	0.72	0.71
99% RH	1.32	1.05	1.00	1.13

5.5.3 Carbon/Epoxy (IM7/EX-1522) Absorption Model and Equilibrium Fluid Content

The hindered diffusion absorption prediction and experimental mass gain data for carbon/epoxy laminates is shown in Figure 5.7. The equilibrium fluid contents associated with the model fits for carbon/epoxy laminates are provided in Table 5.3. The equilibrium fluid content reduced slightly as the fabrication pressure increased. For several prepreg conditioning treatments and fabrication pressures, the experimental mass gain data for carbon/epoxy laminates have not appeared to approach saturation after 18 months of contamination. One limitation of the hindered diffusion model approach is that pseudo-equilibrium (i.e. first stage absorption complete with continuing gradual absorption) must be achieved to validate the absorption parameters. Thus, accurately determining the equilibrium fluid content proved troublesome for several specimen series. Therefore, additional exposure time is required in order to conclusively determine the extent of damage (i.e. equilibrium fluid content) for carbon/epoxy laminates.

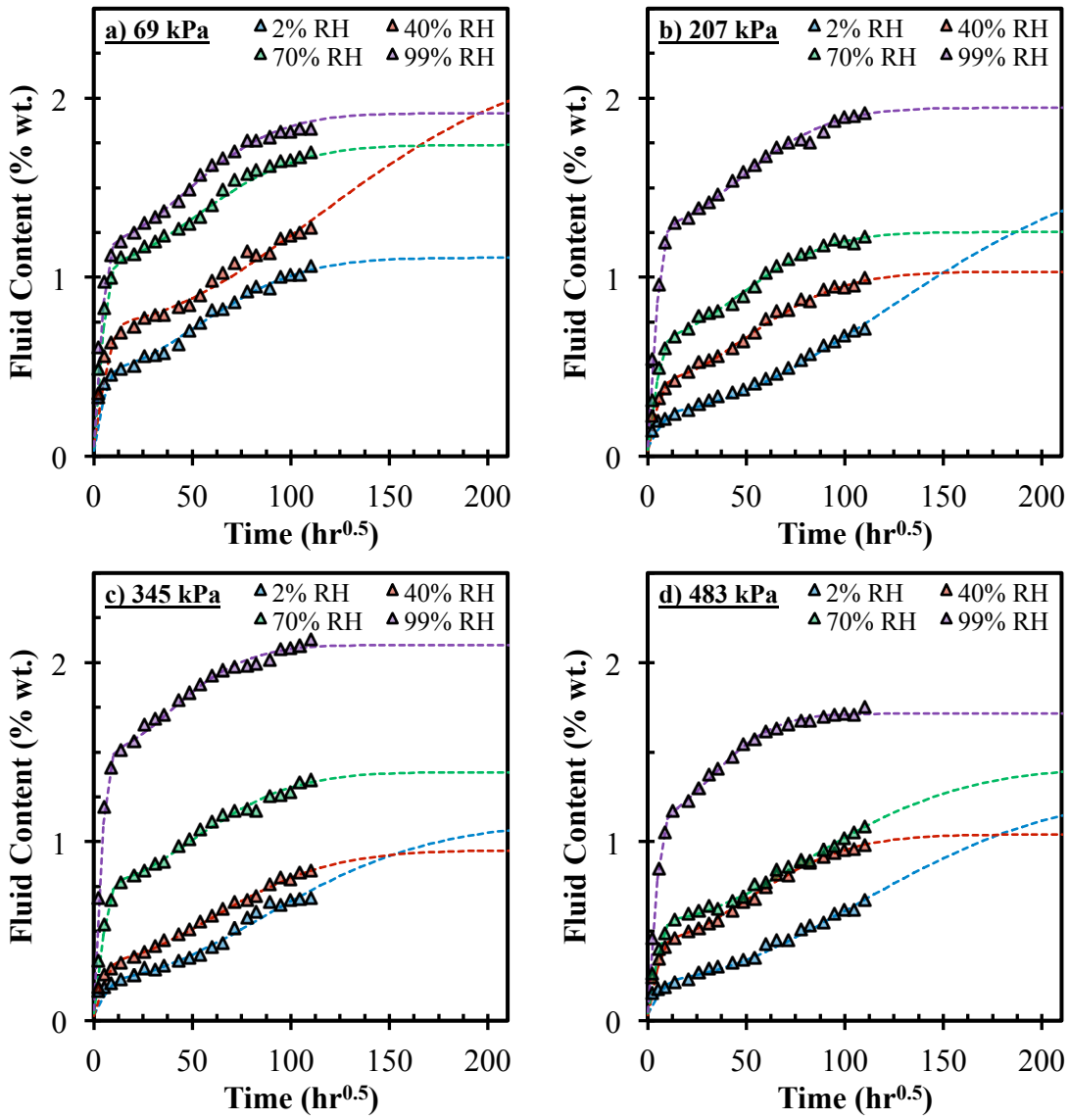

Figure 5.7 Five-year hindered diffusion model prediction for conditioned IM7/EX-1522 prepregs cured at fabrication pressures of (a) 69 kPa, (b) 207 kPa, (c) 345 kPa, (d) 483 kPa

Table 5.3 Equilibrium fluid content for IM7/EX-1522 hydraulic fluid absorption

Prepreg Humidity Exposure	Fabrication Pressure			
	69 kPa	*207 kPa*	*345 kPa*	*483 kPa*
2% RH	1.11	1.68	1.10	1.29
40% RH	2.25	1.03	0.95	1.04
70% RH	1.74	1.25	1.39	1.42
99% RH	1.92	1.95	2.10	1.71

5.6 COMPARISON OF EQUILIBRIUM FLUID CONTENT FOR QUARTZ-REINFORCED LAMINATES

This Section will contain additional analysis of the equilibrium fluid content determined from the hindered diffusion model for quartz/BMI and quartz/epoxy laminates. Comparing the experimental mass gain data and the hindered diffusion model indicated that both of these prepreg materials were near saturation. Therefore, the equilibrium fluid content can be considered a good indicator of the effect that humidity exposure and fabrication pressure had on the level of fluid absorption.

5.6.1 Effect of Humidity Exposure on Equilibrium Fluid Content

The effect of prepreg conditioning on the equilibrium fluid content for quartz/BMI and quartz/epoxy is shown in Figure 5.8. The trend line equations for each prepreg conditioning and fabrication pressure specimen are provided in Table 5.4. For both resin materials, the equilibrium fluid content increased as relative humidity exposure increased. However, the effect was much more pronounced for BMI resin. Additionally, the equilibrium fluid content was significantly higher for laminates fabricated at 69 kPa. Meanwhile, the equilibrium fluid content was grouped tightly together for all other fabrication pressures. This closely mirrors the laminate fiber volume fraction for each material, where the largest incremental improvement was achieved when pressure was increased from 69 kPa to 207 kPa. The rate of increase for equilibrium fluid content was significantly higher, by six fold, for BMI when compared to epoxy resin. The rate of increase for quartz/BMI (Figure 5.8a) gradually declined as fabrication pressure increased. This indicates that prepreg humidity exposure must be closely monitored and accounted for when fabrication pressures are low so as to limit

hydraulic fluid absorption. The rate of increase for quartz/epoxy (Figure 5.8b) was very similar, regardless of the fabrication pressure. Therefore, the equilibrium fluid content is influenced to a larger degree by the fabrication cure pressure.

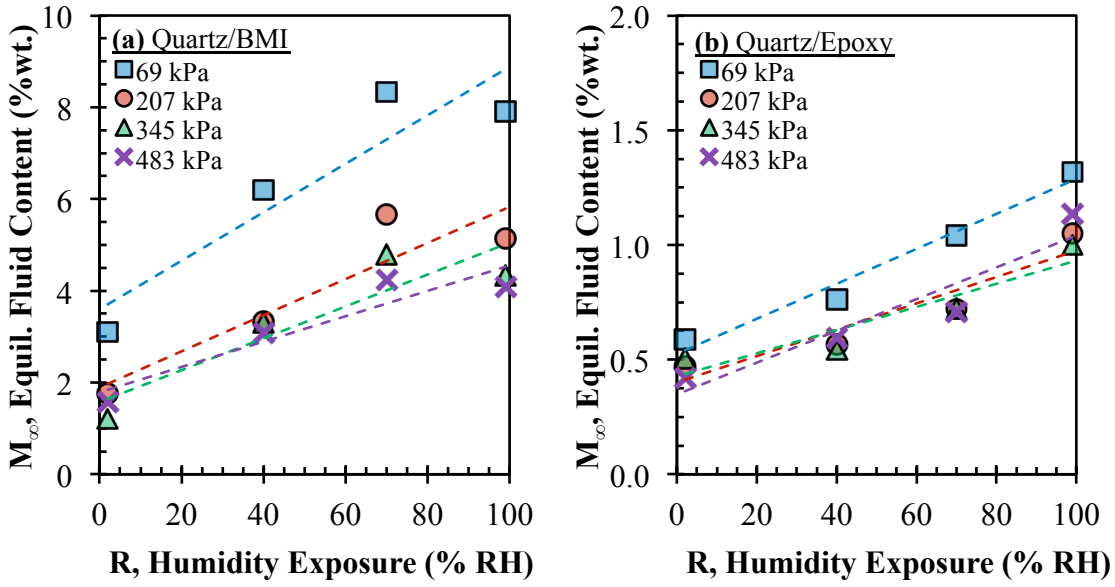

Figure 5.8 Effect of humidity exposure on equilibrium fluid content for quartz-reinforced (AQIII) laminates with either (a) BMI resin or (b) EX-1522 epoxy resin

Table 5.4 Trend line equations for effect of humidity exposure on equilibrium fluid content of quartz-reinforced laminates

	Quartz/BMI		**Quartz/Epoxy**	
	Trend Line Fit	*R^2-Value*	*Trend Line Fit*	*R^2-Value*
69 kPa	0.053R + 3.599	0.8510	0.008R + 0.525	0.9724
207 kPa	0.039R + 1.893	0.8413	0.006R + 0.401	0.8916
345 kPa	0.035R + 1.575	0.8171	0.005R + 0.427	0.8638
483 kPa	0.027R + 1.787	0.8766	0.007R + 0.349	0.8916

5.6.2 Effect of Fabrication Pressure on Equilibrium Fluid Content

The effect of fabrication pressure on the equilibrium fluid content for quartz/BMI and quartz/epoxy is shown in Figure 5.9. The trend line equations for each prepreg conditioning and fabrication pressure specimen are provided in Table 5.5. The best trend line fits for equilibrium fluid content as a function of fabrication pressure was achieved by applying power functions. Quartz/BMI generally had higher accuracy of the model fits when compared to quartz/epoxy. Equilibrium fluid content was also more sensitive to changes in fabrication pressure for BMI, which was indicated by the larger exponential values for this material when compared to epoxy. Generally the rate of decrease for BMI was two or three times that for epoxy. This indicates that the applied cure pressure contributes significantly to the amount of hydraulic fluid absorbed for BMI resin applications.

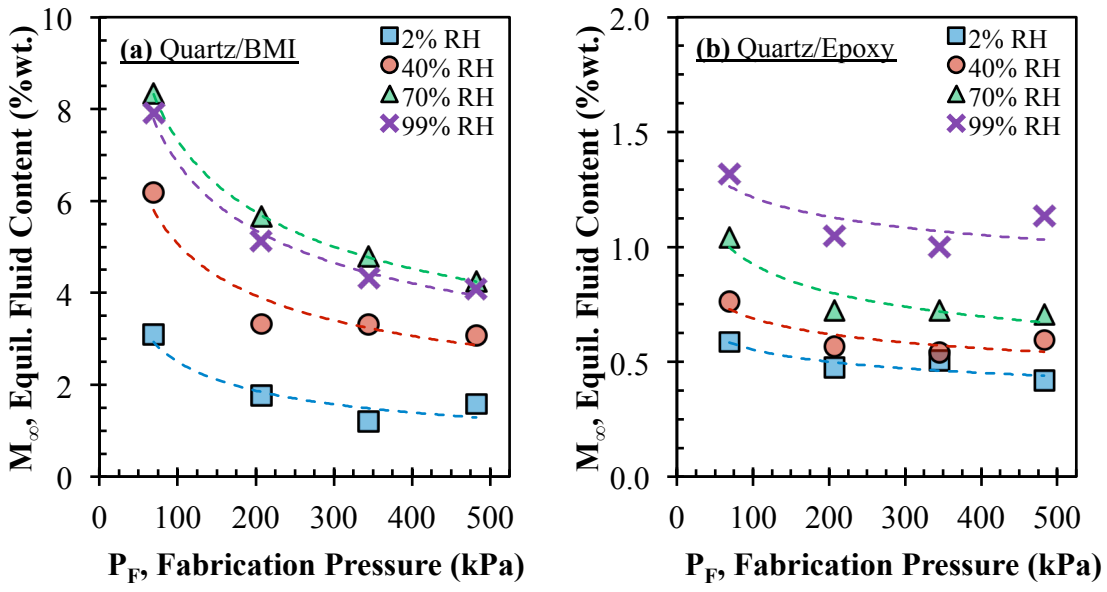

Figure 5.9 Effect of fabrication cure pressure on equilibrium fluid content for quartz-reinforced (AQIII) laminates with either (a) BMI resin or (b) EX-1522 epoxy resin

Table 5.5 Trend line equations for effect of fabrication pressure on equilibrium fluid content of quartz-reinforced laminates

	Quartz/BMI		**Quartz/Epoxy**	
	Trend Line Fit	*R^2-Value*	*Trend Line Fit*	*R^2-Value*
2% RH	$17.412P_F^{-0.421}$	0.8066	$1.082P_F^{-0.146}$	0.7793
40% RH	$27.019P_F^{-0.363}$	0.8911	$1.384P_F^{-0.151}$	0.7167
70% RH	$36.070P_F^{-0.346}$	0.9998	$2.361P_F^{-0.204}$	0.8614
99% RH	$34.030P_F^{-0.349}$	0.9883	$1.969P_F^{-0.105}$	0.5407

5.7 SUMMARY OF LIQUID ABSORPTION BEHAVIOR CHAPTER

This Chapter introduced the effect of long-term hydraulic fluid contamination for the three aerospace-grade composite prepregs. The equipment and experimental procedure used to conduct the long-term absorption study was presented in Section 5.2.

Then, Section 5.3 introduced the long-term experimental absorption data and initial assessment on the effect of varying humidity exposure and fabrication cure. Quartz-reinforced laminates and carbon fiber-reinforced laminates were exposed to hydraulic fluid for a period of 24 months and 18 months, respectively. There are many techniques used for modeling the effect of liquid contaminants in polymer materials, which were discussed in Section 5.4. The hindered diffusion model has been shown to accurately characterize the absorption behavior for anisotropic materials, including the materials used in this study. The equilibrium fluid content determined from the hindered diffusion model indicated that quartz/BMI (Section 5.5.1) and quartz/epoxy (Section 5.5.2) specimens were at or nearing saturation after 24 months of absorption. Alternatively, many carbon/epoxy specimens (Section 5.5.3) continue to absorb fluid after 18 months and do not appear to be approaching saturation. Finally, a comparison of the effect of resin material selection (BMI or epoxy) with identical fiber reinforcement (AQIII Quartz) on the equilibrium fluid content was discussed in Section 5.6. The equilibrium fluid content for BMI resin was shown to be more sensitive to variations in prepreg humidity exposure and fabrication cure pressure when compared to the EX-1522 epoxy resin.

CHAPTER 6

THE EFFECT OF LONG-TERM HYDRAULIC FLUID CONTAMINATION ON FLEXURAL PROPERTIES FOR QUARTZ-REINFORCED LAMINATES

The consensus among researchers is that an increase in void fraction will reduce mechanical performance and cause laminates to be more susceptible to fluid absorption or fatigue damage [1,2,18,20-23,25]. The magnitude of void effect on these parameters is a matter of debate however. A majority of research is focused on the effect on mechanical performance at discrete levels of fiber volume fraction, void volume fractions, or fluid contents. However, a detailed study that examines the combined effect of prepreg humidity exposure, fabrication pressure, and fluid absorption on the mechanical performance has not been reported. Since voids primarily influence matrix-dominated phenomena in laminates, a majority of void research has focused on the laminate flexural strength [15-22, 24, 35]. The remainder of this Chapter will introduce the experimental procedure used to contaminate the two quartz-reinforced prepregs with an aerospace-grade hydraulic fluid. The effect of hydraulic fluid on flexural properties was conducted for quartz-reinforced prepregs because the hindered diffusion model analysis, presented in Chapter 5, indicated that these material systems have approached near saturation. Flexural testing was conducted in accordance with ASTM Standards and identically to the procedure for baseline testing presented in Chapter 3.

6.1 EXPERIMENTAL PROCEDURE FOR HYDRAULIC FLUID ABSORPTION OF QUARTZ-REINFORCED FLEXURAL SPECIMENS

The same experimental equipment and procedure used for hydraulic fluid absorption was used for long-term contamination of flexural specimens described in this Chapter. A summary of the experimental procedure follows, which was described in detail in Section 5.2. Six flexural specimens for each prepreg humidity exposure level and fabrication pressure with approximate planar dimensions of 57 mm by 12.7 mm were prepared for absorption testing. Prior to fluid exposure, any initial moisture present in the composite specimens was removed by drying the specimens in a vacuum-oven at 40°C until an equilibrium weight was achieved. The dried specimens were immersed in sealed glass containers filled with hydraulic fluid. The temperature of each glass container was maintained at room temperature (25°C) with a Thermo Scientific water bath. Similar to the absorption specimens presented in Chapter 5, a significant amount of hydraulic fluid remained on the laminate surface after removing the specimen from the immersion container. Surface fluid was removed from each specimen with a lint-free cloth prior to measuring the fluid uptake for a given immersion time period with a high-precision analytical balance. The fluid absorption was monitored periodically until near-saturation was observed in the mass gain measurements and validated with hindered diffusion model predictions. Equilibrium was achieved for the quartz-reinforced laminates after an absorption period of 21 months. All gravimetric data reported in this Chapter is an average of six specimens for a specific laminate series with uncertainty levels calculated using 95% confidence. After equilibrium, the flexural properties were determined in accordance with the ASTM testing standard for

fiber-reinforced polymers D790. The ASTM Standard D790 was used to determine flexural properties of dry specimens, presented in Section 3.2. Flexural properties were determined from a bar of rectangular cross section resting on two supports and loaded using a nose located midway between the two supports.

With regards to the flexural testing conducted in this study, the support span-to-depth ratio for all prepreg specimens was chosen to be 20:1. This value was chosen because (i) it allowed for a larger span-to-depth ratio to account for the laminated composite specimens, (ii) specimen overall lengths were within the range of useable space for the fabricated laminates, and (iii) was identical to the baseline study presented in Section 3.2. All specimens ruptured prior to the 5.0% maximum strain threshold, and loading was conducted at the specified strain rate of 0.01 mm/mm/min. The flexural properties for hydraulic fluid contaminated specimens were compared with the baseline (i.e. dry) flexural stiffness and flexural strength, presented in Sections 3.2.2 and 3.2.3, respectively. Percent reductions of flexural properties (stiffness and strength) were calculated to evaluate the extent of damage due to hydraulic fluid contamination. The percent reduction, $\%_{red}$, of each specimen series was calculated by:

$$\%_{red} = 1 - \left[\frac{Wet}{Dry}\right] \tag{12}$$

where *Wet* is the flexural stiffness or strength after 21 months of hydraulic fluid contamination, and *Dry* is the flexural stiffness or strength of the baseline study presented in Section 3.2.

6.2 HYDRAULIC FLUID ABSORPTION FOR QUARTZ-REINFORCED LAMINATES

6.2.1 Long-term Hydraulic Fluid Absorption for Quartz/BMI (AQIII/BMI) Flexural Specimens

The fluid mass gain for Quartz/BMI flexural specimens subjected to long-term hydraulic fluid exposure is shown in Figure 6.1. The maximum fluid mass gain ranged from 3.1-8.9 %wt. for laminates fabricated at a low pressure (69 kPa) and reduced to 1.4-4.2 %wt. for laminates fabricated at a high pressure (483 kPa). The average fluid content for flexural specimens was generally slightly greater than the square (aspect ratio 1.0) absorption specimens presented in Section 5.3.1. This may be attributed to some variations with the void volume fraction, or unique interactions due to the different specimen planar dimensions. Similar absorption behavior was observed between the flexural specimens and square-shaped specimens. Such as the largest reduction in fluid mass gain occurring when fabrication pressure increased from 69 kPa to 207 kPa. Additionally, the fluid mass gain was slightly larger for prepregs conditioned at 70% relative humidity when compared to prepregs conditioned at 99% relative humidity for fabrication pressures up to 345 kPa. Additional comparisons between the two specimen planar dimensions will be discussed in the following Sections.

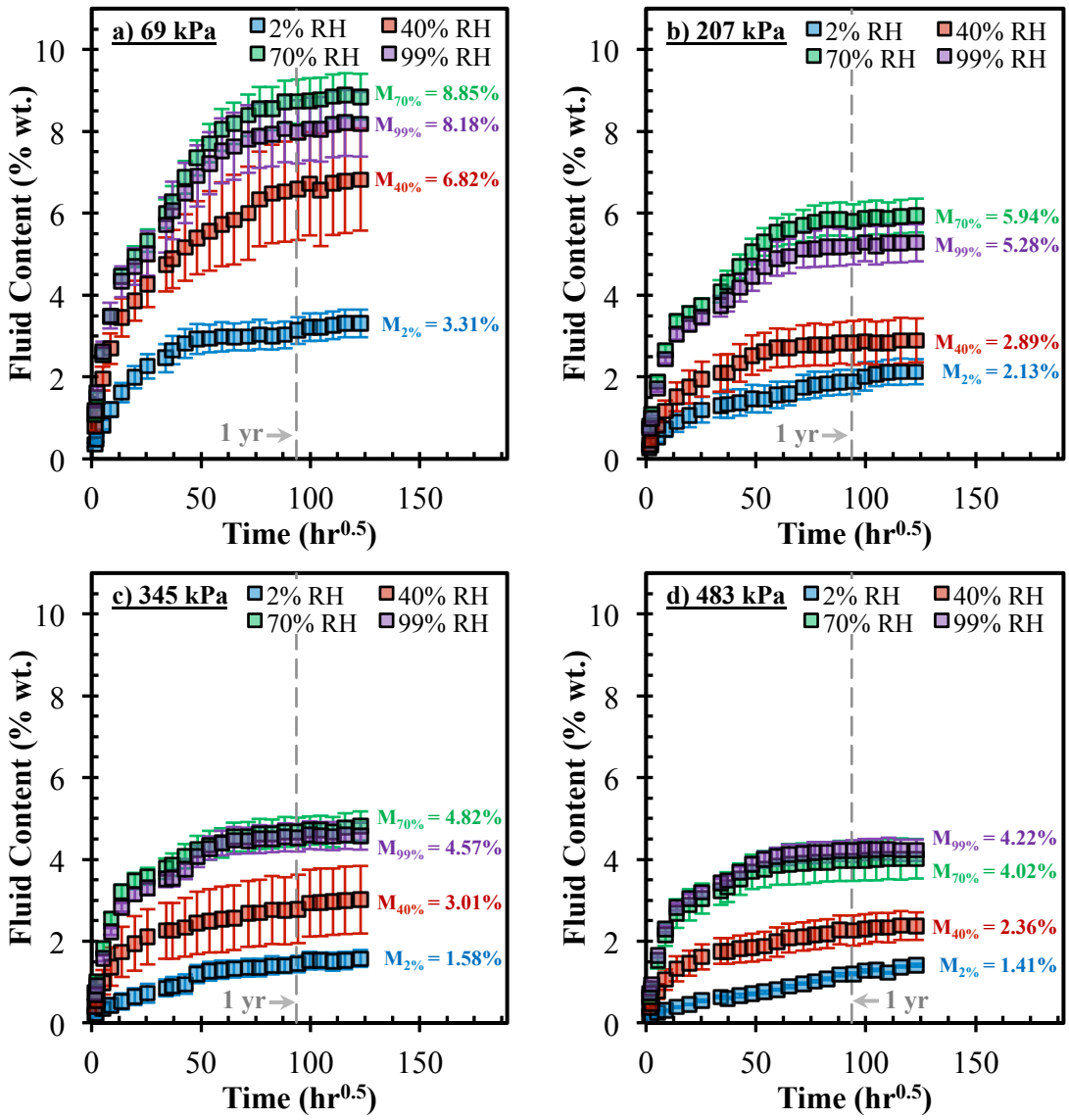

Figure 6.1 Long-term (21 months) hydraulic fluid absorption for flexural specimens of conditioned AQIII/BMI prepregs cured at fabrication pressures of (a) 69 kPa, (b) 207 kPa, (c) 345 kPa, and (d) 483 kPa. Error bars associated with 95% confidence for n=6 samples

6.2.2 Long-term Hydraulic Fluid Absorption for Quartz/Epoxy (AQIII/EX-1522) Flexural Specimens

The fluid mass gain for Quartz/Epoxy flexural specimens subjected to long-term hydraulic fluid exposure is shown in Figure 6.2. The maximum fluid mass gain ranged from 0.6-1.6 %wt. for laminates fabricated at a low pressure (69 kPa) and reduced slightly to 0.5-1.1 %wt. as fabrication pressure increased. Similar to the trend observed with BMI, the average fluid content for flexural specimens was slightly higher, although not by a significant amount, than the square (aspect ratio 1.0) absorption specimens presented in Section 5.3.2. Generally, hydraulic fluid uptake was more gradual when compared to the absorption behavior of BMI. Prepregs conditioned at 99% relative humidity had the most apparent two-stage absorption behavior with rapid diffusion up to $hr^{0.5} \approx 20.0$, followed by a more gradual uptake, particularly at higher fabrication pressures. Sampling variation increased as prepreg humidity exposure increased, which is indicated by the larger confidence intervals for 99% relative humidity specimens in Figure 6.2.

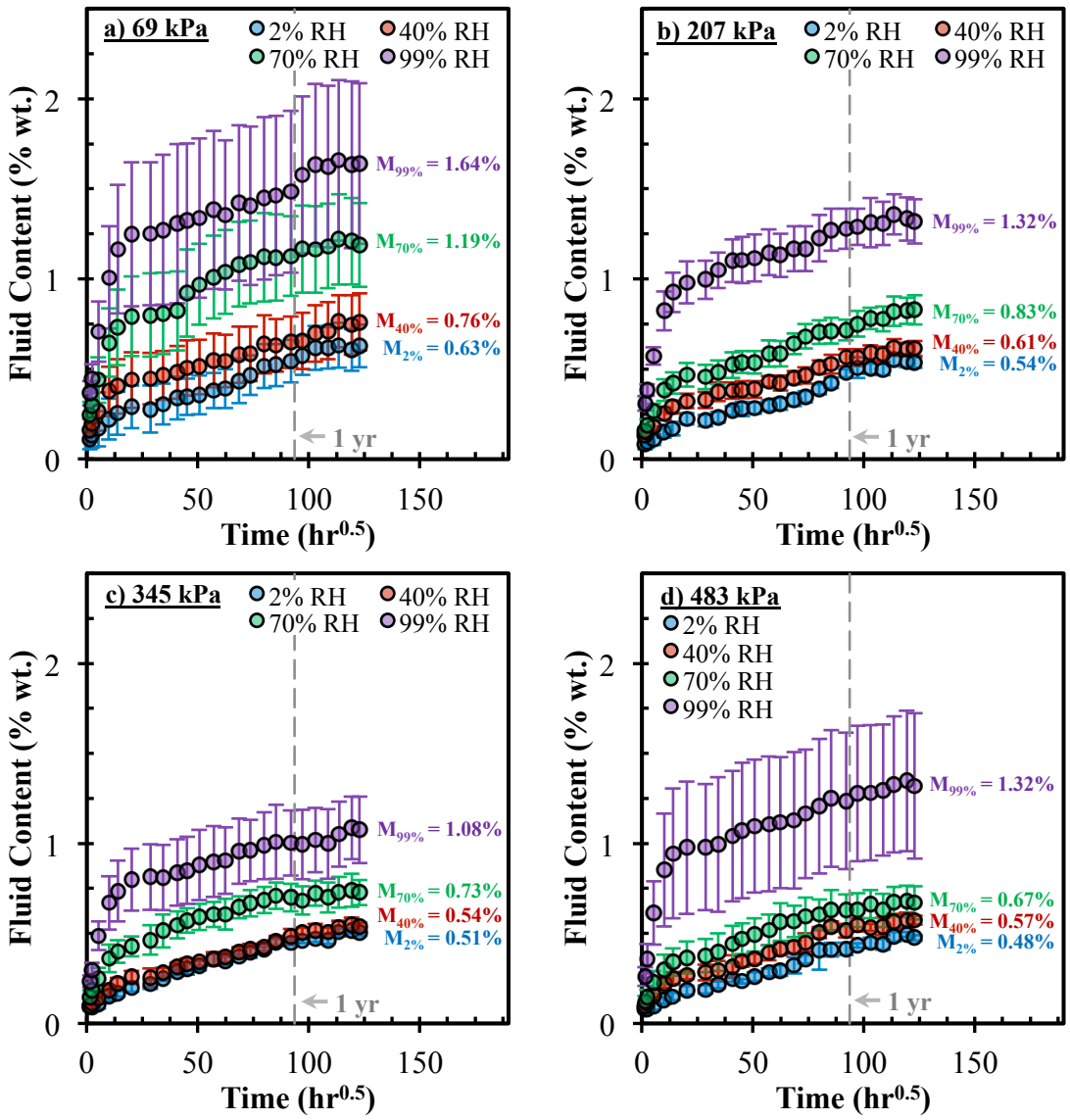

Figure 6.2 Long-term (21 months) hydraulic fluid absorption for flexural specimens of conditioned AQIII/EX-1522 prepregs cured at fabrication pressures of (a) 69 kPa, (b) 207 kPa, (c) 345 kPa, and (d) 483 kPa. Error bars associated with 95% confidence for n=6 samples

6.3 EVALUATION OF HYDRAULIC FLUID CONTAMINATION ON LAMINATE FLEXURAL PROPERTY

6.3.1 Effect of Humidity Exposure, Processing Pressure, and Hydraulic Fluid on Laminate Flexural Stiffness

Figure 6.3a and b indicate both quartz-reinforced laminates have similar flexural stiffness values regardless of the resin material (BMI or epoxy). Stiffness for the baseline specimens ranged from 22 to 29 GPa. Comparatively, stiffness for hydraulic fluid contaminated specimens ranged from 21 to 28 GPa. Flexural stiffness showed a strong dependence on the applied cure pressure, while prepreg humidity exposure did not seem to yield a discernible effect on the laminate flexural stiffness. Both resin systems were fairly resilient to long-term hydraulic fluid contamination. For quartz/BMI, shown in Figure 6.3a, flexural stiffness was reduced by no more than 5% after nearly two years of hydraulic fluid exposure. This trend is seen for nearly all humidity conditioning treatments and fabrication pressures. The only exception was prepregs conditioned in the driest environment (2% RH) and cured at 69 kPa, which observed a flexural stiffness reduction of 9% after nearly two years of hydraulic fluid exposure. The flexural stiffness for quartz/epoxy laminates, shown in Figure 6.3b, was influenced less by hydraulic fluid when compared to the BMI resin. All humidity exposure levels and fabrication pressures had stiffness reductions of less than 5%. Generally, the stiffness percent reduction for quartz/epoxy increased as both humidity exposure and cure pressure increased. Additional observations and trends associated with the stiffness percent reduction will be discussed later in Section 6.4.

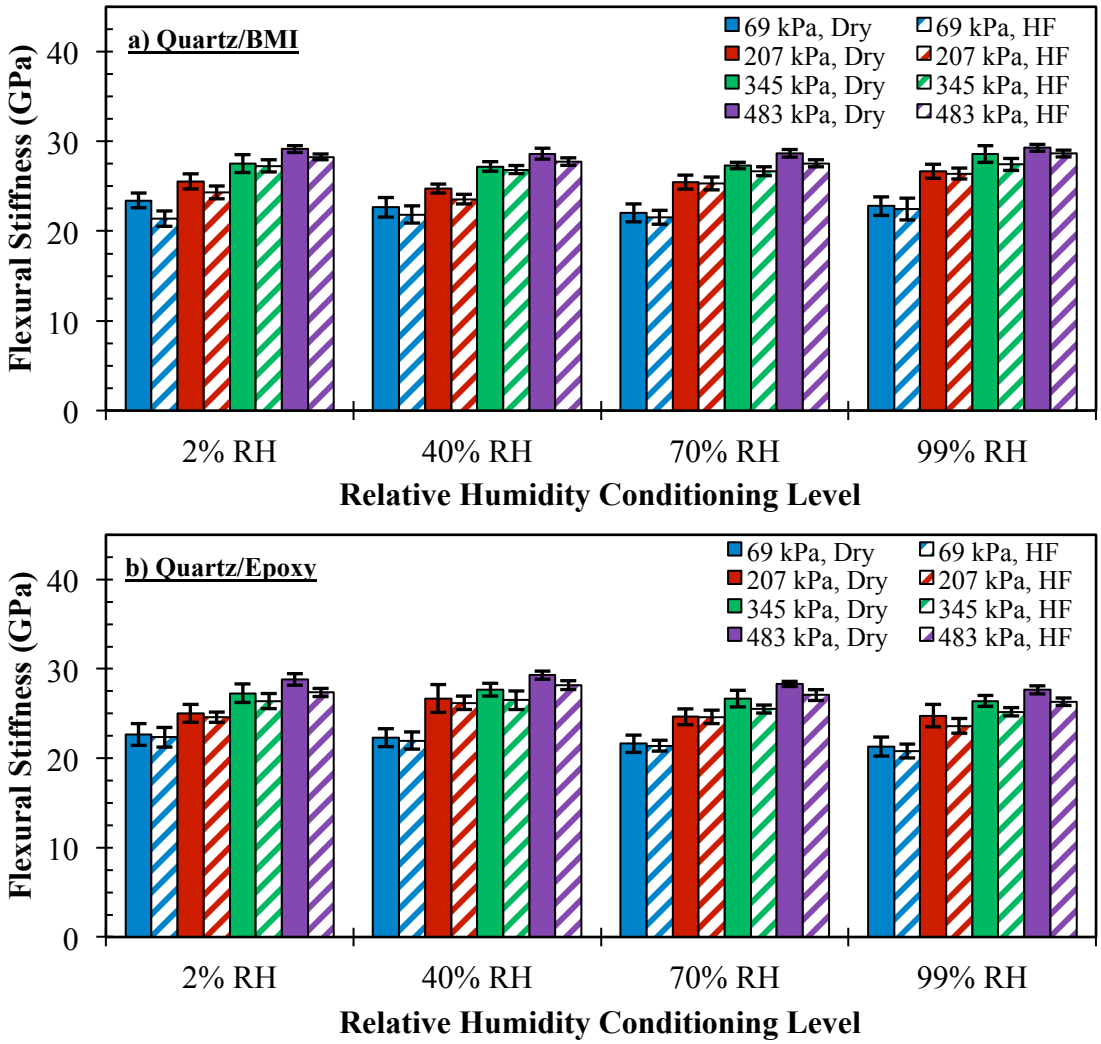

Figure 6.3 Effect of long-term (21 months) hydraulic fluid contamination on flexural stiffness for quartz-reinforced laminates with either (a) BMI resin or (b) EX-1522 epoxy resin. Error bars are associated with 95% confidence for n=6 samples

6.3.2 Effect of Humidity Exposure, Processing Pressure, and Hydraulic Fluid on Laminate Flexural Strength

The average flexural strength for baseline and long-term hydraulic fluid contaminated quartz-reinforced laminates is shown in Figure 6.4. Strength for baseline specimens ranged from 425-603 MPa and 562-967 MPa for quartz/BMI and

quartz/epoxy, respectively. Comparatively, strength for hydraulic fluid contaminated specimens was slightly lower, and ranged from 396-588 MPa and 560-829 MPa for quartz/BMI and quartz/epoxy, respectively. A complex, coupled interaction between humidity exposure and fabrication pressure on the flexural strength was observed for both resin materials. Overall, strength was improved when relative humidity level decreased and fabrication pressure increased. Greater sensitivities to both processing conditions, humidity and pressure, were observed when at low pressures. The effect of long-term hydraulic fluid on flexural strength was less pronounced for quartz/BMI (Figure 6.4a) when compared to quartz/epoxy (Figure 6.4b). Quartz/BMI flexural strength was reduced by no more than 8% after nearly two years of hydraulic fluid exposure for all humidity exposure levels and fabrication pressures. The largest percent reduction for quartz/BMI occurred when at low fabrication pressures. When laminates were fabricated at high pressure (i.e. greater than 350 kPa) the effect of long-term hydraulic fluid contamination on the flexural strength generally declined. Alternatively, the flexural strength for quartz/epoxy was reduced by nearly 15%. Consider also that epoxy resin laminates had higher magnitudes of flexural strength when compared to BMI resin. Therefore, the epoxy laminates had larger variance in flexural strength due to long-term hydraulic fluid contamination. Additional observations and trends associated with the strength percent reduction will be discussed later in Section 6.4.

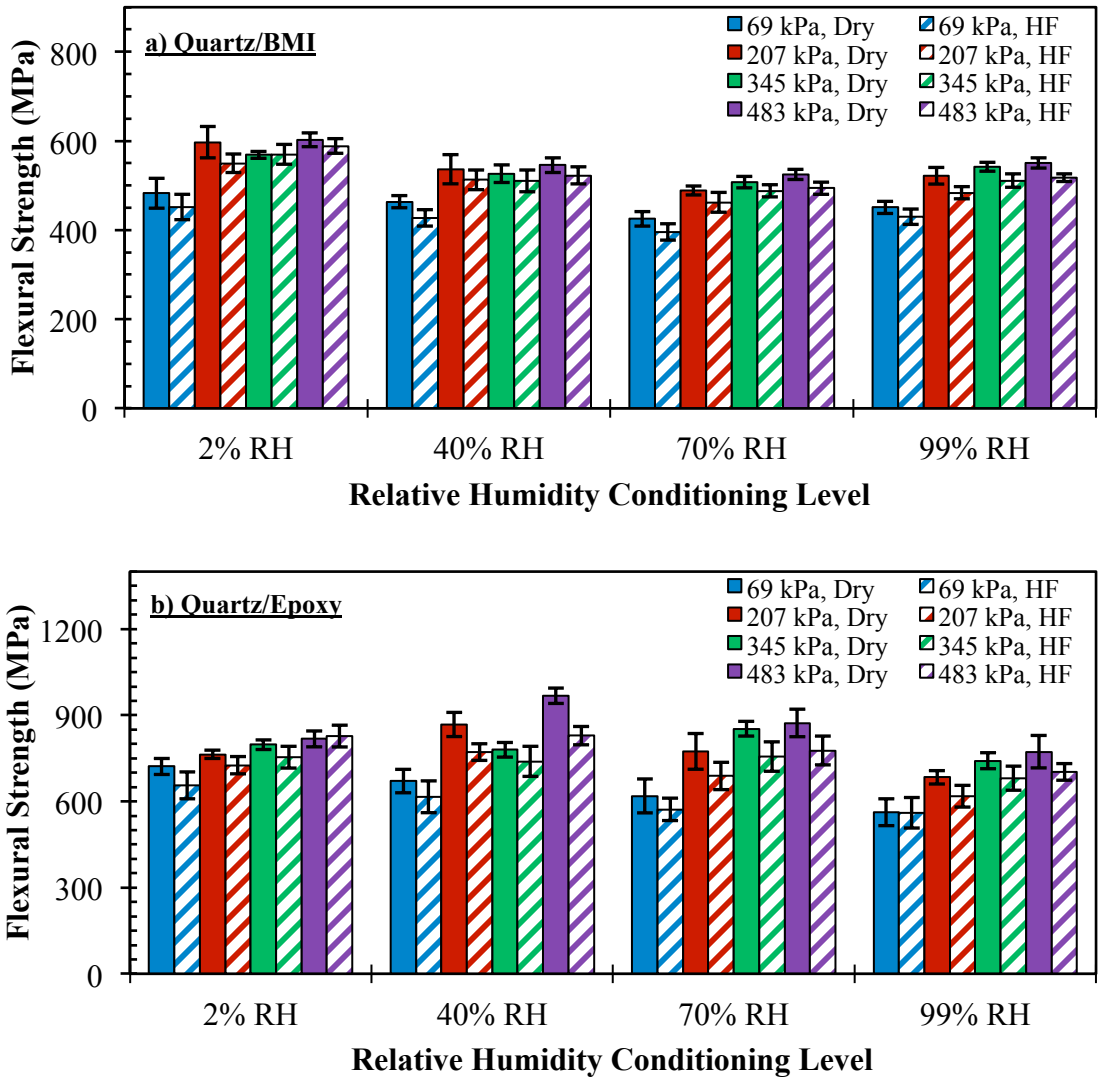

Figure 6.4 Effect of long-term (21 months) hydraulic fluid contamination on flexural strength for quartz-reinforced laminates with either (a) BMI resin or (b) EX-1522 epoxy resin. Error bars are associated with 95% confidence for n=6 samples

6.4 PERCENT REDUCTION OF FLEXURAL PROPERTIES DUE TO LONG-TERM HYDRAULIC FLUID CONTAMINATION

6.4.1 Effect of Prepreg Humidity Exposure on Flexural Stiffness Percent Reduction

The effect of prepreg humidity conditioning on the laminate flexural stiffness percent reduction is shown in Figure 6.5. Although obvious trends (i.e. linear or power functions) of the effect of humidity exposure on the reduction of flexural stiffness were not immediately apparent for either resin material, some general conclusions can be deduced. Hydraulic fluid influenced flexural stiffness for quartz/BMI, shown in Figure 6.5a, to larger degree when humidity exposure was low. For prepregs conditioned at 2% relative humidity, stiffness had a percent reduction range of 1.0-8.8%. For prepregs exposed to low humidity levels, the effect of hydraulic fluid on flexural stiffness could be minimized by using sufficiently high cure pressures (i.e. 345 kPa and above). Additionally, laminates fabricated at high cure pressures were generally the most resilient to hydraulic fluid affects on flexural stiffness. Stiffness reduced by 1.0-4.1% and 2.2-3.9% for laminates fabricated at 345 and 483 kPa, respectively. Mentioned previously, stiffness for epoxy resin specimens were generally affected to a lower degree when compared to BMI. Variations in humidity exposure had little affect on level of damage caused by hydraulic fluid absorption. Therefore, it can be concluded that long-term hydraulic fluid exposure did not have a significant detrimental effect on the fibers' used for either prepreg. Additional analysis regarding the effect of fabrication pressure on flexural stiffness percent reduction will be discussed in the next Section

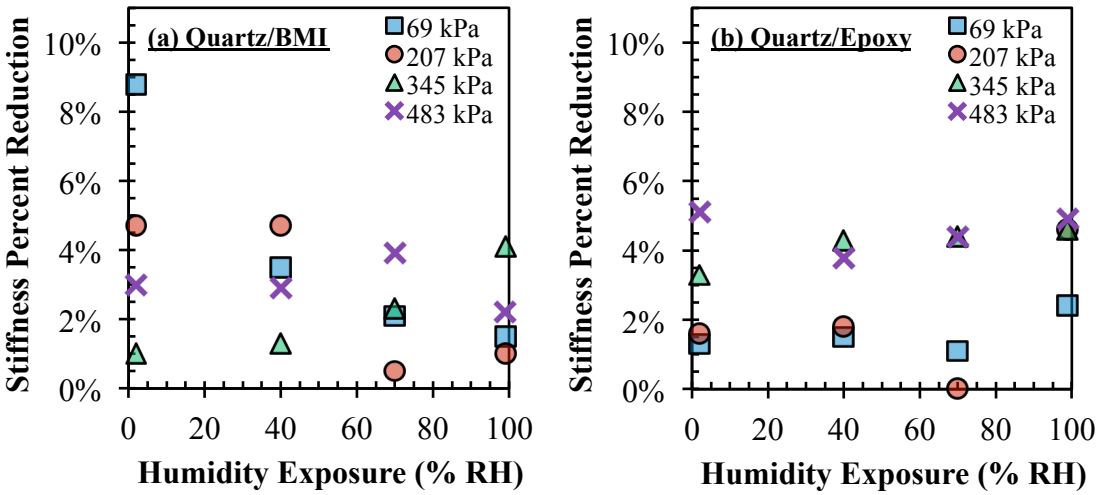

Figure 6.5 Effect of prepreg humidity exposure on the flexural stiffness percent reduction for (a) Quartz/BMI, and (b) Quartz/EX-1522 epoxy

6.4.2 Effect of Fabrication Pressure on Flexural Stiffness Percent Reduction

The effect of applied cure pressure on the laminate flexural stiffness percent reduction is shown in Figure 6.6. As fabrication pressure increased for quartz/BMI laminates, shown in Figure 6.6a, the difference in flexural stiffness percent reduction progressively narrowed. At 69 kPa, the range of stiffness percent reduction was 1.5-8.8%. Meanwhile, the range of stiffness percent reduction was 2.2-3.9% when pressure increased to 483 kPa. With regards to quartz/epoxy, shown in Figure 6.6b, hydraulic fluid contamination reduced stiffness to a larger degree when fabrication pressure was high. At a specific cure pressure, the stiffness percent reduction was tightly grouped for varying humidity exposures.

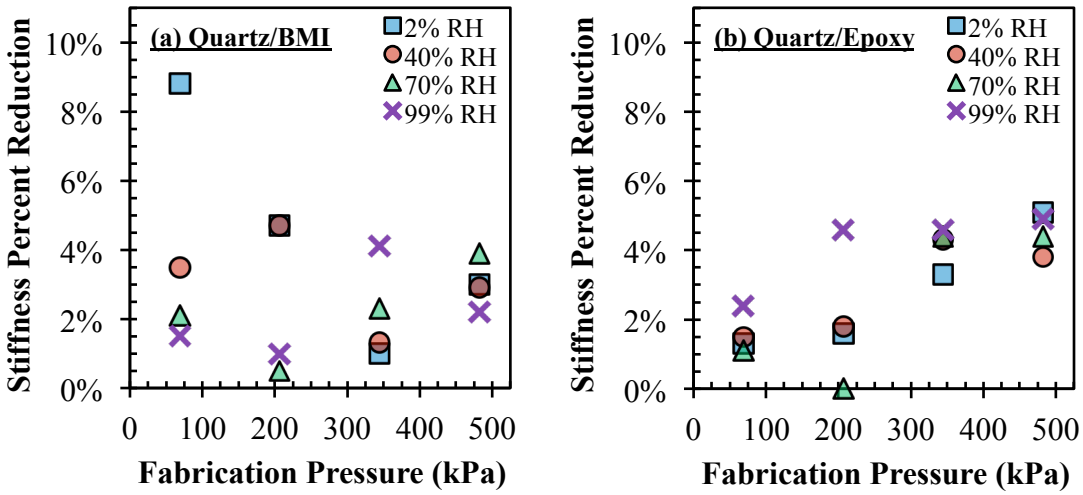

Figure 6.6 Effect of fabrication pressure on the flexural stiffness percent reduction for (a) Quartz/BMI, and (b) Quartz/EX-1522 epoxy

6.4.3 Effect of Prepreg Humidity Exposure on Flexural Strength Percent Reduction

The effect of prepreg humidity exposure on the laminate flexural strength percent reduction is shown in Figure 6.7. Overall, both resin materials demonstrated slight increases in the strength degradation due to hydraulic fluid as humidity exposure increased. With regards to quartz/BMI, shown in Figure 6.7a, detrimental effects of hydraulic fluid can be minimized by increasing the fabrication pressure. Additionally, the effect of hydraulic fluid was much more substantial for quartz/BMI, when humidity exposure was low. Therefore, it is increasingly important to utilize high cure pressures for this scenario. Overall, the strength percent reduction for quartz/epoxy, shown in Figure 6.7b, narrowed as humidity exposure increased. The largest detrimental effect of hydraulic fluid contamination on quartz/epoxy strength was observed when prepregs were exposed to mid-range humidity levels of 40-70% relative humidity.

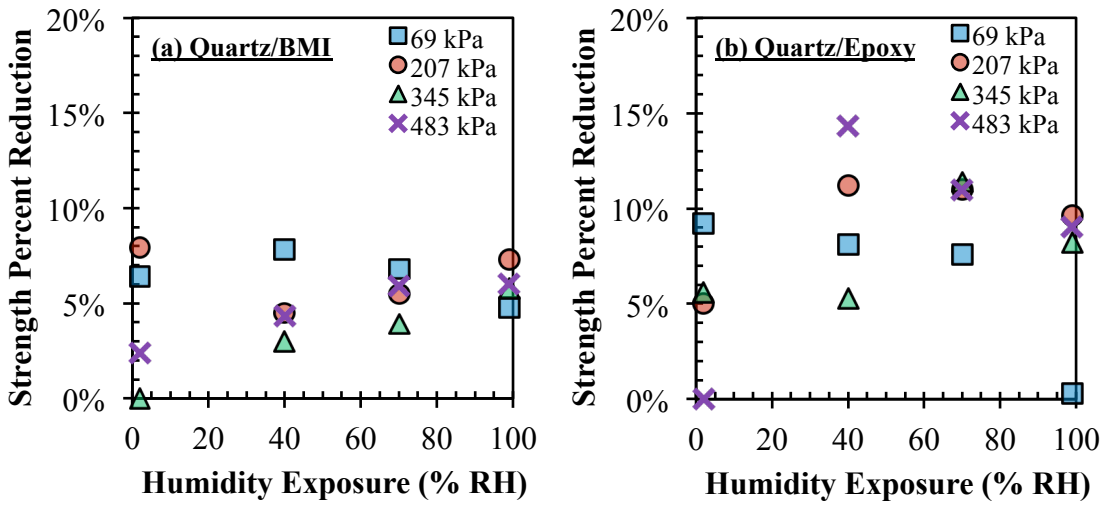

Figure 6.7 Effect of prepreg humidity exposure on the flexural strength percent reduction for (a) Quartz/BMI, and (b) Quartz/EX-1522 epoxy

6.4.4 Effect of Fabrication Pressure on Flexural Strength Percent Reduction

Figure 6.8 illustrates the effect of applied cure pressure on the laminate flexural strength percent reduction. Figure 6.8a clearly indicate that the effect of hydraulic fluid contamination on flexural strength reduces as cure pressure increases. The range of strength reduction at low pressure (69 kPa) was 4.8-7.8%, and reduced to 2.4-6.0% as pressure increased to 483 kPa. Conversely, high pressure fabrication for quartz/epoxy (Figure 6.8b) produced laminates more susceptible to hydraulic fluid damage. The strength reduction range at a particular cure pressure was much larger for epoxy resin when compared to BMI resin, which may be attributed to the quartz/epoxy laminates having a wide range of void fractions.

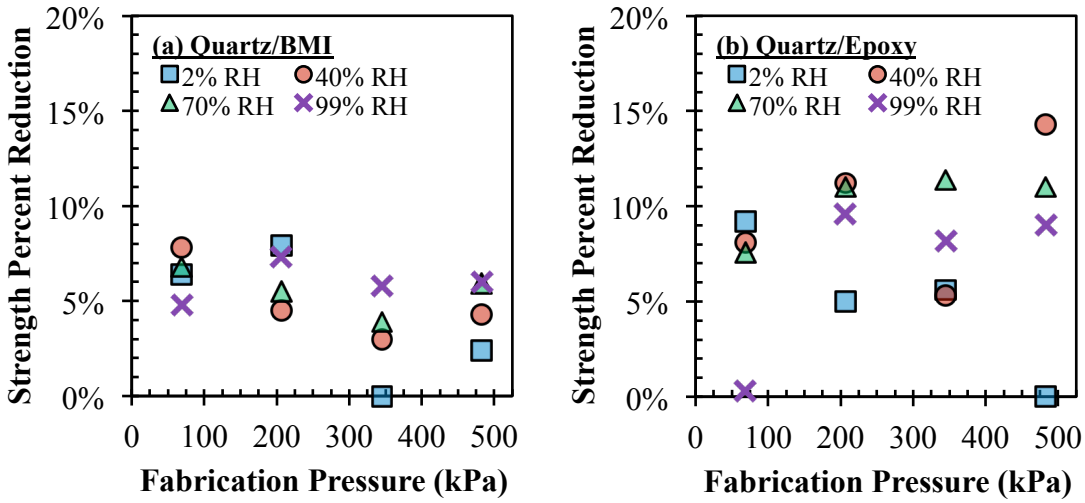

Figure 6.8 Effect of fabrication cure pressure on the flexural strength percent reduction for (a) Quartz/BMI, and (b) Quartz/EX-1522 epoxy

6.5 CONTRIBUTION OF EQUILIBRIUM FLUID CONTENT ON FLEXURAL PROPERTIES OF QUARTZ-REINFORCED LAMINATES

6.5.1 Effect of Equilibrium Fluid Content on Flexural Stiffness Percent Reduction

The effect of hydraulic fluid content on the laminate flexural stiffness percent reduction for varying humidity exposure levels is shown in Figure 6.9. For both resin materials, the largest variation and sensitivity to hydraulic fluid contamination was observed for prepregs conditioned in a dry environment (i.e. 2% RH). Nearly all quartz/BMI laminates (Figure 6.9a) had stiffness reductions of less than 5%, even with a substantially wide range of hydraulic fluid content levels of up to 9 %wt. Conversely, the quartz/epoxy laminates (Figure 6.9b) also observed stiffness reductions of no more than 5%, but for less than 1.7 %wt. maximum observed hydraulic fluid content. Higher levels of hydraulic fluid content generally increased the level of stiffness percent reduction for epoxy resin.

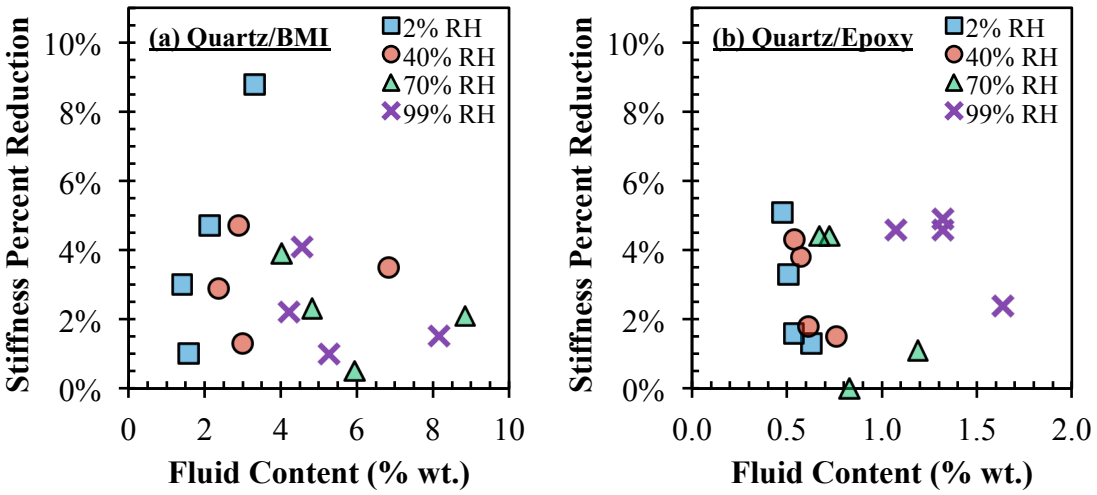

Figure 6.9 Comparison of humidity exposure and hydraulic fluid content on the flexural stiffness percent reduction for (a) Quartz/BMI, and (b) Quartz/EX-1522 epoxy

The effect of hydraulic fluid content on the laminate flexural stiffness percent reduction for varying fabrication pressures is shown in Figure 6.10. BMI resin, shown in Figure 6.10a, had the largest sensitivity to hydraulic fluid contamination when hydraulic fluid content was low. Therefore, utilizing higher fabrication pressures becomes necessary to minimize the effect of hydraulic fluid on flexural stiffness. The stiffness reduction for epoxy resin (Figure 6.10b) was not influenced significantly by varying hydraulic fluid contents. The selected fabrication pressure dictates the percent reduction much more, evidenced by all laminates fabricated at 345 kPa and above having the largest percent reduction values.

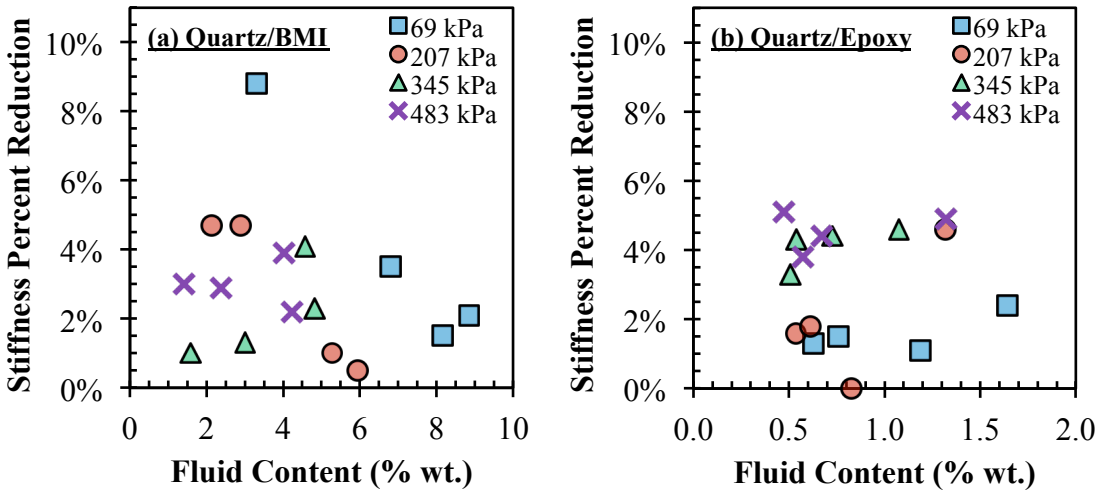

Figure 6.10 Comparison of fabrication pressure and hydraulic fluid content on the flexural stiffness percent reduction for (a) Quartz/BMI, and (b) Quartz/EX-1522 epoxy

6.5.2 Effect of Equilibrium Fluid Content on Flexural Strength Percent Reduction

The effect of hydraulic fluid content on the laminate flexural strength percent reduction for varying humidity exposure levels is shown in Figure 6.11. Although some specimens at low fluid contents had large reductions in flexural strength, the overall trend observed for both resin materials was that higher levels of hydraulic fluid content resulted in larger reductions in flexural strength. When hydraulic fluid content was greater than 5 %wt. all quartz/BMI laminates (Figure 6.11a) had strength reductions larger than 4.8%. As hydraulic fluid content declined, the effect of hydraulic fluid on flexural strength also declined. Wide variations for strength reduction were observed for quartz/epoxy laminates (Figure 6.11b), with no significant discernible trends resulting from varying fluid contents. The largest strength reductions were observed when prepregs were conditioned at either 40% or 70% relative humidity.

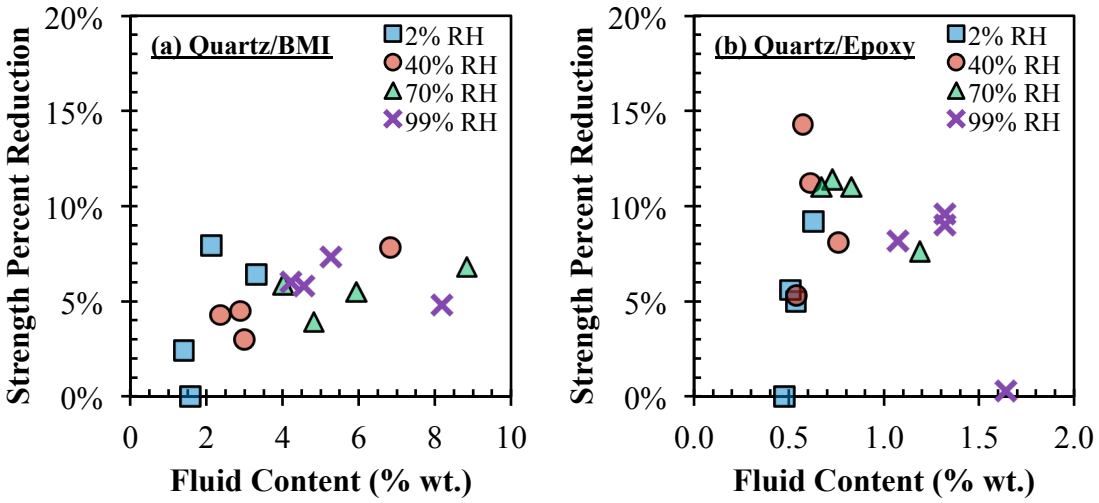

Figure 6.11 Comparison of humidity exposure and hydraulic fluid content on the flexural strength percent reduction for (a) Quartz/BMI, and (b) Quartz/EX-1522 epoxy

The effect of hydraulic fluid content on the laminate flexural strength percent reduction for varying fabrication pressures is shown in Figure 6.12. Both resin materials demonstrated the largest range in strength reductions when fluid content was low, which progressively narrowed as fluid content increased. Overall, the effect of hydraulic fluid on flexural strength slightly increased as hydraulic fluid content increased. Hydraulic fluid contamination affects for BMI resin, shown in Figure 6.12a, were generally minimized when higher fabrication pressures (345 kPa and above) were used, which also resulted in lower overall hydraulic fluid contents. Hydraulic fluid affects on flexural strength for epoxy resin (Figure 6.12b) increased substantially (0.0-14.3%) as hydraulic fluid content increased to 1.0 %wt. Meanwhile, hydraulic fluid content values greater than 1.0 %wt. generally did not degrade the flexural strength by more than 9%.

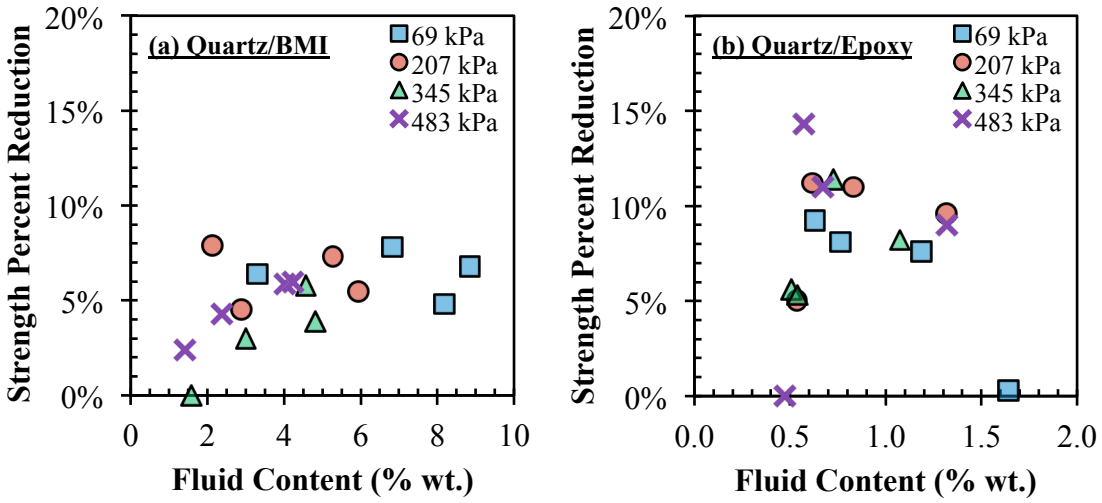

Figure 6.12 Comparison of fabrication pressure and hydraulic fluid content on the flexural strength percent reduction for (a) Quartz/BMI, and (b) Quartz/EX-1522 epoxy

6.6 SUMMARY OF HYDRAULIC FLUID CONTAMINATION EFFECT ON LAMINATE FLEXURAL PROPERTIES CHAPTER

The effect of long-term hydraulic fluid contamination on the flexural stiffness and flexural strength for quartz-reinforced laminates was introduced. Specimens were immersed in hydraulic fluid for 21 months until saturation was achieved and validated with diffusion model predictions. Long-term hydraulic fluid exposure resulted in a reduction in flexural stiffness of no more than 9% for BMI resin and less than 5% for epoxy resin. With regards to flexural strength, BMI was slightly more resilient when compared to the epoxy matrix laminates. Strength reductions for BMI were no more than 8%, whereas the epoxy laminates were closer to 15%. Generally, there was not a discernible trend with regards to varying hydraulic fluid content levels on flexural stiffness. As fabrication pressure seemed to be the driving force for altering the flexural

stiffness. Meanwhile, the effect of hydraulic fluid contamination on flexural strength increased as hydraulic fluid content increased for both resin materials.

CHAPTER 7

CONCLUDING REMARKS AND RECOMMENDATIONS

7.1 SUMMARY OF DISSERTATION

Process-induced defects of composite laminates are often complex in nature and can have a detrimental and varying effect on expected performance of components. The following two processing parameters that drive process-induced defects were examined in this research: (1) the moisture content present in composite prepregs prior to laminate cure, and (2) the cure pressure used to fabricate laminates. Although operational procedures such as storing prepregs in a dry environment and utilizing substantially high cure pressures will minimize process-induced defects, maintaining such restrictive requirements on the laminate fabrication procedure can often be cost prohibitive and impractical. Even when prepregs are stored in vacuum-sealed barriers and at low temperatures, the prepreg moisture content can vary due to changes in the ambient humidity of the storage or fabrication environment. Because components fabricated using prepregs are cured at high temperatures, any moisture present will vaporize during the curing process and form microvoids. This is particularly true for fabrication methods utilizing low cure pressures or without vacuum-assistance, as laminates produced under these scenarios are more susceptible to remaining volatiles, such as microvoids.

As technology improves, composite structures are being implemented into many non-structural applications for the aerospace industry due to their customization and

lightweight potential. Examples of nonstructural components include engine cowlings, panels, and radomes. Nonstructural components have flexibility in the manufacturing process by utilizing less costly, low-pressure methods such as vacuum-bagging or heated compression. However, low-pressure fabrication methods are more susceptible to higher void fractions due to possible presence of moisture absorbed by the prepregs before cure. The relative humidity environment of prepregs in storage or during the lay-up process can contribute to the prepreg moisture content. The local humidity environment may not be actively monitored or controlled at composite manufacturing facilities. During routine operation, aerospace structures are frequently exposed to a variety of liquid contaminants, such as hydraulic fluid. Additionally, composite materials are increasingly being utilized in systems that require a long service-life with minimal repair and maintenance downtime. Therefore, it is becoming increasingly important to accurately characterize the effect of process-induced defects and liquid contamination on the long-term durability of composite materials.

High-performance composite materials are typically used in a variety of aerospace and space structures, including radomes, antenna reflectors, and low observable radar transparent structures. Bismaleimide (BMI) resin with Quartz (AQ581) fiber reinforcement is one such high-performance composite material that was developed to overcome existing limitations for use on complex structures and ducting in advanced military aircraft, helicopters, and many high temperature applications. Quartz/BMI has a high glass transition temperature, with superior burn characteristics and excellent electrical properties, making it an ideal candidate for radomes and other electronic applications. Another high-performance composite material is EX-1522 epoxy resin

system that has been reinforced with either quartz AQIII or carbon IM7 fibers. EX-1522 is a modified and toughened upgrade for high performance applications over traditional epoxy resin systems. This material displays both excellent mechanical and thermal properties, in addition to a low propensity to absorb liquids. EX-1522's has good electrical properties, making it a low cost option for radomes, antenna, and other critical electrical applications.

The research presented in this dissertation was formulated to address numerous gaps identified in literature. The first objective was to examine the coupled effect of prepreg humidity exposure and fabrication pressure on the formation of microvoids and laminate mechanical properties. Although the effect of processing conditions on the formation of microvoids and mechanical properties have been studied extensively, a detailed study that independently varies the void volume fraction by varying the moisture in prepregs before cure and the fiber volume fraction by varying the fabrication pressure has not been reported. The second gap was to examine the effect of long-term hydraulic fluid contamination on the performance of aerospace-grade composite laminates. Addressing these gaps in a comprehensive way could be useful in the design or manufacturing stage and assist in understanding the effect of processing conditions and hydraulic fluid contamination on high-performance, aerospace-grade composites. Therefore, the following research objectives were identified:

- ***Research Objective 1:*** *Coupled effect of varying prepreg humidity exposure level and fabrication pressure on the laminate fiber volume fraction and void formation for aerospace-grade composite prepregs*

- ***Research Objective 2:*** *In addition to fiber volume fraction and void volume fraction, effect of prepreg humidity exposure level and fabrication pressure on the laminate flexural stiffness, flexural strength, and hydraulic fluid absorption behavior*
- ***Research Objective 3:*** *Effect of long-term hydraulic fluid contamination on the flexural properties of aerospace-grade composite laminates*

Several Research Tasks were developed to investigate the research objectives. Research Task 1 was a complete characterization of the laminate microstructure for the three prepregs due to variations in the humidity exposure and fabrication pressure. Laminate fiber volume fractions and void volume fractions were investigated on two distinct fronts. The first part was a comprehensive assessment of the fiber volume fraction and void volume fraction using experimental methods, including specimen suspension, acid digestion, and pycnometer studies. The second part was a visual inspection of the void shape and spatial distribution using images from scanning electron microscopy. Results from Research Task 1 were used to address the first research objective. Research Task 2 was an assessment of the laminate mechanical properties, specifically the flexural stiffness and flexural strength. The first study for Task 2 was an assessment of the laminates after fabrication, (i.e. dry baseline condition). This study served as a comparative to the second study for Task 2, which was an assessment of flexural performance after long-term hydraulic fluid contamination. The first study for Task 2 was used to partially address the second research objective; meanwhile the second study for Task 2 was used to address the third

research objective. Research Task 3 was an investigation of the long-term absorption behavior, with an emphasis on investigating the effect of prepreg humidity exposure and fabrication pressure on the equilibrium fluid content. Research Task 3 was used to address the second research objective. To summarize, the main study topics for each Research Tasks were:

Task 1: Laminate Microstructure Characterization

- Experimental analysis of fiber volume fraction and void volume fraction (Section 2.5)
- Scanning Electron Microscopy image analysis (Section 2.6)

Task 2: Laminate Mechanical Property Assessment

- Laminate flexural stiffness and flexural strength analysis of dry baseline condition prior to environmental degradation (Section 3.2)
- Laminate flexural stiffness and flexural strength analysis after hydraulic fluid contamination for 21 months (Section 6.3)

Task 3: Laminate Hydraulic Fluid Absorption Behavior

- Assessment of long-term absorption behavior and equilibrium fluid content (Section 5.3)

Laminates containing a wide range of void volume fractions and fiber volume fractions were desirable to address the research objectives. Therefore, prepreg sheets were exposed to varying relative humidity levels and subsequently cured with a heated compression mold without a vacuum-bag so as to artificially induce varying void

fractions independently of the laminate fiber volume fraction. In the context of this research, prepreg conditioning was the procedure of exposing prepreg sheets at specific relative humidity exposure levels using a Thermotron 8200 environmental chamber. The prepreg sheets were conditioned at room temperature (25°C) for a period of 24 hours at relative humidity set points of i) 2%, ii) 40%, iii) 70%, or iv) 99%. Higher humidity exposures resulted in more absorbed moisture in the prepreg sheets, which in turn vaporized during the heated cure process and generated large void fractions. BMI resin was significantly more sensitive to humidity exposure when compared to the epoxy resin prepregs. Therefore, proper storage techniques are critical when utilizing BMI products. To vary the fiber volume fraction, laminates were fabricated at different applied cure pressures. Using the conditioned prepreg sheets, eight-ply laminates were fabricated using a Carver hot-press at the applied cure pressures of i) 68.9 kPa (10 psi), ii) 206.8 kPa (30 psi), iii) 344.7 kPa (50 psi), and iv) 482.6 kPa (70 psi). Therefore for each prepreg material, a total of 16 unique laminates were fabricated from a combination of four prepreg conditioning levels and four fabrication pressures. The manufacturer suggested temperature cure profile for each resin material was utilized (Section 2.3).

The resulting fiber volume fraction and void volume fraction was presented in Section 2.5. The fiber volume fraction for each prepreg material ranged from about 50% to 66%, with consistent results for a specific fabrication pressure. The fiber volume fraction for both quartz-reinforced laminates (quartz/BMI and quartz/epoxy) gradually increased from about 50% to 61% as fabrication pressure increased from 69 to 345 kPa. At higher fabrication pressures, the fiber volume fraction increased at a

decreasing rate. The fiber volume fraction for carbon/epoxy laminates increased at a faster rate from 53% to 60% as pressure increased from 69 to 207 kPa, whereas further increases in pressure increased the fiber volume fraction at a lower rate. This behavior was most likely due to fibers' increased role in supporting the applied pressure.

The range of void volume fractions was significantly different for each prepreg material. Overall, void volume fraction increased as relative humidity exposure level increased and as the fabrication pressure decreased. Higher sensitivities were observed when at low pressures and high humidity. The high levels of voids and how the void volume fraction changes among the different material systems clearly illustrated the importance of: (a) removing volatiles and trapped microvoids during cure by a vacuum bag, (b) proper storage of prepregs in a low humidity environment, and (c) applying proper level of fabrication pressure. Both quartz-reinforced laminates (quartz/BMI and quartz/epoxy) contained the highest void levels. Meanwhile BMI were more susceptible to volatiles as the lowest void volume fraction observed was 8%, even when laminates were produced at high pressures. The carbon/epoxy laminates had a void volume fraction range of about 1% to 5%, which was much lower than the other two prepregs with the quartz fiber reinforcement. IM7/EX-1522 prepreg was much less susceptible to prepreg storage conditions compared to AQIII/EX-1522, which had the same epoxy resin but quartz fiber, AQIII, reinforcement instead of the carbon IM7. The fiber/resin interphase or the sizing used in the AQIII/EX-1522 prepregs may act as storage sites for the moisture if the prepreg is stored in a highly humid environment. Overall, the epoxy resin EX-1522 seems to have less volatiles and a high quality

laminate can be produced even without the vacuum bag if the prepreg is stored properly in a dry environment and a sufficiently high fabrication pressure is applied.

Analysis of SEM images for each prepreg material was presented in Section 2.6. The SEM images for quartz/BMI revealed the formation of many large-scale voids, which were primarily located in the intra-tow regions and ply-to-ply interface. Each fabrication pressure for BMI matrix laminates featured several elongated voids that were located between plies and fiber bundles. Some of the larger voids measured over 1 mm in length, which equates to about 50% of the through-the-thickness measurement. Similar to quartz/epoxy, the spatial distribution throughout the thickness of the quartz/BMI laminate did not change as a result of increasing prepreg conditioning level or fabrication pressure. As fabrication pressure increased, the void morphology became more elongated, or void aspect ratio increased. In addition to the many large-scale voids, the laminates exhibited many microscale voids with diameters equivalent to the fiber diameter. The microscale voids were predominantly located within the fiber tows. Varying prepreg moisture content with different humidity levels did not have a discernible effect on the void morphology or distribution for the laminates.

SEM images for Quartz/Epoxy laminates revealed more spherically shaped voids, which were primarily located in resin-rich regions and the ply-to-ply interface. The largest voids occurred at the lowest fabrication pressure, and measured up to 0.5 mm in length and had aspect ratios ranging from 1 to 3. As fabrication pressure increased, the effective area of the voids significantly decreased with voids having diameters on the microscale level and being of a similar scale to the quartz fiber reinforcement. The spatial distribution throughout the thickness of the laminate did not change as a result of

increasing prepreg conditioning level or fabrication pressure. Increasing prepreg humidity exposure resulted in the void effective diameter and aspect ratios increasing substantially.

The microvoid content for carbon-reinforced laminates was significantly lower than the other two prepreg materials in this study. The SEM images for Carbon/Epoxy laminates revealed sporadic, slightly elongated voids, which were primarily located in resin-rich regions and the ply-to-ply interface. As fabrication pressure increased, the effective area of the voids significantly decreased and the void aspect ratio increased. Additionally, larger voids were predominantly located within plies close to the laminate mid-plane. Increasing prepreg relative humidity conditioning levels did not have a significant effect on overall microvoid content, however the microvoids did become more spherical in shape and slightly larger in diameter.

The effect of humidity exposure and fabrication pressure on the laminate flexural stiffness and flexural strength was presented in Chapter 3. All laminate flexural property testing was conducted in accordance with the ASTM testing standard for fiber-reinforced polymers D790. Rectangular cross section specimens were tested using a three-point bending apparatus. The support span-to-thickness ratio was 20:1 for all specimen tests, which was selected because (i) it allowed for a larger span-to-depth ratio to account for the laminated composite specimens and (ii) specimen overall lengths were within the range of useable space for the fabricated laminates.

The resulting flexural stiffness and flexural strength was presented in Section 3.2. Both quartz-reinforced laminates (quartz/BMI and quartz/epoxy) had similar flexural stiffness values ranging from 22 to 29 GPa, regardless of the resin material. Carbon

fiber-reinforced laminates, on the other hand, had the highest flexural stiffness values, ranging from 42 to 53 GPa. As expected, the flexural stiffness demonstrated strong dependence on the pressure, while the prepreg moisture content did not seem to yield a discernible effect on the laminate flexural stiffness.

The flexural strength for quartz/BMI laminates was the lowest values of the three prepreg material systems used in this study, with strength values ranging from 425 to 600 MPa. Meanwhile, the two epoxy-matrix laminates have higher flexural strength values, both with a maximum of about 950 MPa. The flexural strength of quartz/epoxy varied from 562 to 967 MPa, or approximately 40%, which was most likely due to this prepreg material having the highest variation in void fraction. Meanwhile, the flexural strength for carbon/epoxy varied by 23%. This range was similar to that reported by Liu et al. [17], who observed a strength reduction of nearly 20% for a similar range of void fractions. Typically, reducing the relative humidity level of the prepreg conditioning level and increasing fabrication pressure achieved the largest improvement in flexural strength.

Property function equations used to characterize fiber volume fraction, void volume fraction, flexural stiffness, and flexural strength, along with the associated contour plots were presented in Chapter 4. Contour plots are a useful tool for analyzing the coupled contributions of two parameters and identifying unique behaviors such as local minimums or maximums, and sensitivities. Each property function equation was normalized with respect to the maximum observed value so that similar process-induced trends between the three prepregs could be easily identified.

The effect of long-term hydraulic fluid contamination on the prepreg materials was presented in Chapter 5. High-performance aerospace-grade composite materials are frequently exposed to a variety of liquid contaminants through routine operating conditions. Absorbed fluids in polymer structures can have a detrimental effect on the durability and affect the reliability of other subsystems, such as electronics calibration. Even a relatively low level of moisture absorption in polymers and composites can cause resin plasticization, swelling, and residual stresses in the material; which are correlated to be primary sources of material property degradation. Excessive mechanical property degradation due to moisture or hydraulic fluid absorption limits the design and effectiveness of composites. Therefore, predicting the fluid absorption behavior of a composite laminate is essential to account for losses in performance or durability. From each prepreg conditioning type and fabrication pressure, six specimens with planar dimensions 31.5 mm by 31.5 mm were prepared for absorption testing. Prior to fluid exposure, any initial moisture present in the composite specimens was removed by drying the specimens in a vacuum-oven at 40°C until an equilibrium weight was achieved. The dried specimens were then immersed in sealed glass containers filled with hydraulic fluid. The temperature of each glass container was maintained at room temperature (25°C) with a Thermo Scientific water bath. The fluid uptake for a given immersion time period was periodically measured with a high-precision analytical balance. The data was collected over a period of 24 months for quartz-reinforced laminates and 18 months for carbon fiber-reinforced laminates.

After two years of immersion, the fluid mass gain for quartz/BMI ranged from 2.7-8.5 %wt. for laminates fabricated at low pressure (69 kPa) and reduced to 1.4-4.1 %wt.

for laminates fabricated at high pressure (483 kPa). The largest reduction in fluid mass gain was observed when fabrication pressure was increased from 69 kPa to 207 kPa, whereas additional increases in applied pressure did not reduce the fluid content to the same degree. This correlated closely with the fiber volume fraction at each fabrication pressure, in that the largest delta was observed between 69 and 207 kPa. Hydraulic fluid diffusion was very rapid for an absorption period up to approximately $hr^{0.5} \approx 25.0$, or approximately one month. Longer exposure periods (i.e. greater than $hr^{0.5} \approx 25.0$) resulted in more gradual fluid uptake. After two years of immersion, three distinct regions were observed in the absorption data that correlated with the relative humidity exposure level. Prepregs conditioned in a dry environment (i.e. 2% RH) exhibited the lowest fluid contents, of about 1.2-2.7 %wt. Prepregs conditioned in a mild environment (i.e. 40% RH) exhibited a mid-range fluid content range, of about 3.1-6.1 %wt. Prepregs conditioned in a humid environment (i.e. 70% and 99% RH) exhibited the highest fluid content range, of about 4.1-8.5 %wt. After two years of immersion, the fluid mass gain for quartz/epoxy laminates was significantly lower than quartz/BMI. The fluid mass gain ranged from 0.5-1.2 %wt. for laminates fabricated at a low pressure (69 kPa) and reduced slightly to 0.4-1.0 %wt. as fabrication pressure increased. The hydraulic fluid uptake was more gradual for quartz/epoxy when compared to the absorption behavior of BMI. The fluid content for prepregs conditioned at 99% relative humidity was significantly higher than any other conditioning treatment level. This is most likely due to these specimens having the highest void fraction values. At a given fabrication pressure, the laminate fiber volume fraction was very similar for quartz/epoxy laminates. Therefore, the effect of high void fractions, which serve as

storage sites for liquid, was clearly illustrated with this prepreg material. The fluid mass gain for carbon/epoxy laminates after 18 months was similar to that for quartz/epoxy laminates, which was expected as the same EX-1522 resin was used in both laminates. When humidity exposure was less than 70% relative humidity, the fluid mass gain ranged from 1.1-1.8 %wt. for laminates fabricated at a low pressure (69 kPa) and reduced to 0.7-1.1 %wt. for laminates fabricated at a high pressure (483 kPa). The fluid mass gain for laminates fabricated from 99% relative humidity prepregs was similar (1.8-2.1 %wt.) and had large sampling variance, regardless of the fabrication pressure. As humidity exposure increased, the two-stage hydraulic fluid absorption behavior became more prevalent. The carbon/epoxy laminates did not appear to be approaching saturation after 18 months of fluid exposure. The equilibrium fluid content for the experimental mass gain data was determined using a hindered diffusion model. The model indicated that both quartz-reinforced laminates were near saturation after 24 months of immersion, whereas additional absorption is required for the carbon/epoxy laminates.

A detailed study that examined the combined effect of prepreg humidity exposure, fabrication pressure, and fluid absorption on the mechanical performance of quartz-reinforced laminates has not been reported in literature. Therefore, the effect of long-term hydraulic fluid contamination on the flexural properties was presented in Chapter 6. The effect of hydraulic fluid on flexural properties was conducted for quartz-reinforced prepregs because the hindered diffusion model indicated that these material systems have approached near saturation. The effect of hydraulic fluid was analyzed by comparing flexural properties with the dry baseline condition presented in Chapter 3.

Flexural stiffness for the baseline specimens ranged from 22 to 29 GPa. Meanwhile, stiffness for hydraulic fluid contaminated specimens ranged from 21 to 28 GPa. Flexural stiffness showed a strong dependence on the applied cure pressure, while humidity exposure did not yield a discernible effect on stiffness. Therefore, both resin systems were fairly resilient to long-term hydraulic fluid contamination. For quartz/BMI, flexural stiffness was reduced by no more than 5% after nearly two years of hydraulic fluid exposure. This trend was seen for nearly all humidity conditioning treatments and fabrication pressures. The only exception was prepregs conditioned in the driest environment (2% RH) and cured at 69 kPa, which observed a flexural stiffness reduction of 9% after nearly two years of hydraulic fluid exposure. The flexural stiffness for quartz/epoxy laminates was influenced less by hydraulic fluid when compared to the BMI resin. All humidity exposure levels and fabrication pressures had stiffness reductions of less than 5%. Flexural strength for baseline specimens ranged from 425-603 MPa and 562-967 MPa for quartz/BMI and quartz/epoxy, respectively. Comparatively, strength for hydraulic fluid contaminated specimens was slightly lower, and ranged from 396-588 MPa and 560-829 MPa for quartz/BMI and quartz/epoxy, respectively. A complex, coupled interaction between humidity exposure and fabrication pressure on the flexural strength was observed for both resin materials. The effect of long-term hydraulic fluid on flexural strength was less pronounced for quartz/BMI when compared to quartz/epoxy. Quartz/BMI flexural strength was reduced by no more than 8% after nearly two years of hydraulic fluid exposure for all humidity exposure levels and fabrication pressures, with the largest

percent reduction occurring at low cure pressures. Alternatively, the flexural strength for quartz/epoxy was reduced by nearly 15%.

7.2 ADDRESSING RESEARCH OBJECTIVE 1

Coupled effect of varying prepreg humidity exposure level and fabrication pressure on the laminate fiber volume fraction and void formation for aerospace-grade composite prepregs

The first research objective was addressed by the studies presented in Chapters 2 and 4. Sixteen laminates from a combination of four prepreg humidity conditioning treatments and four fabrication pressures were manufactured for each prepreg material. The conditioning and fabrication method decouples the laminate fiber volume fraction and void volume fraction, which allows for each property to be investigated independently.

The laminate fiber volume fraction was not influenced greatly by varying levels of humidity exposure for any prepreg. For example, in the most extreme case, the fiber volume fraction for BMI increased less than 4.7% when humidity exposure increased from 0% RH to 100% RH. Thus, the hypothesis that exposing prepregs to varying humidity levels would primarily affect the laminate void volume fraction without significantly affecting the laminate fiber volume fraction was confirmed. The two epoxy-resin systems (quartz/epoxy and carbon/epoxy) were even more resilient to varying humidity levels. The fiber volume fraction for quartz/epoxy was nearly exclusively influenced by fabrication pressure. Meanwhile, the carbon/epoxy laminates demonstrated slight decreases in fiber volume fraction as humidity exposure increased.

Generally, increasing fabrication pressure increased the fiber volume fraction similarly for each prepreg. However, there were some distinct differences among the three prepregs. When the two quartz-reinforced laminates (BMI and epoxy) were compared, the BMI resin yielded higher fiber volume fractions for the same cure pressure. Additionally, the BMI resin had a slightly larger range of fiber volume fractions, 50.7-66.6%, when compared to the range for epoxy resin, 48.2-62.6%. Excluding very high pressures (483 kPa) the fiber volume fraction for quartz/epoxy laminates was very consistent at a specific cure pressure and typically did not vary by more than ±1.3%. The two epoxy-resin prepregs (quartz/epoxy and carbon/epoxy) had identical delta changes in the fiber volume fraction of 14.4%, albeit the carbon fiber reinforcement had a higher overall magnitude.

All prepregs observed an increase in void volume fraction as the prepreg humidity exposure level increased. Laminates produced with BMI were generally more susceptible to a high void fraction. When the two epoxy resin prepregs were compared, it was observed that utilizing quartz reinforcement would cause a rate of increasing void fraction over five times that of carbon fiber-reinforcement. The quartz/BMI laminates on the other hand had a reasonably low rate of increasing void fraction as humidity exposure increased. The largest rate of increasing void volume fraction for quartz/BMI was 2.5% per 100% relative humidity increase. Thus it can be concluded that although BMI is susceptible to a high void fraction when high-pressure fabrication procedures or vacuum-bag assistance is not utilized, BMI is very resistant to further increases in the void volume fraction as a result of high humidity exposures.

Contour plots of the functional property equations were developed to illustrate the synergistic effect of humidity conditioning and fabrication pressure on fiber volume fraction and void volume fraction. The contour plots are useful in identifying the relative sensitivity of each variable, as well as any local phenomena such as minimums and maximums. Contour plots revealed that fiber volume fraction was predominantly dependent on fabrication pressure for all prepregs. Near vertical contour lines for quartz/epoxy indicated that humidity exposure had very little effect on the fiber volume fraction, regardless of the applied cure pressure. Meanwhile, humidity did play a minor role for quartz/BMI and carbon/epoxy when the applied cure pressure was high. The fiber volume fraction for both epoxy resin prepreg materials (quartz/epoxy and carbon/epoxy), changed by about 20%. On the other hand, the fiber volume fraction for quartz/BMI changed by nearly 30%. Contour plots for normalized void volume fraction revealed a more complex-coupled relationship between prepreg humidity exposure and fabrication cure pressure. For all prepreg materials, the rate of increasing void volume fraction progressively increased as fabrication pressure declined and relatively humidity exposure increased. The contour plots clearly depicted the highest void fractions when laminates were produced at low pressure from prepregs conditioned in high humidity for all prepregs. Both quartz-reinforced laminates (BMI and epoxy) had similar maximum void volume fractions of 14.1% for epoxy resin and 13.9% for BMI resin. However, the quartz/BMI laminates had the smallest change in void fraction for varying levels of humidity exposure and fabrication pressure. At the minimum, the void fraction for BMI reduced to about 8%, or a normalized percent reduction of about 40%. Alternatively, the void volume fraction for quartz/epoxy was progressively reduced to

1.7%, which represents a normalized percent reduction of 90%. Even at low humidity exposure levels, BMI absorbed significantly more moisture during the conditioning process. The void volume fraction for carbon/epoxy laminates reduced from 4.8% to 1.3% as pressure increased and humidity exposure decreased, which represents a normalized percentage range of approximately 70%.

This research study contributed a detailed evaluation of the effect of storage conditions and processing environment in the form of relative humidity exposure and fabrication pressure on the laminate fiber volume fraction and void volume fraction for aerospace-grade composite prepregs. The effect of cure pressure or prepreg conditioning has been addressed occasionally in literature; a systematic study that varies both independently for three composite prepregs has not been studied previously. Fiber volume fraction was found to generally depend on the fabrication pressure, whereas more complex and coupled behavior was noted for void volume fraction. Additionally, the property function equations and associated contour plots are a useful tool in identifying the sensitivity of relative humidity and fabrication pressure on the laminate microstructure.

7.2.1 Limitations and Future Work Associated with Research Objective 1

Uncertainties associated with experimental fiber volume fraction and void fraction results

Some experimentally determined fiber volume fractions and void volume fractions had unusually high variations about the mean, which may have been due to local variations within the specimens used for this study. In the current study, all laminate microstructure specimens were extracted from the perimeters of the laminate. The

central region of each laminate was used exclusively for flexural specimens and tensile specimens for future studies. If given the opportunity again, specimens would have been extracted from the central location within each laminate as a crosschecking means with the other specimens.

Limitations of the statistical approaches and curve fits associated with the effect of humidity or pressure on the laminate microstructure

The selected trend line representations were sufficient in capturing the desired trends and behaviors of the effect of humidity exposure and fabrication pressure on the laminate fiber volume fraction and void volume fraction. Generally, the effect of humidity or fabrication pressure on fiber volume fraction or void volume fraction can be assumed to be 1st-order relationships, such as linear functions or power-functions. One limitation of the approach is that it is a data-driven model; therefore it is only as accurate as the experimental data available. Another limitation for the current study is that only a single average of a limited number of specimens was ascertained. This was sufficient to address the research objectives of analyzing general trends due to varying parameters, however higher levels of statistical analysis was not possible and could be the focus of future research studies.

7.3 ADDRESSING RESEARCH OBJECTIVE 2

In addition to fiber volume fraction and void volume fraction, effect of prepreg humidity exposure level and fabrication pressure on the laminate flexural stiffness, flexural strength, and hydraulic fluid absorption behavior

The studies developed to address the second research objective were presented in Chapters 3, 4, and 5. For each prepreg material, varying humidity exposure did not significantly affect flexural stiffness. For example, the most extreme case was observed with carbon fiber reinforced epoxy laminates fabricated at 345 kPa, which had a slope of just 0.035 GPa / % relative humidity. Both quartz-reinforced laminates (quartz/BMI and quartz/epoxy) had even lower stiffness slopes due to humidity exposure, of no more than 0.015 GPa / % relative humidity for all fabrication levels. Regardless of the matrix material (BMI and epoxy), both quartz-reinforced laminates had similar stiffness offsets for the same fabrication pressure. As fabrication pressure increased, all materials demonstrated near linear flexural stiffness increases. Regardless of the humidity exposure, the rate of stiffness increase and offset was similar for quartz/epoxy and quartz/BMI laminates. The rate of stiffness increase for quartz-reinforcement was within the range of 0.014-0.016 GPa/kPa. Comparing the two epoxy matrix materials (quartz/epoxy and carbon/epoxy) revealed that flexural stiffness for carbon fiber reinforced laminates was slightly more sensitive to changes in pressure than quartz-reinforced laminates. This was indicated by the larger increasing slopes of carbon fiber (0.016-0.023 GPa/kPa) as opposed to that of quartz fiber (0.015-0.016 GPa/kPa).

Each material demonstrated complex, polynomial-like behavior on flexural strength when considering humidity exposure. Strength was lower when BMI resin was used instead of epoxy resin. However, strength for BMI was not influenced to the same degree by changes in humidity. Additionally, utilizing BMI for the resin material resulted in a local minimum for flexural strength near 70% relative humidity. Epoxy resin on the other hand generally had a local maximum near 50% relative humidity.

Both epoxy resin systems (quartz/epoxy and carbon/epoxy) had initial strength values between 700-840 MPa that were in close proximity to each other at a specific fabrication pressure. However, the effect of humidity exposure was distinctly different for each fiber reinforcement type, with quartz-reinforced laminates being influenced by humidity to a larger degree. There were instances for carbon fiber that was more sporadic and random in nature. For example, samples fabricated at 483 kPa demonstrated a large local minimum near 40% relative humidity, which was caused by the unusually low flexural strength for the specimens conditioned at 40% relative humidity. The overall trend of a slight decline as humidity increased from zero to 100% relative humidity remained true, therefore it is believed that this behavior was more likely due to uncertainties with experimental data. The flexure strength increased as fabrication pressure increased for each prepreg material. Excluding dry humidity environments (i.e. 2% RH), the flexural strength for quartz/epoxy increased substantially as fabrication pressure increased. Generally, all quartz-reinforced materials (quartz/BMI and quartz/epoxy) had similar initial strength values ranging from 270-350 MPa. However, the rate of increase for epoxy was nearly double that for BMI. Therefore this results in a flexural strength range of 562-967 MPa and 425-602 MPa for quartz/epoxy and quartz/BMI, respectively. The flexural strength for carbon fiber reinforced laminates was influenced the least due to fabrication pressure.

Contour plots for normalized flexural stiffness were primarily dependent on the fabrication pressure for all prepregs. Since stiffness is fiber-dominated phenomenon, it was expected that humidity exposure would have a limited effect on the flexural stiffness, which was confirmed by the near vertical contour lines. Overall, the spacing

between contour lines remained similar throughout the entire fabrication pressure range. The constant contour line spacing indicated near-linear increases in stiffness as fabrication pressure increased. The maximum flexural stiffness was 29.3 GPa for both quartz-reinforced prepregs, regardless of whether BMI or epoxy was used. The stiffness for each quartz-reinforced prepreg had a normalized percent change of about 25%. Meanwhile, the flexural stiffness for carbon fiber-reinforcement was significantly higher, with a maximum of 53.3 GPa. The load-bearing capability of carbon fiber is well known to be superior when compared to quartz fiber, which was reflected by the high stiffness values. Carbon fiber-reinforcement also had a much narrower range of flexural stiffness values, as the normalized percent change was less than 20% for all fabricated specimens. Contour plots for normalized flexural strength reveal significant contributions by prepreg humidity exposure and fabrication pressure. Flexural strength requires good fiber-matrix interface to transfer loads between plies. Therefore as laminate defects increase (i.e. void fraction) the strength potential significantly degrades. The flexural strength for quartz/BMI and quartz/epoxy followed this trend very closely, in that the highest flexural strength was observed when humidity exposure was low and fabrication pressure was high, and correlated with the lowest void volume fraction. Additionally, the spacing between contour lines was the closest in the same region when void volume fraction similarly had the closest intervals, which was at high humidity exposure and low fabrication pressure. An interesting note was the complex procedure required to improve strength for these laminates. If starting at a low fabrication pressure, a majority of improvement could be achieved simply by increasing the cure pressure. However, as pressure increased to higher amounts (greater than 350

kPa), it became increasingly necessary to reduce the humidity exposure level to continue improving the flexural strength. Resin type has a significant role on the maximum flexural strength, which is corroborated by BMI being much lower (603 MPa) when compared to epoxy (967 MPa). The normalized strength reduction for carbon/epoxy was much lower than the two quartz-reinforced laminates. Additionally, the strength for carbon/epoxy laminates was influenced by humidity changes to the same degree.

The experimental mass gain data for long-term hydraulic fluid absorption was analyzed using a hindered diffusion model. The model had good agreement with the experimental data and was successful in recovering the absorption parameters and equilibrium fluid contents for each laminate. Both quartz-reinforced laminates (quartz/BMI and quartz/epoxy) were nearing saturation after two years of immersion. Meanwhile, the carbon/epoxy laminates have not neared saturation after 18 months of immersion. For quartz/BMI and quartz/epoxy, the equilibrium fluid content increased as relative humidity exposure increased. However, the effect was much more pronounced for BMI resin. Additionally, the equilibrium fluid content was significantly higher for laminates fabricated at 69 kPa. Meanwhile, the equilibrium fluid content was grouped tightly together for all other fabrication pressures. This behavior closely mirrors the laminate fiber volume fraction for each material, where the largest incremental improvement was achieved when pressure was increased from 69 kPa to 207 kPa. The rate of increase for equilibrium fluid content was significantly higher, by six fold, for BMI when compared to epoxy resin, which gradually declined as fabrication pressure increased. This indicates that prepreg humidity exposure must be

closely monitored and accounted for when fabrication pressures are low so as to limit hydraulic fluid absorption. The rate of increase for quartz/epoxy (Figure 5.8b) was very similar, regardless of the fabrication pressure. Therefore, the equilibrium fluid content is influenced to a larger degree by the fabrication cure pressure when epoxy resin is utilized. Quartz/BMI generally had higher accuracy of the model fits when compared to quartz/epoxy. Equilibrium fluid content was also more sensitive to changes in fabrication pressure for BMI, with increasing rates of two or three times that epoxy. This indicated that the applied cure pressure contributes significantly to the amount of hydraulic fluid absorbed for BMI resin applications.

One contribution of this research study was a detailed evaluation of the effect of humidity exposure and fabrication pressure on the laminate flexural properties and absorption behavior of aerospace-grade composite prepregs. Flexural stiffness was generally dependent on the fabrication pressure, whereas flexural strength demonstrated a coupled relationship with humidity exposure and cure pressure. Property function equations and contour plots are a useful tool in identifying trends associated with flexural properties. Finally, a detailed analysis of the equilibrium fluid content for each prepreg was developed using a hindered diffusion model.

7.3.1 Limitations and Future Work Associated with Research Objective 2

Discrepancies at high relative humidity exposure levels

For some studies within this project, the 70% relative humidity prepreg conditioning had higher equilibrium fluid contents or higher flexural strength when compared to the 99% relative humidity specimens. This localized behavior contradicts the overall trends in that increasing prepreg conditioning will increase the equilibrium fluid content and

decrease the flexural strength. This behavior may be due to experimental uncertainty inherent in characterizing laminates with considerable voids. A more detailed investigation at several high relative humidity levels (i.e. 60%, 70%, 80% and 90% RH) would be desirable so as to further examine this phenomenon.

Elevated temperature effects

Researchers have frequently identified different absorption behaviors of composite laminates when exposed to liquid contaminations at elevated temperatures. Frequently, the equilibrium fluid content will be achieved in a shorter duration when temperature increases. Therefore, one area of future work could include examining elevated temperature effects on the absorption behavior of high-performance composite laminates.

7.4 ADDRESSING RESEARCH OBJECTIVE 3

Effect of long-term hydraulic fluid contamination on the flexural properties of aerospace-grade composite laminates

The effect of hydraulic fluid content on the laminate flexural properties (Chapter 6) was analyzed for the two quartz-reinforced materials (quartz/BMI and quartz/epoxy) as those materials had approached saturation after nearly two years of immersion. This study was developed to address the third research objective. For both resin materials, the largest variation and sensitivity to hydraulic fluid contamination was observed for prepregs conditioned in a dry environment (i.e. 2% RH). Nearly all quartz/BMI laminates had stiffness reductions of less than 5%, even with a substantially wide range

of hydraulic fluid contents of up to 9 %wt. Conversely, the quartz/epoxy laminates (Figure 6.9b) observed stiffness reductions of no more than 5%, but for less than 1.7 %wt. maximum observed hydraulic fluid content. Therefore, higher levels of hydraulic fluid content generally increased the level of stiffness percent reduction for epoxy resin. BMI resin was generally more sensitive to hydraulic fluid contamination when fabrication pressure was low. Therefore, utilizing higher fabrication pressures becomes necessary to minimize the effect of hydraulic fluid on flexural stiffness. The stiffness reduction for epoxy resin was not influenced significantly by varying hydraulic fluid contents. The selected fabrication pressure dictates the percent reduction much more, evidenced by all laminates fabricated at 345 kPa and above having the largest percent reduction values.

Although some specimens at low fluid contents had large reductions in flexural strength, the overall trend observed for both resin materials was that higher levels of hydraulic fluid content resulted in larger reductions in flexural strength. When hydraulic fluid content was greater than 5 %wt. all quartz/BMI laminates had strength reductions larger than 4.8%. As hydraulic fluid content declined, the effect of hydraulic fluid on flexural strength also declined. Wide variations for strength reduction were observed for quartz/epoxy laminates with no discernible trends due to varying fluid contents. Both resin materials demonstrated the largest range in strength reductions when fluid content was low, which progressively narrowed as fluid content increased. Overall, the effect of hydraulic fluid on flexural strength slightly increased as hydraulic fluid content increased. Hydraulic fluid contamination affects for BMI resin were generally minimized when higher fabrication pressures (345 kPa and above) were used.

Hydraulic fluid affects on flexural strength for epoxy resin increased substantially (0.0-14.3%) up to a hydraulic fluid content of 1.0 %wt. Higher hydraulic fluid content values generally did not degrade the flexural strength by more than 9%.

One contribution of this research study was a detailed evaluation of not only the effect of humidity exposure and fabrication pressure on the laminate flexural properties, but also the effect of long-term hydraulic fluid contamination. Overall, the flexural performance for both quartz-reinforced laminates was not significantly degraded as a result of long-term hydraulic fluid contamination. For the most extreme cases, flexural strength was reduced by less than 9% and 15% after nearly two years of hydraulic fluid contamination for quartz/BMI and quartz/epoxy, respectively.

7.4.1 Limitations and Future Work Associated with Research Objective 3

Discrepancy with equilibrium fluid content for two specimen planar dimensions

One discrepancy that could not be resolved with the current work was the different equilibrium fluid contents for specimens of two planar dimensions (i.e. absorption specimens from Chapter 5 and flexural specimens from Chapter 6). Usually, different planar dimensions should only affect the initial slope of fluid diffusion that correlates with Fickian absorption. As non-Fickian behavior begin to dominate for large time periods, both specimen dimensions should converge to a single equilibrium fluid content. For most cases, the convergence never occurred and the equilibrium fluid content for two specimen sizes remained separated by 10-20%. Local variations within specimens (i.e. unusually high void content) may be the cause. However this hypothesis could not be confirmed by the current study. Therefore, a comprehensive future study of multiple planar dimensions (e.g. aspect ratios of 1.0, 2.0, 3.0 and 4.0)

would be helpful in determining the three-dimensional absorption behavior for laminates subjected to different humidity levels and fabrication pressures.

REFERENCES

[1] J. P. Anderson and M. C. Altan, Properties of composite cylinders fabricated by bladder assisted composite manufacturing. *Journal of Engineering and Material Technology,* **134**, 4 (2012).

[2] J. P. Anderson and M. C. Altan, Formation of voids in composite laminates: Coupled effect of moisture content and processing pressure. *Polymer Composites,* **36**, 2 (2015).

[3] C. Maggana and P. Pissis, Water sorption and diffusion studies in an epoxy resin system. *Journal of Polymer Science, Part B: Polymer Physics,* **37**, 11 (1999).

[4] R. M. V. G. K. Rao, M. Chanda, and N. Balasubramanian, A Fickian diffusion model for permeable fibre polymer composites. *Journal of Reinforced Plastics and Composites,* **2**, 4 (1983).

[5] T. C. Wong and L. J. Broutman, Moisture diffusion in epoxy resins. Part I. Non-Fickian sorption processes. *Polymer Engineering and Science,* **25**, 9 (1985).

[6] J. Vina, E. A. Garcia, A. Arguelles, and I. Vina, The effect of moisture on the tensile and interlaminar shear strengths of glass or carbon fiber reinforced PEI. *Journal of Materials Science Letters,* **19**, (2000).

[7] L. Aktas, Y. Hamidi, and M. C. Altan, Effect of moisture absorption on mechanical properties of resin transfer molded composites - Part I: Absorption. *Journal of Materials Processing and Manufacturing Science,* **10**, 4 (2002).

[8] S. Popineau, C. Rondeau-Mouro, C. Sulpice-Gaillet, and M. E. R. Shanahan, Free/bound water absorption in an epoxy adhesive. *Polymer,* **46**, 24 (2005).

[9] W. Chu, and V. M. Karbhari, Effect of water sorption on performance of pultruded E-glass/Vinylester composites. *Journal of Materials in Civil Engineering,* **17**, 1 (2005).

[10] L-R. Bao and A. F. Yee, Moisture diffusion and hygrothermal aging in Bismaleimide matrix carbon fiber composites - Part I: Uni-weave composites. *Composites Science and Technology,* **62**, 16 (2002).

[11] L-R. Bao, and A. F. Yee, Moisture diffusion and hygrothermal aging in Bismaleimide matrix carbon fiber composites - Part II: Woven and hybrid composites. *Composites Science and Technology,* **62**, 16 (2002).

[12] L-R. Bao, and A. F. Yee, Effect of temperature on moisture absorption in a Bismaleimide resin and its carbon fiber composites. *Polymer,* **43**, 14 (2002).

[13] Y. Li, J. Miranda, and H-J. Sue, Hygrothermal diffusion behavior in Bismaleimide resin. *Polymer,* **42**, 18 (2001).

[14] Y. Li, J. Miranda, and H-J. Sue, Moisture diffusion behavior in Bismaleimide resin subjected to hygrothermal cycling. *Polymer Engineering and Science,* **42**, 2 (2002).

[15] V. L. Saponara, Environmental and chemical degradation of carbon/epoxy and structural adhesive for aerospace applications: Fickian and anomalous diffusion, Arrhenius kinetics. *Composite Structures,* **93**, 9 (2011).

[16] M. Al-Qadhi, N. Merah, Z. M. Gasem, N. Abu-Dheir, and B. J. Abdul Aleem, Effect of water and crude oil on mechanical and thermal properties of epoxy-clay nanocomposites. *Polymer Composites,* **35**, 2 (2013).

[17] L. Liu, B-M. Zhang, D-F. Wang, and Z-J Wu, Effects of cure cycles on void content and mechanical properties of composite laminates. *Composite Structures,* **73**, 3 (2006).

[18] K. R. Hurdelbrink II, J. P. Anderson, Z. Siddique, and M. C. Altan, Effects of Processing Conditions on Mechanical Properties of Quartz/BMI Laminates. *American Society of Composites 30th Technical Conference*. East Lansing, MI. (2015).

[19] S. J. Li, L. H. Zhan, R. Chen, W. F. Peng, Y. A. Zhang, Y. Q. Zhou, and L. R. Zeng, The influence of cure pressure on microstructure, temperature field and mechanical properties of advanced polymer-matrix composite laminates. *Fibers and Polymers,* **15**, 11 (2014).

[20] S. R. Ghiorse, Effect of void content on the mechanical properties of carbon/epoxy laminates. *Sampe Quarterly,* **24**, 2 (1993).

[21] K. A. Olivero, H. J. Barraza, E. A. O'Rear, and M. C. Altan, Effect of injection rate and post-fill cure pressure on properties of resin transfer molded disks. *Journal of Composite Materials,* **36**, 16 (2002).

[22] N. C. W. Judd, and W. W. Wright, Voids and their effects on the mechanical properties of composites - An appraisal. *Sampe Journal,* **14**, 1 (1978).

[23] P-O. Hagstrand, F. Bonjour, and J-A. E. Manson, The influence of void content on the structural flexural performance of unidirectional glass fibre reinforced polypropylene composites. *Composites Part A: Applied Science and Manufacturing,* **36**, 5 (2005).

[24] S. F. Muller de Almeida, and Z. d. S. N. Neto, Effect of void content on the strength of composite laminates. *Composite Structures,* **28**, 2 (1994).

[25] Gorkem E. Guloglu, K. R. Hurdelbrink II, J. P. Anderson, and M. C. Altan, Experimental and Theoretical Investigation of Non-Fickian Moisture Absorption of Quartz/BMI Laminates Fabricated by Preconditioned Prepregs. *31st International Conference of the Polymer Processing Society*. Jeju Island, Korea. (2015).

[26] M. J. Robinson, A qualitative analysis of some of the issues affecting the cost of composite structures. *Advanced Materials/Affordable Processes,* **23** (1991).

[27] S. Hernández, F. Sket, C. González, and J. Llorca, Optimization of curing cycle in carbon fiber-reinforced laminates: void distribution and mechanical properties. *Composites Science and Technology,* **85** (2013).

[28] S. M. Sisodia, E. K. Gamstedt, F. Edgren, and J. Varna, Effects of voids on quasi-static and tension fatigue behavior of carbon-fibre composite laminates. *Journal of Composite Materials,* **49**, 17 (2015).

[29] M. A. Suhot, and A. R. Chambers, The effects of voids on the flexural properties and failure mechanisms of carbon/epoxy composites. *Jurnal Teknologi,* **71**, 2 (2014).

[30] A. Zhang, H. Lu, and D. Zhang, Research on the mechanical properties prediction of carbon/epoxy composite laminates with different void contents. *Polymer Composites,* **37**, 1 (2014).

[31] M. L. Costa, S. F. M. de Almeida, and M. C. Rezende, The influence of porosity on the interlaminar shear strength of carbon/epoxy and carbon/bismaleimide fabric laminates. *Composites Science and Technology,* **61**, 14 (2001).

[32] S. Hernández, F. Sket, J. M. Molina-Aldareguia, C. González, and J. Llorca, Effect of curing cycle on void distribution and interlaminar shear strength in polymer-matrix composites. *Composites Science and Technology,* **71**, 10 (2011).

[33] H. Yoshida, T. Ogasa, and R. Hayashi, Statistical approach to the relationship between ILSS and void content of CFRP. *Composites Science and Technology,* **25**, 1 (1986).

[34] W. V. Liebig, C. Viets, K. Schultze, and B. Fiedler, Influence of voids on the compressive failure behaviour of fibre-reinforced composites. *Composites Science and Technology,* **117** (2015).

[35] Z-S. Guo, L Liu, B-M. Zhang, and S Du, Critical void content for thermoset composite laminates. *Journal of Composite Materials,* **43**, 17 (2009).

[36] G. Seon, A. Makeev, Y. Nikishkov, and E. Lee, Effects of defects on interlaminar tensile fatigue behavior of carbon/epoxy composites. *Composites Science and Technology,* **89** (2013).

[37] L. K. Grunenfelder, and S. R. Nutt, Void formation in composite prepregs–effect of dissolved moisture. *Composites Science and Technology,* **70**, 16 (2010).

[38] H. Jeong, Effects of voids on the mechanical strength and ultrasonic attenuation of laminated composites. *Journal of Composite Materials,* **31**, 3 (1997).

[39] T. S. Lundström, and B. R. Gebart, Influence from process parameters on void formation in resin transfer molding. *Polymer Composites,* **15**, 1 (1994).

[40] G. R. Sherwin, Non-autoclave processing of advanced composite repairs. *International Journal of Adhesion and Adhesives,* **19**, 2 (1999).

[41] M. Shen, M. S. Wagner, D. G. Castner, B. D. Ratner, and T. A. Horbett, Multivariate surface analysis of plasma-deposited tetraglyme for reduction of protein adsorption and monocyte adhesion. *Langmuir,* **19**, 5 (2003).

[42] A. Kumar, and R. G. Reddy, Effect of channel dimensions and shape in the flow-field distributor on the performance of polymer electrolyte membrane fuel cells. *Journal of Power Sources,* **113**, 1 (2003).

[43] S. L. Campanelli, A. D. Ludovico, C. Bonserio, P. Cavalluzzi, and M. Cinquepalmi, Experimental analysis of the laser milling process parameters. *Journal of Materials Processing Technology,* **191**, 1 (2007).

[44] V. Yong, and H. T. Hahn, Moisture absorption modeling using design of experiments. *Journal of Applied Polymer Science,* **103**, 3 (2007).

[45] L. R. Grace, and M. C. Altan, Characterization of anisotropic moisture absorption in polymeric composites using hindered diffusion model. *Composites Part A: Applied Science and Manufacturing,* **43**, 8 (2012).

[46] L. R. Grace, and M. C. Altan, Non-fickian three-dimensional hindered moisture absorption in polymeric composites: Model development and validation. *Polymer Composites,* **34**, 7 (2013).

[47] L. R. Grace, and M. C. Altan, Three-dimensional anisotropic moisture absorption in quartz-reinforced Bismaleimide laminates. *Polymer Engineering and Science,* **54**, 1 (2014).

[48] E. Perez-Pacheco, J. I. Cauich-Cupul, A. Valadez-Gonzalez, and P. J. Herrera-Franco, Effect of moisture absorption on the mechanical behavior of carbon fiber/epoxy matrix composites. *Journal of Materials Science,* **48**, 5 (2013).

[49] F. Pomies, and L. A. Carlsson, Analysis of modulus and strength of dry and wet thermoset and thermoplastic composites loaded in transverse tension. *Journal of Composite Materials,* **28**, 1 (1994).

[50] W. L. Bradley, and T. S. Grant, The effect of the moisture absorption on the interfacial strength of polymeric matrix composites. *Journal of Materials Science,* **30**, 21 (1995).

[51] E. P. Sideridis, and G. S. Bikakis, Shear properties and load-deflection response of cross-ply glass-epoxy composite short-beams subjected to three-point-bending tests, and the effect of moisture absorption. *Journal of Applied Polymer Science,* **129**, 4 (2013).

[52] T. A. Bullions, A. C. Loos, and J. E. McGrath, Moisture sorption effects on and properties of a carbon fiber-reinforced phenylethynyl-terminated poly(etherimide). *Journal of Composite Materials,* **37**, 9 (2003).

[53] R. M. V. G. K. Rao, H. V. S. Kumari, and K. S. Raju, Moisture diffusion behavior of T300-914C laminates. *Journal of Reinforced Plastics and Composites,* **14**, 5 (1995).

[54] N. Abacha, M. Kubouchi, T. Sakai, and K. Tsuda, Diffusion behavior of water and sulfuric acid in epoxy/organoclay nanocomposites. *Journal of Applied Polymer Science,* **112**, 2 (2009).

[55] T. Glaskova, and A. Aniskevich, Moisture absorption by epoxy/montmorillonite nanocomposite. *Composites Science and Technology,* **69**, 15-16 (2009).

[56] K. R. Hurdelbrink II, Z. Siddique, and M. C. Altan. The coupled effect of microvoids and hydraulic fluid absorption on mechanical properties of quartz/BMI laminates. *American Society of Composites 29th Technical Conference*. San Diego, CA. (2014).

[57] L Aktas, Y. K. Hamidi, and M. C. Altan, Combined edge and anisotropy effects on Fickian mass diffusion in polymer composites. *Journal of Engineering and Material Technology,* **126**, 4 (2004).

[58] J. Crank, The mathematics of diffusion. *Oxford University Press* (1975).

[59] H. G. Carter, and K. G. Kibler, Langmuir-Type Model for Anomalous Moisture Diffusion in Composite Resins. *Journal of Composite Materials,* **12** (1978).

[60] H. L. Frisch, and C. E. Rogers, Transport in Polymers. *Journal of Polymer Science Part C-Polymer Symposium,* **12**, 12PC (1966).

[61] S. Roy, W. X. Xu S. J. Park, and K. M. Liechti, Anomalous moisture diffusion in viscoelastic polymers: modeling and testing. *Journal of Applied Mechanics,* **67**, 2 (2000).

APPENDIX A: SPECIMEN AVERAGES FOR PROPERTY FUNCTIONS

Table A.1 Average fiber volume fraction and 95% confidence interval for the three prepreg materials

Prepreg Conditioning (% RH) & Fabrication Pressure (kPa)		Quartz / BMI	Quartz / Epoxy	Carbon / Epoxy
2% RH	68.9	50.72 ± 2.88	49.04 ± 4.23	55.24 ± 3.14
	206.8	60.67 ± 5.12	53.21 ± 2.30	61.73 ± 1.67
	344.7	61.82 ± 2.49	58.17 ± 3.25	62.00 ± 3.02
	482.6	66.78 ± 1.33	60.53 ± 2.57	66.06 ± 1.55
40 % RH	68.9	51.45 ± 2.93	48.44 ± 3.57	51.71 ± 2.34
	206.8	58.97 ± 2.27	54.55 ± 3.24	56.91 ± 2.37
	344.7	63.71 ± 2.16	58.33 ± 2.02	59.48 ± 1.28
	482.6	64.76 ± 3.65	61.75 ± 3.10	61.95 ± 3.08
70% RH	68.9	55.43 ± 4.52	48.21 ± 2.84	53.61 ± 3.53
	206.8	62.00 ± 3.07	53.74 ± 2.17	61.61 ± 5.99
	344.7	64.93 ± 1.33	58.29 ± 1.77	62.67 ± 5.03
	482.6	66.62 ± 2.79	62.58 ± 3.97	61.90 ± 0.38
99% RH	68.9	52.63 ± 4.37	49.21 ± 4.06	52.67 ± 1.78
	206.8	64.94 ± 2.56	53.91 ± 2.80	60.46 ± 1.65
	344.7	65.57 ± 2.56	58.17 ± 2.00	59.14 ± 2.29
	482.6	64.12 ± 0.98	59.28 ± 0.46	61.16 ± 1.95

Table A.2 Average void content and 95% confidence interval for three composite prepreg materials

Prepreg Conditioning (% RH) & Fabrication Pressure (kPa)		Quartz / BMI	Quartz / Epoxy	Carbon / Epoxy
2% RH	68.9	12.41 ± 1.29	3.52 ± 1.01	3.21 ± 1.25
	206.8	9.23 ± 1.88	2.33 ± 0.53	1.67 ± 0.23
	344.7	8.23 ± 1.15	2.15 ± 0.54	1.28 ± 0.47
	482.6	8.22 ± 1.48	1.73 ± 0.52	1.26 ± 0.48
40 % RH	68.9	12.83 ± 1.21	7.00 ± 2.00	3.96 ± 0.32
	206.8	9.40 ± 0.52	4.60 ± 0.58	1.89 ± 0.60
	344.7	8.99 ± 1.05	3.87 ± 0.86	2.04 ± 0.18
	482.6	8.21 ± 1.30	3.65 ± 1.83	1.65 ± 0.58
70% RH	68.9	13.35 ± 3.50	10.23 ± 1.57	3.91 ± 1.01
	206.8	10.38 ± 2.05	7.03 ± 1.16	2.37 ± 0.56
	344.7	9.52 ± 0.19	5.95 ± 0.95	2.18 ± 1.20
	482.6	8.09 ± 0.79	5.44 ± 0.15	1.72 ± 0.42
99% RH	68.9	13.88 ± 2.36	14.12 ± 0.82	4.75 ± 0.62
	206.8	11.69 ± 0.98	10.47 ± 1.29	3.33 ± 0.77
	344.7	10.05 ± 0.90	8.30 ± 0.84	3.63 ± 0.85
	482.6	7.93 ± 0.79	7.86 ± 0.44	1.89 ± 0.14

Table A.3 Average flexural stiffness and 95% confidence interval for the three composite prepreg materials

Prepreg Conditioning (% RH) & Fabrication Pressure (kPa)		Quartz / BMI	Quartz / Epoxy	Carbon / Epoxy
2% RH	68.9	23.42 ± 0.83	22.65 ± 1.22	43.89 ± 1.49
	206.8	25.53 ± 0.83	25.00 ± 1.00	48.61 ± 1.20
	344.7	27.54 ± 1.01	27.27 ± 1.04	47.11 ± 2.31
	482.6	29.14 ± 0.38	28.83 ± 0.66	51.88 ± 0.94
40 % RH	68.9	22.64 ± 1.08	22.31 ± 1.01	42.58 ± 1.82
	206.8	24.71 ± 0.50	26.69 ± 1.56	46.94 ± 2.38
	344.7	27.19 ± 0.55	27.68 ± 0.74	49.60 ± 0.88
	482.6	28.60 ± 0.61	29.29 ± 0.45	51.55 ± 0.94
70% RH	68.9	22.01 ± 0.99	21.62 ± 0.98	43.65 ± 2.38
	206.8	25.45 ± 0.79	24.63 ± 0.88	47.90 ± 1.65
	344.7	27.31 ± 0.37	26.69 ± 0.94	49.72 ± 0.76
	482.6	28.68 ± 0.43	28.32 ± 0.30	53.30 ± 2.60
99% RH	68.9	22.79 ± 1.06	21.31 ± 1.07	42.85 ± 1.25
	206.8	26.67 ± 0.80	24.75 ± 1.25	50.69 ± 1.37
	344.7	28.58 ± 0.92	26.41 ± 0.61	50.70 ± 1.55
	482.6	29.30 ± 0.39	27.66 ± 0.46	51.76 ± 1.59

Table A.4 Average flexural strength and 95% confidence interval for three composite prepreg materials

Prepreg Conditioning (% RH) & Fabrication Pressure (kPa)		Quartz / BMI	Quartz / Epoxy	Carbon / Epoxy
2% RH	68.9	482.32 ± 33.32	721.94 ± 28.44	692.19 ± 53.51
	206.8	596.79 ± 34.98	763.16 ± 14.32	784.38 ± 32.17
	344.7	568.87 ± 7.96	797.86 ± 17.30	722.97 ± 92.38
	482.6	602.85 ± 15.84	818.05 ± 28.03	847.21 ± 93.35
40 % RH	68.9	463.28 ± 13.75	670.77 ± 40.64	665.69 ± 34.29
	206.8	536.74 ± 33.04	868.07 ± 42.30	781.01 ± 48.76
	344.7	526.25 ± 19.57	779.78 ± 25.55	690.29 ± 78.89
	482.6	545.67 ± 16.61	967.33 ± 26.62	607.56 ± 69.23
70% RH	68.9	425.04 ± 16.22	619.12 ± 59.67	653.18 ± 53.89
	206.8	488.61 ± 10.28	773.84 ± 61.85	733.73 ± 34.26
	344.7	507.71 ± 13.04	852.99 ± 26.19	774.24 ± 71.65
	482.6	524.81 ± 11.40	872.99 ± 48.63	793.83 ± 93.63
99% RH	68.9	450.96 ± 13.74	562.19 ± 46.51	689.36 ± 42.11
	206.8	521.82 ± 18.93	683.90 ± 23.26	720.31 ± 67.30
	344.7	542.24 ± 10.31	741.68 ± 28.37	741.84 ± 83.50
	482.6	550.10 ± 11.71	772.77 ± 56.02	787.59 ± 51.47

Table A.5 Average flexural stiffness for hydraulic fluid contaminated specimens and 95% confidence interval for two quartz-reinforced prepregs. Percent reduction determined from dry flexural results

Relative Humidity (% RH) & Fabrication Pressure (kPa)		Quartz / BMI	*Wet / Dry Reduction*	Quartz / Epoxy	*Wet / Dry Reduction*
2% RH	68.9	21.37 ± 0.84	*8.8%*	22.36 ± 1.12	*1.3%*
	206.8	24.32 ± 0.73	*4.7%*	24.60 ± 0.58	*1.6%*
	344.7	27.26 ± 0.68	*1.0%*	26.38 ± 0.83	*3.3%*
	482.6	28.27 ± 0.32	*3.0%*	27.36 ± 0.46	*5.1%*
40% RH	68.9	21.85 ± 0.95	*3.5%*	21.97 ± 0.95	*1.5%*
	206.8	23.55 ± 0.54	*4.7%*	26.20 ± 0.77	*1.8%*
	344.7	26.85 ± 0.43	*1.3%*	26.50 ± 1.05	*4.3%*
	482.6	27.77 ± 0.43	*2.9%*	28.17 ± 0.48	*3.8%*
70% RH	68.9	21.56 ± 0.79	*2.1%*	21.39 ± 0.59	*1.1%*
	206.8	25.31 ± 0.73	*0.5%*	24.62 ± 0.77	*0.0%*
	344.7	26.69 ± 0.51	*2.3%*	25.51 ± 0.45	*4.4%*
	482.6	27.55 ± 0.41	*3.9%*	27.08 ± 0.62	*4.4%*
99% RH	68.9	22.45 ± 1.20	*1.5%*	20.80 ± 0.77	*2.4%*
	206.8	26.42 ± 0.64	*1.0%*	23.61 ± 0.83	*4.6%*
	344.7	27.42 ± 0.66	*4.1%*	25.20 ± 0.49	*4.6%*
	482.6	28.65 ± 0.38	*2.2%*	26.31 ± 0.40	*4.9%*

Table A.6 Average flexural strength for hydraulic fluid contaminated specimens and 95% confidence interval for two quartz-reinforced prepregs. Percent reduction determined from dry flexural results

Relative Humidity (% RH) & Fabrication Pressure (kPa)		Quartz / BMI	*Wet / Dry Reduction*	Quartz / Epoxy	*Wet / Dry Reduction*
2% RH	68.9	451.68 ± 28.40	*6.4%*	655.42 ± 46.48	*9.2%*
	206.8	549.68 ± 20.61	*7.9%*	725.33 ± 29.93	*5.0%*
	344.7	569.87 ± 22.61	*-0.2%*	753.29 ± 37.82	*5.6%*
	482.6	588.28 ± 16.08	*2.4%*	827.44 ± 38.26	*-1.1%*
40% RH	68.9	427.11 ± 18.23	*7.8%*	616.38 ± 55.57	*8.1%*
	206.8	512.82 ± 22.25	*4.5%*	771.03 ± 28.84	*11.2%*
	344.7	510.44 ± 24.62	*3.0%*	738.81 ± 52.72	*5.3%*
	482.6	522.42 ± 18.89	*4.3%*	829.16 ± 32.04	*14.3%*
70% RH	68.9	396.03 ± 18.64	*6.8%*	571.97 ± 39.50	*7.6%*
	206.8	461.70 ± 22.33	*5.5%*	688.57 ± 47.48	*11.0%*
	344.7	487.80 ± 13.99	*3.9%*	755.78 ± 51.33	*11.4%*
	482.6	493.98 ± 13.90	*5.9%*	777.24 ± 50.30	*11.0%*
99% RH	68.9	429.29 ± 17.20	*4.8%*	560.34 ± 52.92	*0.3%*
	206.8	483.73 ± 14.12	*7.3%*	618.46 ± 38.10	*9.6%*
	344.7	510.78 ± 15.38	*5.8%*	680.59 ± 41.61	*8.2%*
	482.6	517.33 ± 9.06	*6.0%*	703.03 ± 29.66	*9.0%*